Design and Applications of Inkjet-Printed Flexible Sensate Surfaces

by

Nan-Wei Gong

**Submitted to the Program in Media Arts and Sciences,
School of Architecture and Planning,
in partial fulfillment of the requirements for the degree of
Doctor of Philosophy in Media Arts and Sciences**

at the

MASSACHUSETTS INSTITUTE OF TECHNOLOGY

September 2013

Signature redacted

Author_____

Program in Media Arts and Sciences
September 2013

Signature redacted

Certified by_____

Joseph A. Paradiso
Associate Professor of Media Arts and Sciences
Massachusetts Institute of Technology
Thesis Supervisor

Signature redacted

Accepted by_____

Pattie Maes
Associate Academic Head, Professor of Media Arts and Sciences
Massachusetts Institute of Technology

Design and Applications of Inkjet-Printed Flexible Sensate Surfaces

by

Nan-Wei Gong

Submitted to the Program in Media Arts and Sciences,
School of Architecture and Planning,
in partial fulfillment of the requirements for the degree of
Doctor of Philosophy in Media Arts and Sciences

Abstract

We live in a world where everyday artifacts begin to be designed and augmented as media interfaces. New technologies based on this mission enable us to more easily sense, interact, and communicate with objects. However, the world is highly variable in physical forms. To achieve the vision of ubiquitous computing, common man-made objects need to be designed from the ground up to incorporate computers and sensors. Often, we find ourselves confined by existing sensing infrastructures that are not designed to adapt the complexity of the physical world.

This dissertation presents a research platform to investigate design principles and applications for flexible sensate surfaces. This platform utilizes recent advancements in low-cost, roll-to-roll conductive inkjet printing technology as an enabler for creating a scalable, physically and functionally adaptive and customizable sensing system. This collection of work demonstrates design principles and examples in the following four areas: manufacturing, customizable computer aided design, fabrication with physical manipulation and multi-modal sensing techniques. Two types of manufacturing methods are used and characterized. The first approach customizes the sensing design in a digital environment, where users define the geometry, shape and sensing inputs in a computer and print out customized functional patterns. The second approach is sensor fabrication via physical manipulation, where the sensate surface is pre-manufactured and through an additive method (paneling linear sensor tape stripes), or a subtractive method (cutting a sensor sheet), and the shape and sensing targets are processed post-manufacturing. Lastly, I demonstrate three techniques for multi-modal sensing - designing "target specific shapes" for different sensing targets, multiplexing single input electrodes with various analog circuits for near surface sensing (pressure, touch, folding, proximity sensing), and adding extra layers of chemical for the designed ad-hoc sensing target alteration.

The outcome of this exploration combines emerging technologies to realize a new way of designing sensate surfaces for smart environments and objects and helps us rethink sensing as both a graphical design and a physical manipulation process. In the course of this thesis, I demonstrate these principals by designing, testing, and evaluating a variety of flexible sensate surfaces.

Thesis Supervisor: Dr. Joseph A. Paradiso,
Associate Professor, Program in Media Arts and Sciences
Massachusetts Institute of Technology

Design and Applications of Inkjet-Printed Flexible Sensate Surfaces

by

Nan-Wei Gong

Signature redacted

Thesis Reader_____

Pattie Maes
Associate Academic Head, Professor of Media Arts and Sciences
MIT Media Lab

Signature redacted

Thesis Reader_____

Jürgen Steimle
Head of the Embodied Interaction Group
Max Planck Institute for Informatics

Acknowledgement

To my adviser Joe Paradiso for being a great adviser and a friend, for offering me this life-changing experience at the Media Lab.

To my readers, Pattie Maes and Jürgen Steimle, for your advice and feedback.

To my colleagues from the Responsive Environments Group:

Mat Laibowitz, for being my mentor and offering me the best ninja survival-training program in town. Bo Morgan, for showing me what it means to love what you do, for putting the band together, and eventually, for saving the world with funk2. Mark Feldmeier, for being our rock. Gershon Dublon, for playing music with me and creating wonderful moments for everyone. Nan Zhao, for being the best officemate and friend, for listening and being patience with me, and lastly, for introducing me to Sushi and Gyro Jones. Amit Zoran, for always trying hard to make me a better person. Nick Gillian, for great discussions and always explaining things patiently to me. Michael Lapinski and Matt Aldrich, for being supportive and giving me great advice. Amna Carreiro, for taking care of everyone. Brian Mayton, Laurel Pardue, Alex Reben, Behram Mistree, Manas Mittal, David Way, and Pragun Goyal for being great friends and colleagues.

To my friends:

Anette von Kapri, for being amazing and bringing me the most positive energy. Simon Olberding, for being a great friend and collaborator, for the real-time translation service and being there for me in front of SIAM. Valentin Huen, for giving me great advice and help whenever I need the most. To David Mellis and Jennifer Jacobs, for always being supportive and constructive. To Yu Chen, for being #1 on my speed dial for the past 12 years. To Chiu-Yen Wang, for being a great friend, someone I can always count on, and Liang-Yi Chang, for being my friend and running/studying buddy over the past decade.

To my collaborators:
Steve Hodges, for giving me great advice and help in my research direction. Jürgen Steimle, for brainstorming and collaborating with me and giving me great momentum to complete my research. Yoshihiro Kawahara, for exciting technologies to us.

Lastly, to my family: mom, dad and Chia-Wei for your unconditional love and support.

Table of Contents

Chapter 1 15

Introduction 15

Chapter 2 19

Related Work 19

2.1 Flexible Electronics and Sensor Skin Surfaces 19

2.2 Augmenting Smart Objects with Near Surface Sensing 22

2.3 Toolkits for physical computing and prototyping 24

2.4 Inkjet-Printed Sensors 25

Chapter 3 28

Manufacturing: Conductive Inkjet Printing 28

3.1 Conductive Inkjet Technology (CIT) 29

3.2 Off-the-shelf Inkjet Printing with Silver Nanoparticles 30

3.3 Component Attachment Techniques 31

Chapter 4 34

4.1 Motivation and Related Works 35

4.2 A Customizable Sensate Surface for Music Control 40

4.2.1 Functional patterns as inputs 40

4.2 Mapping Strategies 44

4.2.1 Mapping Strategies - Physical Mappings 44

4.2.2 Mapping Strategies - Signal Mapping 46

Proximity 46

Pressure 47

Activity trigger 47

Slider 48

4.5 Customization 49

4.6 The Zebra Skin 51

4.6.1 Parametric Pattern Design 52

4.6.2 Rapid Prototyping with Conductive Inkjet Printing 54

4.6.3 Hardware Interface for Sensing and Communication 54

4.6.4 Signal Mapping 55

4.7 Hardware toolkit for user customization 55
4.8 Conclusions 59
Chapter 5 61
5.1 The Making of Sensate Structures for User Customization – Cuttable Sensor Sheet and Sensor Tape 61
5.2 Subtractive Manufacturing: Cuttable Multi-touch Sensor Sheet 64
5.3 Additive Manufacturing – Sensor Tape 66
5.3.1 Method and Experiment 67
Chapter 6 74
6.1 Sensor floor –background and related work 74
6.2 Overall Architecture and Construction 75
6.3 PCB module circuitry 78
6.4 Physical topology 81
6.5 Sensing Modalities 81
6.5.1 Passive Mode Capacitive Sensing 82
6.5.2 Active Mode Capacitive Sensing 82
6.5.3 UHF and HF Sensing 84
6.5.4 Piezoelectric pickup 85
6.6 Evaluation 85
6.6.1 Detecting users with passive mode 85
6.6.2 Sensing with active mode 87
6.6.3 Piezoelectric sensor 89
6.6.4 Cellular signals versus localization and identification 90
6.7 Conclusions 94
Chapter 7 97
7.1 Example Scenarios 97
7.1.1 Enabling rich input on and above smart objects 97
7.1.2 Interactions with, on and above flexible surfaces 99
7.2 Design and Fabrication Principals of PrintSense 100
7.3 Sensing Principles of PrintSense 104
7.3.1 Capacitive Touch Sensing 104
7.3.2 Capacitive Proximity Sensing 105
7.3.3 Other sensing modalities 106

7.4 Electrode substrate 107
7.5 Hardware implementation 108
7.6 Characterization of operation 109
7.6.1 Resistive Sensing 109
7.6.2 Capacitive proximity sensing 116
7.7 Example use cases 117
7.7.1 Use Case 1: Grasp Detection on Curved Objects 117
7.7.2 Use Case 2: Manipulation of Flexible Surfaces 118
7.8 Discussion and conclusion 119
Chapter 8 121
Conclusion 121
Appendices 124
A.1 Sensor Floor schematics 125
A.2 PrintSense schematics 129
A.3 Design example of a sensate music controller surface 137
Bibliography 138

Table of Figures

FIGURE 2.1 EXAMPLE PLATFORMS FOR SKIN-LIKE SENSOR SYSTEMS BUILT WITH RIGID PCBS. LEFT TO RIGHT: TRIBBLE [22] , S.N.A.K.E [23], AND CHAINMAIL [21]. 19
FIGURE 2.2 ROLL-TO-ROLL PRINTING PROCESSES, WIDELY USED IN DISPLAY CONNECTOR CIRCUITS FOR PROVIDING EXTRA ELASTICITY TO THE CONNECTION WHILE EMBEDDING AND CONSTRAINING THE BACK PANEL [25]. 20
FIGURE 2.3 LEFT: UNMOUSEPAD - RESISTIVE, PRESSURE-SENSITIVE TOUCHBASED INPUT DEVICE FOR TRACKING BOTH TOUCHES AS WELL AS PENS BASED ON INTERPOLATING FORCE SENSITIVE RESISTANCE (IFSR). RIGHT: PYZOFLEX, A PRESSURE SENSING INPUT DEVICE THAT IS BASED ON A FERROELECTRIC MATERIAL. IT IS CONSTRUCTED WITH A SANDWICH STRUCTURE OF FOUR LAYERS THAT CAN BE SCREEN-PRINTED EASILY ON ANY MATERIAL. 21
FIGURE 2.4 LEFT: MODULAR AND DEFORMABLE TOUCH-SENSITIVE SURFACES BASED ON TIME DOMAIN REFLECTOMETRY. RIGHT: TACTILETAPE: LOW-COST TOUCH SENSING ON CURVED SURFACES. 22
FIGURE 2.5 (A)THE TANGO: A TANGIBLE RECEPTIVE WHOLE-HAND INTERFACE [35]. (B) FLEXAURA, A FLEXIBLE NEAR-SURFACE RANGE SENSOR [26], (C) THE BAR OF SOAP, HANDHELD DEVICES THAT COMBINE GRASP AND ORIENTATION SENSING, (D) GRIPS AND MULTI-TOUCH PEN [34]. 23
FIGURE 2.6 EXAMPLE HARDWARE TOOLKITS FOR COMPUTATIONAL RAPID PROTOTYPING. THESE OPEN-SOURCE ELECTRONICS PROTOTYPING PLATFORMS SUPPORT COLLABORATION THROUGH THE SHARING OF PERSONAL PROJECTS AND SOURCE CODES. 24
FIGURE 2.7 TOOLKITS FOR PROTOTYPING INTERACTIVE OBJECTS. (A)MIDAS, (B) SKETCH-A-TUI, (C) DRAW THE ELECTRIC, (D) MAKEY MAKEY. 25

FIGURE 2.8 ILLUSTRATION OF A FLEXIBLE PRINTED SENSOR TAPE FOR DIAGNOSTICS OF MILD TRAUMATIC BRAIN INJURY. THE SENSOR TAPE INTEGRATES PRESSURE AND ACCELERATION SENSORS, SIGNAL-PROCESSING ELECTRONICS, NON-VOLATILE MEMORY, AND A THIN FILM BATTERY [50] 26
FIGURE 2.9 LEFT: SENSPROUT: INKJET-PRINTED SOIL MOISTURE AND LEAF WETNESS SENSOR. RIGHT: RFID TAG MODEULE DESIGNED ON FLEXIBLE SUBSTRATE, WITH INKJET-PRINTED SINGLE WALL CARBON NANOTUBES (SWCNT) FILM AS A LOAD. 27
FIGURE 3.1 CONDUCTIVE INKJET FLEX PRINTING TECHNOLOGY WITH 2 STAGE ADDITIVE PROCESS. (A) STAGE 1, INKJET PRINTING (360 DPI) WITH ONBOARD UV AND IR CURING. (B) STAGE 2 - ELECTRO-LESS COPPER PLATING. (C) EXAMPLE FLEXIBLE CIRCUIT WITH COPPER TRACES ON MYLAR SUBSTRATE 30
FIGURE 3.2 CONDUCTIVE INKJET PRINTING WITH OFF-THE-SHELF PRINTING AND CONDUCTIVE SILVER PARTICLE INK. (A) AN EXAMPLE INKJET PRINTER WITH SILVER NANO PARTICLE FILLED INK CARTRIDGES. (B) SILVER NANO INK AND REPLACEMENT INK CARTRIDGES. (C) EXAMPLE PRINTOUT FROM MITSUBISHI PAPER MILLS LIMITED. 31
FIGURE 3.3 COMPONENT ATTACHMENT WITH LOW-TEMPERATURE SOLDER PASTE AND A SOLDER PASTE DISPENSER. 32
FIGURE 3.4 ILLUSTRATION OF THE CONDUCTIVE ADHESIVE TRANSFER TAPE FROM 3M [55]. 33
FIGURE 4.1. (A) EXAMPLE OF EXTRA MOVEMENT REQUIRED BETWEEN INSTRUMENT AND MUSIC CONTROLLERS. (B) IMPLEMENTATION OF OUR SYSTEM WITH ADDITIONAL GUITAR CONTROL INPUTS TO SEND THE MOST COMMONLY USED COMMANDS AND MINIMIZE NEEDED FINGER MOTION FOR THE EXTRA CONTROL DURING A LIVE PERFORMANCE 37
FIGURE 4.2 LEFT: WAYNE COYNE OF THE FLAMING LIPS [63], AND RIGHT: DIY KORG KAOSSILATOR GUITAR [64]. 38
FIGURE 4.3. (A) POTENTIAL SPACES (BLUE ZONES) FOR EXTRA CONTROL INPUTS. (B) ILLUSTRATION OF TRADITIONAL IMPLEMENTATION OF ADDITIONAL CONTROL INPUTS (C) CONTROL SURFACE DESIGN PATTERN WITH THE SAME EFFECT AS (B) WITHOUT PHYSICALLY CHANGING THE ORIGINAL INSTRUMENT. 40
FIGURE 4.4. (A) PRINTOUT OF OUR EXAMPLE DESIGNS. (B) CAPACITIVE SENSING BUTTONS (INDICATED BY ORANGE ARROWS) AND ASSOCIATED CIRCUIT WITH SURFACE MOUNT COMPONENTS (CY8C20) ATTACHED TO THE FLEXIBLE SURFACE. 41
FIGURE 4.5. CONNECTION DETAILS ABOUT THE CONTROLLER CIRCUIT. THE MICROCONTROLLER UNIT TALKS TO THE CAPACITIVE SENSING CHIP WITH A TWO WIRE COMMUNICATION PROTOCOL, WHICH ALLOWS MANY INPUT DEVICES TO BE COMMUNICATING ON THE SAME BUS. 42
FIGURE 4.6. SYSTEM BLOCK DIAGRAM – THE MAIN HARDWARE IS ATTACHED TO A MUSICAL INSTRUMENT OR ESSENTIALLY ANY OBJECT. A SENSATE SURFACE COMMUNICATES WITH THE CONTROL CIRCUITRY, WHICH TALKS TO A WIRELESS MODULE. THE OTHER END OF THE WIRELESS DATA TRANSMISSION SITS ON TOP OF A COMPUTER, WHICH PARSES AND PASSES THE INFORMATION TO MIDI INTERFACING SOFTWARE. THE SOFTWARE THEN SENDS MIDI MESSAGES TO A SOFTWARE SYNTHESIZER. 43
FIGURE 4.7. POTENTIAL MAPPING ON A PLUCKED STRING INSTRUMENT BASED ON GESTURES SUCH AS FINGER TAPPING, PICKING AND STRUMMING. 46
FIGURE 4.8 DESIGN REFERENCE OF A LINEAR SLIDER [72]. TOP: SENSOR ELECTRONICS. MIDDLE: CHEVRON-SHAPED INPUT ELECTRODE ARRAY, BOTTOM: ELECTRODE SIGNALS FOR FINGER AT RED REGION ABOVE. THE SLIDER POSITION IS GIVEN BY THE DISTRIBUTION'S CENTROID. 49
FIGURE 4.9. THREE EXAMPLE DESIGNS FOR DIFFERENT COVERAGE AND INPUT LOCATIONS. 50
FIGURE 4.10. AN EXAMPLE OF INKJET-PRINTED CONDUCTIVE PATTERNS FOR PHYSICAL MANIPULATION OF ELECTRIC UKULELE SIGNALS. ALL FEATURES ON THE SURFACE CAN GENERATE RESPONSIVE CONTROL SIGNALS WITH TOUCHING, BRIDGING, AND HOVERING 52
FIGURE 4.11. DESIGN PROCESS: (A) FROM VECTORS TO CONTOURS, (B) TWO EXAMPLES OF PATTERNS DESIGNED WITH DIFFERENT FORCE VECTORS. 53

FIGURE 4.12. DIFFERENT REGIONS IN THE FORCE VECTOR FIELD ARE DEFINED AS FUNCTIONAL INPUTS SUCH AS BUTTONS, SLIDERS, ETC. LEFT: COMPLETE DESIGN, COMBINING WITH COLORED PIGMENT. RIGHT: CONNECTED REGIONS OF EACH INPUT. 53
FIGURE 4.13. (A) TWO EXAMPLES OF TRACING CONTINUITY IN SUB-PATTERNS, (B) THE PRINTING PROCESS. 54
FIGURE 4.12. EXAMPLE MAX PATCH FOR THE ZEBRA SKIN INTERFACE. 55
FIGURE 4.15. TOOLKIT FOR BASIC IMPLEMENTATION. TWO DESIGN PATTERNS WERE MADE. EACH BATTERY-POWERED UNIT, AS SEEN IN THE BACK, CAN TRANSMIT SENSOR DATA WIRELESSLY THOUGH BLUETOOTH. 56
FIGURE 4.14. DATA PLOTS FROM FOUR DIFFERENT SIGNAL MAPPING STRATEGIES – (A) PROXIMITY, (B) BUTTON, (C) PRESSURE, (D) ACTIVITY INTEGRATION. 58
FIGURE 4.15. OUR MODULAR TEST SETUP – AN ARRAY OF BUTTONS CONNECTED TO A BATTERY-POWERED MICROCONTROLLER MODULE THAT TRANSMITS DATA WIRELESSLY. THE FIGURE ON THE RIGHT SHOWS INPUT SIGNALS FROM SLIDING ONE FINGER ALONG THE SENSOR ARRAY. 59
FIGURE 5.1. (A) SENSOR SHEET - THE GREEN BLOCK REPRESENTS THE CONNECTOR OR ASSOCIATED CIRCUITRY. (B) SENSOR TAPE, WHICH CAN BE UNLIMITED IN LENGTH WITH REPEATED CONNECTORS, WIRED TAPS, OR SCALABLE MUX. (C) WITH THE SUBTRACTIVE APPROACH, ONE CAN CUT OUT THE DESIRABLE SENSING AREA WHILE IN (D) ONE CAN PASTE, OR ADD MULTIPLE LINEAR TAPE SENSORS TO MAKE THE SAME SENSING SURFACE. THE DOTTED LINE IN (C) AND (D) INDICATES CUTTING LINES. 63
FIGURE 5.2. AN EXAMPLE OF SENSOR SHEET BEING CUT TO A SPECIFIC SHAPE AND THE VISUALIZATION ITS SIGNAL INPUT READINGS. 64
FIGURE 5.4: A) PROTOTYPE OF A DUAL-LAYER SENSOR (B) WITH OVERLAID TREE AND STAR TOPOLOGIES (A) FOR A 4X4 SENSOR SHEET. THE TREE TOPOLOGY IS PRINTED ON A TRANSPARENT PET FILM. BOTH LAYERS ARE CONNECTED USING 3M CONDUCTIVE Z-TAPE. 65
FIGURE 5.5 (A) SENSOR DESIGN – COPPER ELECTRODE ON POLYESTER SUBSTRATE COATED WITH LOW-TEMPERATURE CURABLE POLYIMIDE. (B) SPIN COATING 20 MM THICK POLYIMIDE ONTO CONDUCTIVE INKJET-PRINTED SUBSTRATE. (C) PRE-BAKE AND CURING ON A HOT PLATE. (D) APPARATUS FOR IV SWEEP MEASUREMENTS WITH 2 POINT PROBE. 68
FIGURE 5.6 I-V CURVE OF A 0.8 CM2, 20 μM THICK FILM AT 58 % RELATIVE HUMIDITY. 69
FIGURE 5.7 (A) CIRCUIT DIAGRAM FOR MEASURING RESISTANCE CHANGE AT A FIXED VOLTAGE. (B) PICTURE OF THE ACTUAL CIRCUIT AND COMPONENTS. THE FOUR PINS ARE CONNECTED TO POWER, GROUND, REFERENCE VOLTAGE AND AMPLIFIER VOLTAGE OUTPUT LINKED TO THE ANALOG-TO-DIGITAL INPUT OF A MICROPROCESSOR. 70
FIGURE 5.8 IMPEDANCE VARIANCE OF 30 K Ω FROM 99% TO 58% RH WITHIN 300 SECONDS UNDER 1.4 VOLTS.. 71
FIGURE 5.9 (A) ILLUSTRATION OF SENSOR TAPE AS A TEMPLATE FOR DIFFERENT SENSOR COATING, WHILE (B) CHANGING THE SENSING TARGET THROUGH MECHANICAL DRAWING, OR DROP CASTING. 72
FIGURE 6.1. TOP LEFT: THE TOP VIEW OF THE SIGNAL PROCESSING PCB MODULE SHOWS THE ELECTRONIC COMPONENTS. TOP RIGHT: THE SURFACE-MOUNT PADS ON THE UNDERSIDE OF THE PCB MODULE, WHICH ARE USED TO CONNECT WITH THE SUBSTRATE BELOW. BOTTOM: THE SUBSTRATE IS MADE UP FROM SENSING TILES LIKE THE ONE SHOWN. THE 2X2 MATRIX OF PRINTED ELECTRODES IS CLEARLY VISIBLE; NOTE THAT THE TOP-RIGHT ELECTRODE INCORPORATES A PATTERN OF BREAKS IN THE COPPER DESIGNED TO MINIMIZE EDDY CURRENTS BECAUSE THE NFC HF ANTENNA IS PRINTED AROUND IT (JUST VISIBLE IN THE PHOTO). THE GSM UHF ANTENNA IS JUST ABOVE THE BOTTOM-RIGHT HAND CAPACITIVE ELECTRODE. 77
FIGURE 6.2. (A) A ROLL OF THE SUBSTRATE WITH MULTIPLE SENSING PCB MODULES FITTED AND (B) A CLOSE-UP OF ONE PCB MODULE. (C) A SINGLE SENSING TILE CONSISTS OF THE SUBSTRATE PLUS THE CORRESPONDING PCB MODULE. 78
FIGURE 6.3. BLOCK DIAGRAM OF OPERATION FOR EACH SENSING TILE. FROM LEFT TO RIGHT, SIGNALS PICKED UP BY THE ELECTRODES/ ANTENNAE ARE THEN FILTERED BY ANALOG CIRCUITS AND FINALLY SAMPLED BY THE

MICROCONTROLLER. EACH MICROCONTROLLER ACTS AS A SLAVE DEVICE TO A MASTER MICROCONTROLLER, WHICH CONTROLLED THE ENTIRE FLOOR VIA A TWO-WIRE COMMUNICATION PROTOCOL..... 79
FIGURE 6.4. BASIC OPERATION OF EACH SLAVE SENSOR UNIT. ONCE AN UNIT JOINS THE I^2C NETWORK, IT ENTERS A LOW-POWER IDLE MODE AND CAN BE INTERRUPTED BY PIEZO PICKUP, RF SIGNALS, OR THE NETWORK (SIGNAL DETECTED FROM ADJACENT UNITS) AND ENTERS PRESENCE SENSING, INTERACTION AND RECOGNITION MODE. 80
FIGURE 6.5. EXAMPLE FOLDING SCHEMES THAT ALLOW WIDER AND NON-FLAT AREAS TO BE COVERED USING A SINGLE PIECE OF THE SUBSTRATE WITHOUT ANY CUTTING OR JOINING. BLUE ARROWS INDICATE THE DIRECTION OF CONNECTING UNITS..... 81
FIGURE 6.6. ACTIVE CAPACITIVE SENSING: ONE OF THE ELECTRODES SERVES AS A TRANSMITTER BY WAY OF A SERIES OF RISING AND FALLING EDGES THAT ACT AS AN EXCITATION WAVEFORM (VSOURCE). THE NEIGHBORING ELECTRODES PICK UP THIS SIGNAL (VC). THE AMPLITUDE OF VC IS PROPORTIONAL TO THE CAPACITIVE COUPLING BETWEEN TRANSMIT AND RECEIVE ELECTRODES..... 83
FIGURE 6.7. FOOTSTEP PATTERNS DETECTED BY ELECTRODES EMBEDDED IN THE FLOOR IN PASSIVE CAPACITIVE SENSING MODE. THE FOUR DIFFERENT COLORS IN THE RIGHT-HAND FIGURES REPRESENT THE SIGNALS FROM THE DIFFERENT ELECTRODES IN ONE SENSING TILE..... 86
FIGURE 6.8. DIFFERENT SIGNATURES TYPICALLY DETECTED WITH THE PASSIVE CAPACITIVE SENSING METHOD. (A) FOREFOOT STRIKE, (B) HEEL STRIKE PATTERN (LEFT FEET), (C) AND (D) MID-SWING BETWEEN STEPS (RIGHT FEET), DETECTED BY ADJACENT ELECTRODES. THE DECAY TIME IS FROM THE RC RESPONSE OF THE ENVELOPE DETECTOR. 86
FIGURE 6.9. (A) THE EFFECTIVENESS OF ACTIVE CAPACITIVE SENSING MODE. (B) SHOWS THE ELECTRODE PATTERN OF A SINGLE TILE, WHERE THE ELECTRODE MARKED BY THE RED DOT SERVED AS THE TRANSMITTER. THE USER WAS BRIDGING TWO ELECTRODES, NAMELY TRANSMIT ELECTRODE (4) AND RECEIVE ELECTRODE (1). (A) THE USER WAS TOUCHING THE TRANSMIT ELECTRODE AND MOVED FROM TOWARDS ELECTRODE (1). THE STRENGTH OF THE SIGNAL PICK-UP IS PLOTTED AS A FUNCTION OF DISTANCE. (C) SIGNAL PICKUP ON ALL THE RECEIVE ELECTRODES AS A FUNCTION OF TIME, AS THE USER REPEATEDLY BRIDGES ELECTRODES (4) AND (1) – SIGNIFICANT SIGNALS ARE PICKED UP BY ADJACENT ELECTRODES (2) AND (3) AS WELL AS ELECTRODE (1)..... 87
FIGURE 6.10. WALKING PATTERNS DETECTED BY SHUNT MODE. DURING EACH STEP, THE USER EFFECTIVELY BLOCKS THE ELECTROMAGNETIC FIELD FLUX, HENCE THE SIGNAL DROP: (A) HEEL STRIKES AND (B) MID-SWING. THE RED DOTS MARK THE TRANSMIT ELECTRODES..... 88
FIGURE 6.11. SIGNALS PICKED UP FROM THE PIEZOELECTRIC SENSORS. RED RECTANGLES MARK THE LOCATION OF EACH SENSOR WITHIN THE SENSING SURFACE. WALKING PATTERNS WERE CONSISTENT WITH THE OTHER EXPERIMENTS REPORTED IN THIS PAPER. NOTE THAT VIBRATION FROM ADJACENT UNITS IS ALSO PERCEPTIBLE. 90
FIGURE 6.12. SIGNALS PICKED UP BY ANTENNAS PRINTED ON THE SENSING SUBSTRATE. (A) NFC SIGNAL PATTERN. THE PATTERN AND SIGNAL STRENGTH OF NFC ARE CONSISTENT AND CAN EASILY BE USED TO DETERMINE RANGE BY MEASURING PEAK THRESHOLDS. (B) GSM SIGNALS HAVE STRONGER SIGNAL RESPONSE THAT CAN INFER LONGER DISTANCE TRACKING BY INTEGRATING AND AVERAGING THE SIGNAL PATTERNS. 91
FIGURE 6.13. (A) SIGNAL RESPONSE VERSUS SENSING UNIT LOCATION WHEN A NFC DEVICE IS HELD 30CM FROM THE SURFACE. (B) ILLUSTRATION OF THE EXPERIMENTAL SETUP. (C) CLOSE UP OF THE NFC SQUARE LOOP ANTENNA PRINTED ON EACH TILE. (D) NFC SIGNAL STRENGTH VERSUS DISTANCE..... 92
FIGURE 6.14. (A) SIGNAL RESPONSE VERSUS SENSING UNIT LOCATION WHEN A GSM DEVICE IS HELD 1M FROM THE SURFACE. (B) ILLUSTRATION OF THE EXPERIMENTAL SETUP. (C) CLOSE UP OF THE TILE GSM ANTENNA. (D) GSM SIGNAL STRENGTH VERSUS DISTANCE. 93
FIGURE 7.1. MOTIVATING SCENARIOS. 98
FIGURE 7.4. FOUR DIFFERENT SENSING MODALITIES SUPPORTED BY PRINTSENSE, IN CONJUNCTION WITH INTER-DIGITATED ELECTRODES. ILLUSTRATED FROM TOP TO BOTTOM: CLOSE PROXIMITY ACTIVE TRANSMIT-AND-

RECEIVE CAPACITIVE SENSING, AC HUM DETECTION (PASSIVE CAPACITIVE PROXIMITY SENSING), TRADITIONAL CAPACITIVE SENSING AND RESISTIVE PRESSURE SENSING. NOTE THAT FOLD DETECTION IS NOT ILLUSTRATED. 104
FIGURE 7.5 PRINTSENSE IMPLEMENTATION, 12 X 24 CM2, 6 BY 7 SENSOR ARRAYS FOR MULTIMODAL NEAR-SURFACE GESTURE CONTACT SENSING. FOUR LARGE ELECTRODES AT EACH CORNER ARE FOR LONGER RANGE HOVERING AND FOLDING DETECTION. THE FSR AT UPPER RIGHT IS FOR GSR PRESSURE CALIBRATION. 107
FIGURE 7.6. PRINTSENSE HARDWARE. 108
FIGURE 7.7. PRINTSENSE SENSING BLOCK DIAGRAM. 108
FIGURE 7.8. COMPARISON OF TOUCH AND PRESSURE DETECTION USING DIFFERENT SENSING TECHNIQUES. NOTICE HOW CLOSELY THE RESISTIVE SENSING TRACKS THE FORCE SENSITIVE RESISTOR..... 110
FIGURE 7.9 A TYPICAL TOUCH INPUT OVER TIME ON A FSR AND A GSR ELECTRODE. Y-AXIS IS THE READING FROM A 10-BIT ADC. 111
FIGURE 7.10 FSR VOLTAGE DIVIDER CIRCUIT USED IN OUR SETUP. RM STANDS FOR THE MEASURING RESISTOR. .. 111
FIGURE 7.11 RELATIVE PRESSURE BETWEEN 5 TOUCH INPUTS AMONG 5 USERS ACROSS TIME. EACH INCONTIGUOUS INPUT IS 1000 SAMPLES WITH DURATION OF 1 SECOND. 113
FIGURE 7.12 RELATIVE STANDARD DEVIATION OF FSR AND GSR INPUTS OVER TIME FOR EACH USER. EACH POINT REPRESENTS THE RELATIVE STANDARD DEVIATION OF A TOUCH INPUT WITHIN 1 SECOND, 1000 SAMPLES... 114
FIGURE 7.13 MEAN VALUES OF THE GSR/FSR RATIO FOR EACH USER ACROSS TIME, WITH ERROR BARS REPRESENTING THE STANDARD DEVIATION OF THAT MEAN. 115
FIGURE 7.14 HISTOGRAM OF RELATIVE PRESSURE (GSR OVER FSR) ACROSS 5 USERS. 1500 SAMPLES PER USER FROM 15 TOUCH EVENTS. 115
FIGURE 7.15. NEAR SURFACE SENSING SIGNAL RESPONSES OF ONE ELECTRODE. 117
FIGURE 7.16. GRASP DETECTION AND RAW DATA ON CURVED OBJECTS. (A) ONE FINGER TOUCH. (B) PINCH – TWO FINGERS INPUT. (C) THREE FINGERS TOUCH. (D) FOUR FINGERS TOUCH. (E) WHOLE HAND GRASP. RAW DATA VISUALIZATION BELOW EACH IMAGE IS FROM RESISTIVE SENSING AND CAPACITIVE PRESSURE SENSING. THE LENGTH AND COLOR BOTH REPRESENT THE LEVEL OF PRESSURE. 118
FIGURE 7.17. USING PRINTSENSE TO DETECT FOLDING. (A) THE BASIC SETUP; ELECTRODES 1 AND 3 ARE ACTIVE TRANSMITTERS. (B) FOLDING OVER THE LEFT-HAND CORNER. (C) FOLDING THE RIGHT SIDE. THE RAW CAPACITIVE RECEIVER DATA FROM EACH ELECTRODE IS SHOWN IN THE BOTTOM ROW. 119

Chapter 1

Introduction

"Ultimately, computers would vanish into the background, weaving themselves into the fabric of everyday life until they are indistinguishable from it. "

Mark Weiser [1] (1991)

The vision of ubiquitous computing and pervasive sensing is to create a world where computers and sensors are embedded within every single item around us to facilitate our lives with critical information and services [1]. Yet, the world is populated with highly complex variety in physical form. Creating an intelligent environment implies redesigning our everyday objects completely with custom-made hardware and software systems to comply with this variety of sizes and shapes.

Nevertheless, the cost of customized high granularity sensing platforms still limits the ubiquity of smart objects. As computer systems move beyond desktop computing and into smart objects, the rigid and planar form factor of traditional electronics remains a major challenge for the integration of sensor hardware into the desired form, size and shape. Creating an inexpensive skin-like flexible and stretchable surface that is covered with sensors has been an area that is well-explored in many different disciplines [2], such as in robotics for surface tactile sensing and navigation [3] [4] [5], in human-computer interaction design [6] [7] [8], in wearable computing as e-textiles [9] [10], and biomedical materials science research [11] [12].

However, most of the studies with accessible manufacturing and off-the-shelf parts are based on traditional electronic components or PCBs, the sensors are of considerable thickness, and restricted in flexibility, and can mandate a

fully customized hardware solution for each specific size and shape. Another disadvantage of traditional printed circuit board fabrication is the lead time when ordering from a PCB manufacturer, or process time from a machine such as vinyl cut copper tape or milling a printed circuit board with a milling machine based on the Roland Modela [13]. Lastly, small quantities of customized circuit boards are costly (based on the spec, the cost can range anywhere between tens to hundreds of dollars). The recent advancements in conductive inkjet printing [14], a low-cost process that inkjet prints a material onto roll-to-roll Mylar that is subsequently copper plated, and conductive inks [15] presents great opportunities to solve the above problems.

The advancement of conductive ink and various printing processes (roll-to-roll printing, desktop inkjet printing ...etc.) allow inexpensive mass production of sensors. This opportunity enables us to create customizable low-cost flexible "sensor sheets". They can also be printed with cheap inkjet printers, enabling small-quantity rapid "sensing" prototyping.

This dissertation focuses on the creation of a research platform for investigating principles and approaches for flexible sensate surface design based on conductive inkjet printing technologies. The collection of work in this thesis is categorized in the following four areas: manufacturing, sensing design, sensing fabrication and sensing applications.

In the *"Manufacturing"* area, I look into and characterize two different types of printed electronics manufacturing methods – conductive inkjet-flex printing [14] and conductive silver nanoparticle ink [15] with an off-the-shelf inkjet printer. The first method has great scalability and bendability, whereas the second method can support small-scaled manufacturing at home.

I investigate user customization in two approaches – 1) Sensing Design and 2) Sensing Fabrication.

In the *"Sensing Design"* area, I explore designing sensors in a computer-aided design (CAD) environment. Inputs are digitally designed as functional patterns, and input size can be scaled like vector graphs. The concept is furthermore demonstrated with the exploration of parametric design. The solution allows users to design functional patterns (sensor inputs) in a CAD environment, and rapidly test and modify their sensing surface cheaply through off-the-shelf inkjet printing. This approach also integrates the aesthetic and engineering design processes of an interactive smart object or environment into the same process.

In the *"Sensing Fabrication"* area, users customize sensate surfaces with physical manipulation, where, unlike the former digital design method, the surface is pre-manufactured with built-in sensing capabilities, shapes and sizes. Users define the outcome of this surface through additive methods (paneling linear sensor tapes), or subtractive methods (cutting a sensor sheet) -the shapes and sensing targets are processed post-manufacturing.

Lastly, I explore the *"Sensing Applications"* area with three techniques for the design of multi-modal sensing –

1) Designing "target-specific shapes" for different sensing targets. Examples include special patterns for specific electric field sensing such as electrodes for capacitive sensing, antennas for Near Field Communication (NFC) and Global System for Mobile Communications (GSM) signal pickup [16].

2) Multiplexing an input electrode with various analog circuits for multi-modal near surface sensing (pressure, touch, folding, proximity sensing). Unlike the previous approach, where a series of patterns are needed, this approach only requires one electrode design, in this case, interdigitated electrodes. The same input is processed with different analog circuitry and can infer multiple physical phenomena.

3) Adding extra layers of chemicals for ad-hoc sensing target alteration. The additive approach (printing) supports adding different chemicals onto the same sensing substrates, which enables personalized alteration of sensing functionalities [17]. Another approach is to "draw" sensing elements such as carbon nanotubes [18] on the sensor substrates and alter the sensing targets.

In this thesis, I strive to combine the field of emerging technologies in the manufacturing of low-cost flexible electronics and the field of sensing and industrial design for human computer interaction. This work can serve as a fundamental framework for the future of rapid sensing prototyping and interactive design.

I envision that, in the future, every printer will come with cartridges beyond just different colors, but also conductive ink and sensing materials as ink. Furthermore, there will be software toolkits that can support users to not only design graphics with clipart templates, but also to design rules, geometries and applications for printing circuits and sensors that are integrated with printed image made from the standard inks.

The following chapter describes the related technology and research in flexible electronics and sensor skin surfaces; previous research on augmenting smart objects with near surface sensing, toolkits for physical computing and prototyping, and lastly, inkjet-printed sensors.

Chapter 2

Related Work

2.1 Flexible Electronics and Sensor Skin Surfaces

The concept of sensate media [19], multimodal electronics skins as dense sensor networks, was introduced in recent years as the future of sensing and networking in smart objects [20] [21]. A sensate surface is ideally scalable and potentially requires less computing power for small-scaled sensing, tracking and interactive applications [22]. Many researchers have developed dense, skin-like sensor systems. The benefits and technological requirements of having sensitive skin devices were first demystified by Lumelsky et al. [3]; they envisioned a new paradigm in sensing and control which would be enabled by a large array of sensors embedded in a flexible, stretchable, and/or foldable substrate that could cover the surface of a moving machine. These surfaces can enable unsupervised machinery in unpredictable and unstructured surroundings.

Figure 2.1 Example platforms for skin-like sensor systems built with rigid PCBs. Left to right: Tribble [23], S.N.A.K.E [24], and Chainmail [22].

Most of the research since has focused on robotic tactile sensing [5], matrices for Human-Computer Interaction [7] [8] [5], and ultra-dense distributed sensor networks [22] [20]. Strategies of peer-to-peer communication, and

computer algorithms for dense sensor network platforms were developed to process the massive amount of information generated via a skin interface. Example platforms from the Responsive Environments Group at MIT Media Lab include the Tribble [23], ChainMail [22], PushPin computing [25].

Sensor skin surfaces also provide various resolutions depending on the sensory density for application-specific requirements. In order to integrate the sensor design into an everyday object, researchers started working on the implementation of sensor arrays on flexible electronics.

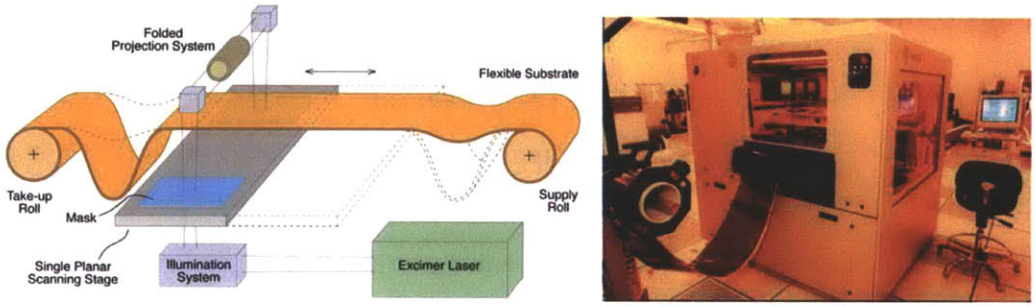

Figure 2.2 Roll-to-roll printing processes, widely used in display connector circuits for providing extra elasticity to the connection while embedding and constraining the back panel [26].

Research in materials and mechanics for flexible and stretchable electronics [2] promise an exciting future in wearable computing and smart object manufacturing, but are still far away from user-customized design

Three major types of manufacturing techniques can be used to fabricate a flexible sensing surface. The first one is fabrication by roll-to-roll processing [2] [15]. Roll-to-roll lithography is capable of very high-resolution conductor placement on flexible substrate materials, but at a relatively high cost. Another manufacturing method for fabricating large-area, low cost flexible materials is additive printing of noble-metal conductors, organic conductors, and even semiconductors [26]. However, the electrical and mechanical characteristics of the resulting materials do not make them an adequate substitute for more conventional manufacturing techniques. The third

approach centers on methods for printing metallic conductors from nanoparticles. These techniques are currently being developed, hence few are yet mainstream. The main contenders appear to be copper-on-kapton substrate (e.g. www.allflexinc.com), conductive inkjet flex technology (e.g. www.conductiveinkjet.com) and metallic nanoparticle inkjet printing (e.g. t-ink.com).

Recent applications of *flexible sensor surfaces* include distributed optical proximity detection such as FlexAura [27], a flexible range sensor based on IR LEDs and phototransistors; Sugiura et. al [10] designed a stretchable tangential force measurement based on measuring IR passing through an elastic membrane; PyzoFlex [8], a 4-layered multi-touch pressure and hover sensing input device that is based on screen-printed ferroelectric material; the unMousePad [7], an interpolating force-sensitive resistor sheet for multi-touch pressure input. However, all of the above approaches require multi-layer construction and special manufacturing tools.

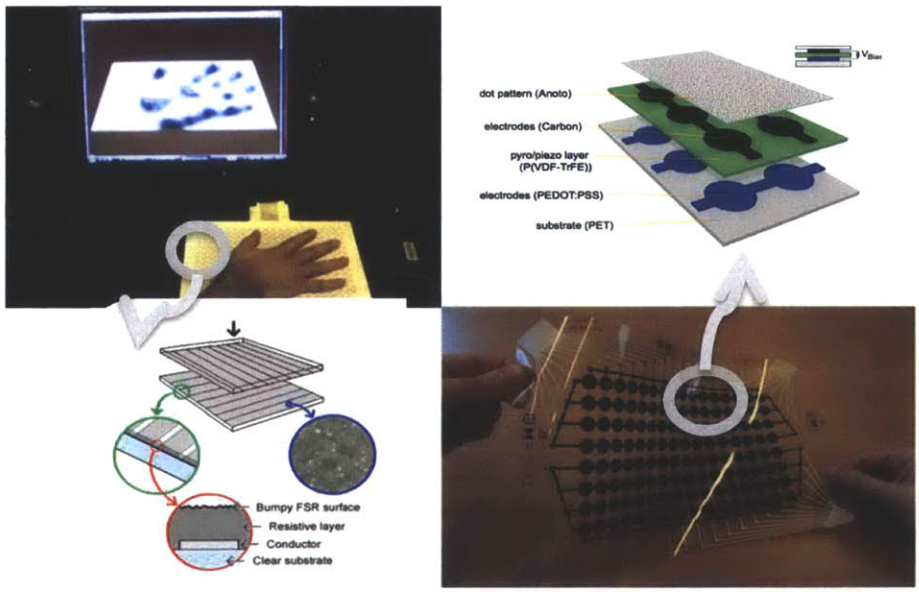

Figure 2.3 Left: UnMousePad - resistive, pressure-sensitive touchbased input device for tracking both touches as well as pens based on Interpolating Force Sensitive Resistance (IFSR). Right: PyzoFlex, a pressure sensing input device that is based on a ferroelectric material. It is constructed with a sandwich structure of four layers that can be screen-printed easily on any material.

There are also linear flexible *sensing strips* such as ShapeTape [28], a 48 x 1 x 0.1 cm flexible rubber strip which measures bend and twist at 6 cm intervals using embeded fiber-optic sensors, allowing the shape of the entire tape to be reconstructed at 30Hz. TactileTape [29] also has a one-dimensional tape form factor, but in this case it senses single-touch input along its length (Figure 2.4). Figure 2.4 (a-c) shows another example of linear sensing structure for touch input that is based on time domain reflectometry for touch location sensing. Time domain reflectometry is originally used in diagnosing cable faults and where a cable is being touched. In this example, Wimmer and Baudish [30] explore how to extend time domain reflectometry in order to touch-enable thin, modular, and deformable surfaces and devices.

Figure 2.4 Left: Modular and Deformable Touch-Sensitive Surfaces Based on Time Domain Reflectometry. Right: TactileTape: low-cost touch sensing on curved surfaces.

Our approach aims at providing a one-layer thin sensor printout without extra hardware components on the surface. The "sensors" can be easily accessible and produced by end users by either ordering conductive ink printing services online or printing at home.

2.2 Augmenting Smart Objects with Near Surface Sensing

The advantage of having a thin layer of printed sensor is the ability to quickly design, modify, and reiterate the shape and size while embedding sensing capabilities into smart objects. Augmenting smart objects with sensing abilities, especially touch input, has been demonstrated on many input

devices for extending interaction capabilities. Mouse 2.0 [31] demonstrated a series of new designs to support the traditional mouse with additional touch sensing on the un-utilized surface. Wigdor et al. presented Under the Table Interaction [32], which explores the design space of a two-sided interactive touch table. Other researchers attempted to capture users' intention by detecting the different ways of implicit grasp inputs as users hold their devices. Examples include Graspables [33], the bar of soap [34], and multi-touch pen for context sensing [35]. However, most of the above examples are all based on planar, non-flexible printed circuit boards. My proposed research can serve as a platform suited to prototyping smart objects for gesture recognition and interaction and enhancing the input capabilities of existing devices. Also, it allows designers and end users to print their desired sensing shape cheaply, which can be folded, cut and integrated with rapid prototyping technologies.

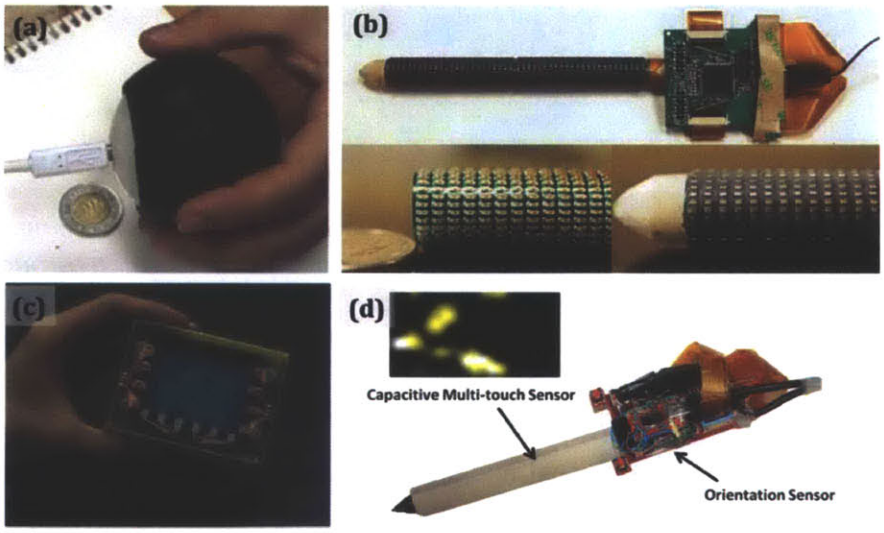

Figure 2.5 (a)The Tango: a tangible receptive whole-hand interface [36]. (b) FlexAura, a flexible near-surface range sensor [27], (c) The Bar of Soap, handheld devices that combine grasp and orientation sensing, (d) Grips and Multi-touch Pen [35].

2.3 Toolkits for physical computing and prototyping

Many toolkits have been developed to support physical computing during the prototyping process. Traditionally, designers use sketches to demonstrate user interface ideas and then prototype, test, analyze and then redesign. Building a customized hardware platform for prototyping design ideas is time-consuming and requires substantial knowledge of electrical engineering and programming.

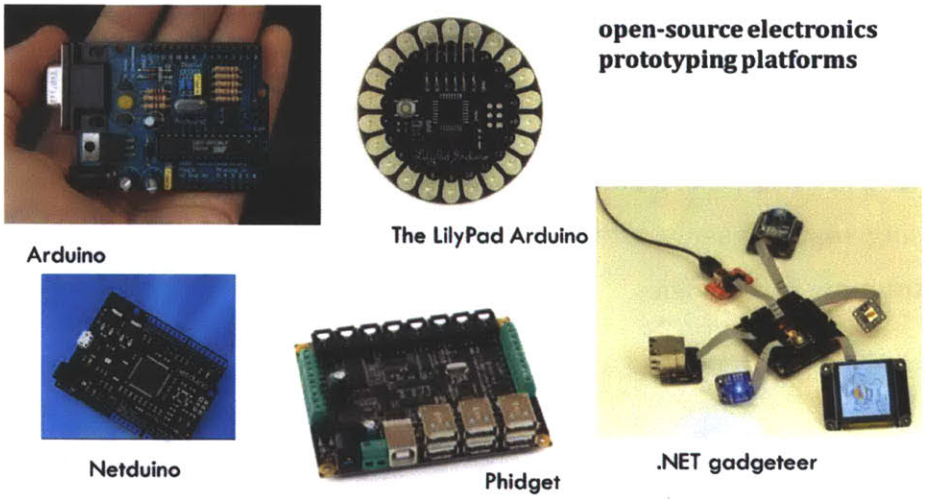

Figure 2.6 Example hardware toolkits for computational rapid prototyping. These open-source electronics prototyping platforms support collaboration through the sharing of personal projects and source codes.

Open-source electronics prototyping platforms like the Phidgets [37], d.tools [38], Calder [39], iStuff [40], LEGO Mindstorms [41] .NET Gadgeteer [42] and Maaestro [43] provide physical widgets (sensor building blocks), and higher level software widgets for a designer to interface and iterate during the design process with little engineering skills required (figure 2.6). The problem with hardware widgets is their lack of flexibility in the function once they are designed and manufactured. For example, a force sensitive resistor (FSR) is commonly used for pressure input. However, the size and the shape of each FSR cannot be changed easily. The design decisions need to be made based on the limited sensor selection that is available in the market.

To solve the physical constraints with existing sensors, prototyping toolkits such as Midas [44], Sketch-a-TUI [45], Drawing the Electric [46], and commercialized products like Makey Makey [47], were developed to enable end users to fabricate custom capacitive touch sensors to prototype interactive objects. The problem with most toolkits is that they are disconnected from the design and the fabrication process.

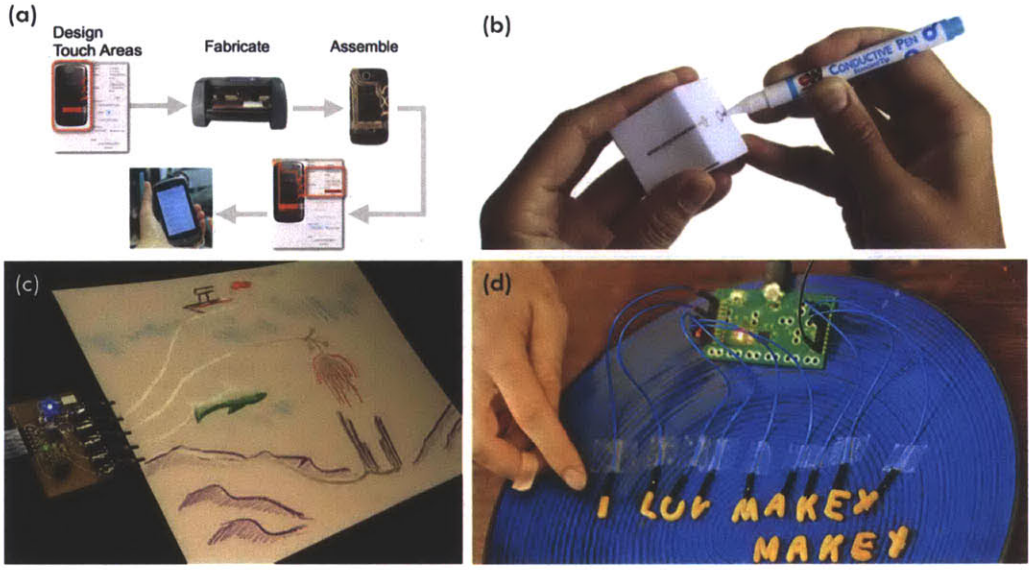

Figure 2.7 Toolkits for prototyping interactive objects. (a)Midas, (b) Sketch-a-TUI, (c) Draw the Electric, (d) Makey Makey.

An inkjet-printed sensor design approach not only provides a fast prototyping sensing surface, but also emphasizes the integration of functional elements with industrial design practice (designing sensing inputs as graphics), as well as different techniques for physical constructions (through cutting and folding). It is also more scalable and reproducible than the handcraft approach, since the files can be scaled, shared and re-printed easily.

2.4 Inkjet-Printed Sensors

To realize the vision of flexible electronics and sensate surfaces, every single component needs to be printed, including sensors, components such as

transistors [48], batteries [49] and even memory arrays [50]. Figure 2.7 is an artist's illustration [50] of the future of flexible electronics, where a sensor tape integrates pressure, acceleration sensors, electronics for signal processing, memory, and a thin film battery. This compact, standalone sensor tape can be attached to a helmet, for accessing the possibility of brain injuries.

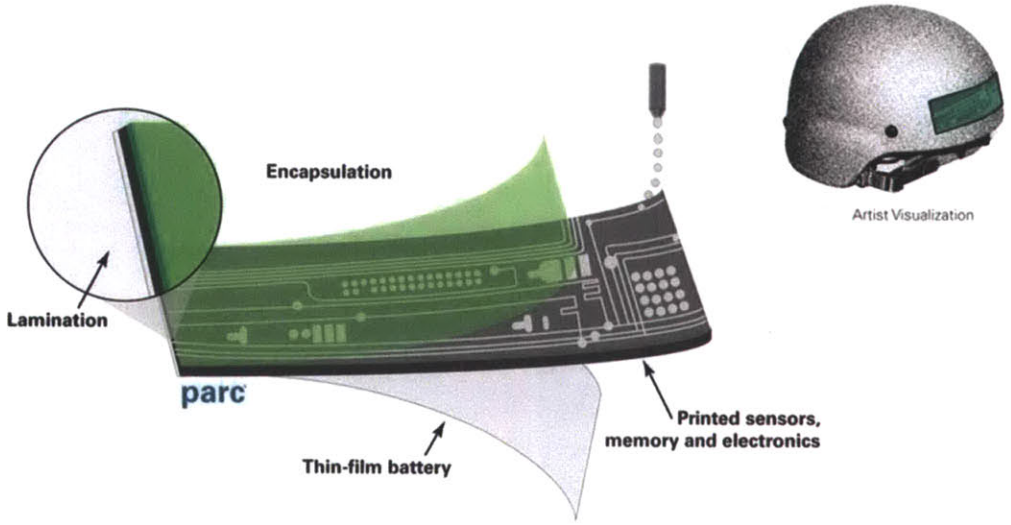

Figure 2.8 Illustration of a flexible printed sensor tape for diagnostics of mild traumatic brain injury. The sensor tape integrates pressure and acceleration sensors, signal-processing electronics, non-volatile memory, and a thin film battery [51].

In this dissertation, I am interested in low-cost processes that not only can support large-scaled deployment, but also be used for rapid sensing prototyping. Therefore, the following examples of related work are focused on making sensors with inkjet printers. Many researchers developed their experimental platforms based on materials printers such as the Dimatix Materials Printer from Fujifilm [52]. It enables the deposition of fluidic materials on an 8x11 inch or A4 substrate, utilizing a disposable piezo inkjet cartridge. Figure 2.9 shows an example of gas sensors printed on a paper substrate with the materials printer. Vyas et al. demonstrated inkjet-printed and self-powered wireless sensors for environmental, gas, and

authentication-based sensing [53]. Another example is Sensprout [54] from Kawahara et al. that integrates an antenna, a soil moisture sensor, and a leaf wetness sensor with a RF energy harvesting antenna.

Figure 2.9 Left: SenSprout: inkjet-printed soil moisture and leaf wetness sensor. Right: RFID tag modeule designed on flexible substrate, with inkjet-printed single wall carbon nanotubes (SWCNT) film as a load.

This dissertation provides an infrastructure for the design and application of printed sensate surfaces, through the combination of the functionalities of printed sensors and various design approaches.

The next chapter describes the characteristics and material processing of two low-cost inkjet printing technologies that are used in this dissertation.

Chapter 3

Manufacturing: Conductive Inkjet Printing

Two manufacturing technologies are selected as experimental platforms in this thesis: 1) Conductive Inkjet Technology (CIT) in Figure 3.1, a two-step electro-less plating process that plates copper on Mylar substrate (http://www.conductiveinkjet.com/). 2) Off-the-shelf desktop inkjet printing (Figure 3.2) with conductive silver nano particle ink on polyester film or resin coated paper (Silver Nano Particle Ink from Mitsubishi Paper Mills Limited - http://www.mpm.co.jp/).

The first technology offers good flexibility, strength and conductivity of circuitry that is unlimited in length with the roll-to-roll process. However, the machines is not accessible by end users and, although the turnaround can be prompt (e.g. two-three days), it takes time for ordering and shipping. Whereas the second technology, off-the-shelf conductive ink printing, only requires users to purchase the ink and can operate with a cheap inkjet printer. Although this method has the disadvantage of less flexibility (the chemical sintering process provides less mechanical strength between conducting particles) and about 2 times lower conductivity, the manufacturing time is the speed of normal printing on a sheet of paper, which provides users with instant feedback on their designs.

Table 3.1 presents properties comparison between these two technologies. Both methods have reasonable sheet resistance for basic circuits, and both print on PET substrates. The conductor is electroless plated copper metal for inkjet flex printing and Silver nanoparticles for conductive ink. It cost about

3-10 times more to print with CIT printing since the price is based on size, instead of materials used from the vendor. The thickness of conducting material is thicker for Inkjet Flex printing, which is beneficial both in conductivity and physical strength against bending. Since the conductive ink printing technology is based on chemical sintering between the ink and the resin coating on the paper, depositing more layers of ink will not make the conducting layer thicker, whereas in a deposition process, the thickness of the conducting layer can be easily controlled by reaction time.

	CIT Printing	Inkjet printing with conductive Ink
Sheet Resistance	20~50 mΩ/□	110mΩ/□
Substrate	Melinex 339, White PET	Resin coated PET film
Conductor	Electroless plated Copper Metal	Chemical sintered Silver nano-particle
Cost	~$10 USD for A4 size	$4 USD for A4 (solid), $0.8 USD for A4 (20%)
Thickness	220 μm	0.75 μm

Table 3.1 Properties comparison between Inkjet Flex Printing and Conductive Inkjet Printing with Silver nanoparticles.

The two complimentary processes in this dissertation are presented in different projects based on the suitability of each application.

3.1 Conductive Inkjet Technology (CIT)

Conductive Inkjet Technology is a two-step process to create solid copper circuitry directly from digital files (Figure 3.1). The first step is inkjet printing patterns with a catalytic ink through a roll-to-roll process (Figure 3.1(a)). The printer is cable of printing in 360 dpi (< 250 um feature size) and

sheet resistance of 20~50 mΩ/□ on a Mylar substrate that is 280 mm in width and unlimited in length. After the first step, the rolls with catalytic patterns are immersed in an electroless plating solution to deposit solid metal onto the desired pattern (Figure 3.1(b)). The process additively creates circuits; therefore the ink and metal are only deposited where required by the design. Compared with the subtractive method of traditional circuit fabrication processes, which etch unwanted material, this approach produces smaller a waste stream and environmental footprint. Figure 3.1 (c) shows an example circuit with components attached to the flexible circuit printout with low-temperature solder or conductive adhesive.

For applications such as navigation of a flexible display, we could replace copper with ITO (Indium tin oxide) on transparent polymers to produce a transparent layer of circuitry, which is a common technique for OLED displays [20]. This process provides a consistent conductivity between folding and bending.

Figure 3.1 CIT printing technology with 2 stage additive process. (a) Stage 1, inkjet printing (360 dpi) with onboard UV and IR curing. (b) Stage 2 - electro-less copper plating. (c) Example flexible circuit with copper traces on Mylar substrate.

3.2 Off-the-shelf Inkjet Printing with Silver Nanoparticles

The primary disadvantage of the CIT printing is the lead time. Like most PCB manufacturing methods, once you design the circuit, there are a few days of manufacturing and shipping time.

The second process we explored is printing conductive traces with silver ink and an off-the-shelf inkjet printer. We adapted conductive silver ink from

Mitsubishi Paper Mill and print conductive traces on paper. The sheet resistance is 0.11Ω/□, $8*10^{-6}$ ohm-cm, with a thickness of 0.75 um. The printing is a chemical sintering process and the sheet resistance reaches steady state after 5~10 minutes, depending on the paper. Although this process has less durability to bending, printing with an off-the-shelf printer presents great advantage in rapid prototyping.

It is a chemical sintering process that reacts with polyester film or resin-coated paper. In our experiment, we replaced the ink cartridge (Figure 3.2(b)) of an off-the-shelf inkjet printer (Brother DCP-J1 40W), and by fine-tuning the print setting; we were able to produce conductive Silver traces with the same quality of conductivity compatible with CIT. The advantage of this technique is having the ability of rapid prototyping on your desktop. Also, it is possible to combine the printout with colored pigments and even sensing materials to have a multi-modal sensor sheet manufactured in the same process.

Figure 3.2 Conductive Inkjet printing with off-the-shelf printing and conductive silver particle ink. (a) An example inkjet printer with silver nano particle filled ink cartridges. (b) Silver nano ink and replacement ink cartridges. (c) Example printout from Mitsubishi paper mills limited.

3.3 Component Attachment Techniques

One of the major challenges of replacing traditional PCB substrates is the component attachment techniques. Traditional PCB technology is based on glass-reinforced epoxy laminated sheets with conducting traces. The

materials have great thermal & mechanical properties and are optimized for reflow soldering processes. For the two flexible circuit printing technologies we explored, both use PET film as substrates. PET has a low melting point and is not compatible with traditional soldering techniques. Here, we present the two component attachment techniques for PET substrates.

The first technique is soldering with low-temperature solder. This technique utilizes existing soldering infrastructures and is compatible with the copper on Mylar circuitry. We used EFD SolderPlus D500 series [55], which is a $Sn_{42}Bi_{58}$ Low Temperature Solder Paste. This solder paste alloy has a eutectic point of 138 °C, which is lower than the melting point of PET films (~260°C). However, this technique does not work with the Silver nanoparticles circuit, since it burns through the resin coated film easily.

Figure 3.3 Component attachment with low-temperature solder paste and a solder paste dispenser.

Another issue is the mechanical bonding force between the components and the conductor traces. Tin and Bismuth in the low temperature solder paste ($Sn_{42}Bi_{58}$) both has poor mechanical strength and the bonding force is weaker than traditional Lead or Silver based solder.

The second method for component attachment is using Conductive Adhesive Transfer Tape from 3M (3M Z-axis conductive tape 9703) [56] that is designed for attaching Flexible Printed Circuits (FPC) to traditional PCBs.

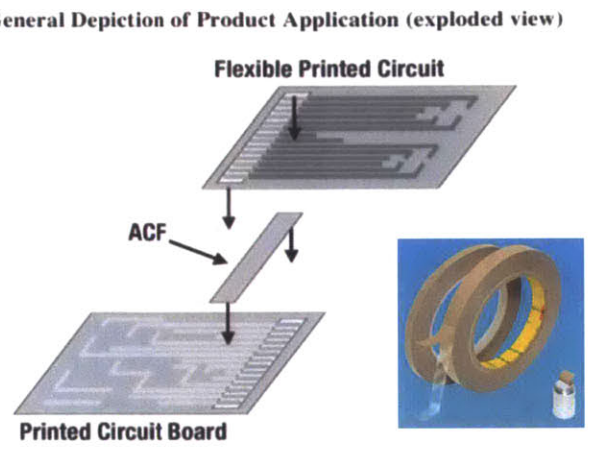

Figure 3.4 Illustration of the conductive adhesive transfer tape from 3M [56].

The tape is a standard adhesion pressure sensitive adhesive (PSA) transfer tape with conductive fillers (silver particles) enabling connectivity through adhesive thickness (the Z-axis) between substrates. The insulation resistance in the plane of the tape is around 3.4×10^{14} Ohms/square and the contact resistance is < 0.3 ohms.

For attaching fine pitch components, the minimum gap between conductors is 15 mils (0.4mm) and the minimum overlap area is 5000 mil^2 (3.2 mm^2).

The disadvantage of this attachment method is the high cost of this material. However, since it is like any adhesion pressure sensitive adhesive tape, one can easily remove and reattach components onto the substrate without damaging the substrate and traces. This presents a great way for solder-less rapid prototyping. The next chapter describes how we utilize the combination of graphic and sensing design aspects for the making and development of interactive surfaces.

Chapter 4

Sensing Design:

Computer Aided Design for Customization

The previous chapter describes the experimental platforms for conductive inkjet printing technology and flexible printed sensor sheets. The strength of this technology is the high flexibility of graphical and physical design and rapid prototyping. This presents a great opportunity in user customization. To that end, I use music controller interfaces as an example to show the possibilities of combining graphics, sensing, and musical interaction design.

This chapter describes music control sensate surfaces, which enable any musical instrument to be outfitted with a versatile, customizable, and essentially cost-effective touch and gesture interface. The first part of this chapter describes a sensate music controller surface based on conductive inkjet printing technology, and the second part describes an exploration that combines color pigments and silver nanoparticle ink to produce a fully-customized, parametrically designed music controller surface that is aesthetically-driven with an off-the-shelf inkjet printer.

The last part of this chapter describes a capacitive sensing controller toolkit, which allows users to define and assign inputs and outputs through the hardware interface. The high dynamic range capacitive sensing electrodes not only can infer touch, but near-range, non-contact gestural nuance in a music performance. With this sensate surface, users can "cut" out their

desired shapes, "paste" the number of inputs, and customize their controller interface, which can then send signals wirelessly to audio effects or software synthesizers.

I seek to find a solution for integrating the form factor of traditional music controllers seamlessly on top of one's music instrument and meanwhile adding expressiveness to the music performance by sensing and incorporating movements and gestures to manipulate the musical output. We present an example of implementation on an electric ukulele and provide several design examples to demonstrate the versatile capabilities of this system.

4.1 Motivation and Related Works

For decades, researchers have been working on exploiting alternative input devices to develop new electronic music controllers with intuitive interfaces and ways to enable people to play synthesizers [57]. Controlling sound with more expression but less complexity has long held the interests of musicians, especially in live performances. A common problem among many music controllers is the lack of a general interface that is specifically designed for integrating and simplifying different playing modes, especially with traditional instruments.

One of the major challenges for an understaffed live performance is to multitask on stage between controlling switches, knobs, effects, pedals and, at the same time, focus on musical expression. Our first music controller project seeks to provide a customizable wireless music controller surface that can be easily adapted by musicians and seamlessly integrated with any existing music instrument.

Our goal is to create a skin-like sensate surface, which allows users to build their desired controller without changing the geometry of their instruments. We believe that this approach is an efficient and cost-effective method to

create a user interface for music since our platform is highly adaptive and can, in practice, be custom-designed by users.

Musical instruments, especially traditional acoustic instruments have long been designed with high visual aesthetic [58]. This is still a strong practice with guitars [59], which are even now adorned with any manners of compelling artwork. This project brings such aesthetic visual adornment into functional electronics skin laminated onto the instrument that responds to the nuance of touch anywhere on a surface, much as biological skin does.

To demonstrate this, we used an electric ukulele as an example and developed circuit implementations and patterns tailored for specific contact or non-contact musical gestures. We printed different designs and explored how the addition of integrated instrument effect controllers could benefit a live performance and how it is possible to have an electronic surface that can add something to the aesthetic to a musical instrument. Besides sensing basic control signals, we also explored the possibilities of embedding sensors in areas where extended hand gestures during a performance can be detected and then use that information to contribute expressiveness to the musical outputs. Studies have been conducted [60]of ancillary gestures musicians make during performances that are not related to sound production over surface can also measure some of these and exploit them in making the instruments sound more expressive.

Performing live on stage and simultaneously using various controllers has never been an easy task. Although the days of manipulation of knobs and switches from racks of synthesizers or arrays of stomp boxes [61] are now replaced by touchscreens on tablets and laptops, it is still not easy to switch back and forth between a traditional instrument and a software interface. It can also be challenging to modify an existing instrument, since the shape design is commonly optimized for acoustics and playing. Figure 4.1(a) illustrates movements frequently required during a regular performance. Our motivation is to create a sensate "skin" for extra control inputs, which

allow musicians to implement their desired sensing components on the surface of their instruments and replace extra movements with additional control inputs (figure 4.1(b)).

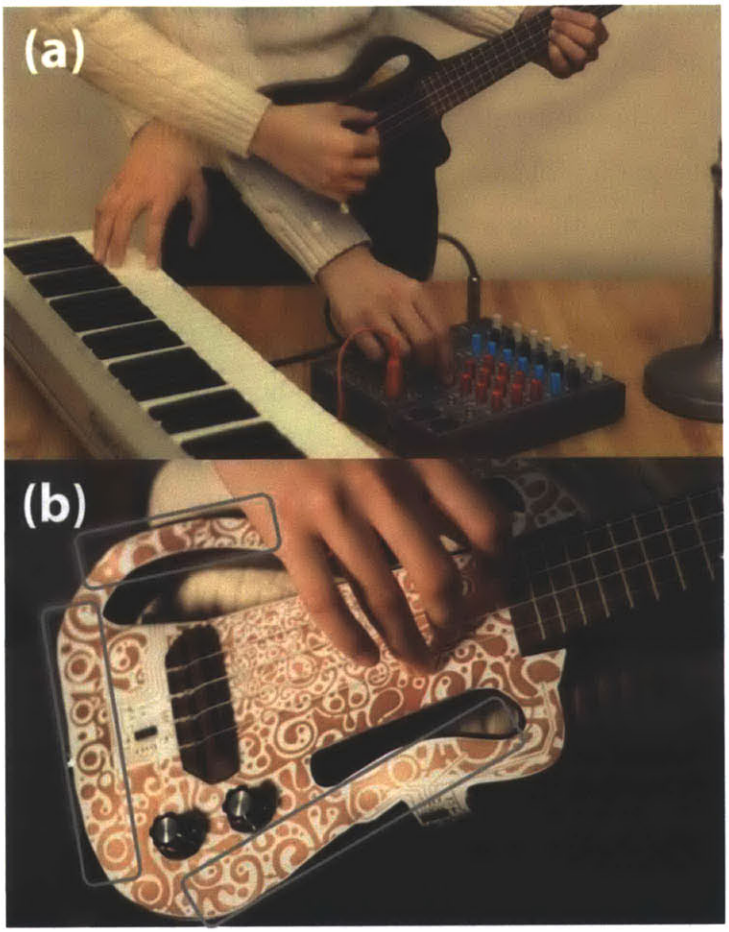

Figure 4.1. (a) Example of extra movement required between instrument and music controllers. (b) Implementation of our system with additional guitar control inputs to send the most commonly used commands and minimize needed finger motion for the extra control during a live performance.

Previous work related to adding extra control through embedding sensing components into musical instruments for alternative control including the Starr Labs "ZTAR" [62], a guitar-like digital instrument with a touch sensitive fingerboard, string triggers, hotkeys and a joystick, Stepp's DG-1 analog guitar synthesizer [63]; or Donald Buchla's Thunder percussion controller, which replaced keyboards with flat pressure and position-sensitive capacitive touch plates [64]. These examples demonstrate the potential of

extending the possibilities in music expression through additional tactile sensing components and creating new ways to interact with digital control. However, there is no existing option for an average user to implement such sensing capabilities besides purchasing control surfaces like a Korg Kaossilator as a building block (more kludging) or attaching an iPhone or button bank to their instrument. Examples of players trying to integrate a touch interface on top of their instruments are shown in Figure 4.2. These indicate that touch screens are not enough to support the need of musicians, mainly because they are not shapeable or conformable; a standard row/column touch screen can not bend across the instrument's body or accommodate the many holes and irregular boundary,

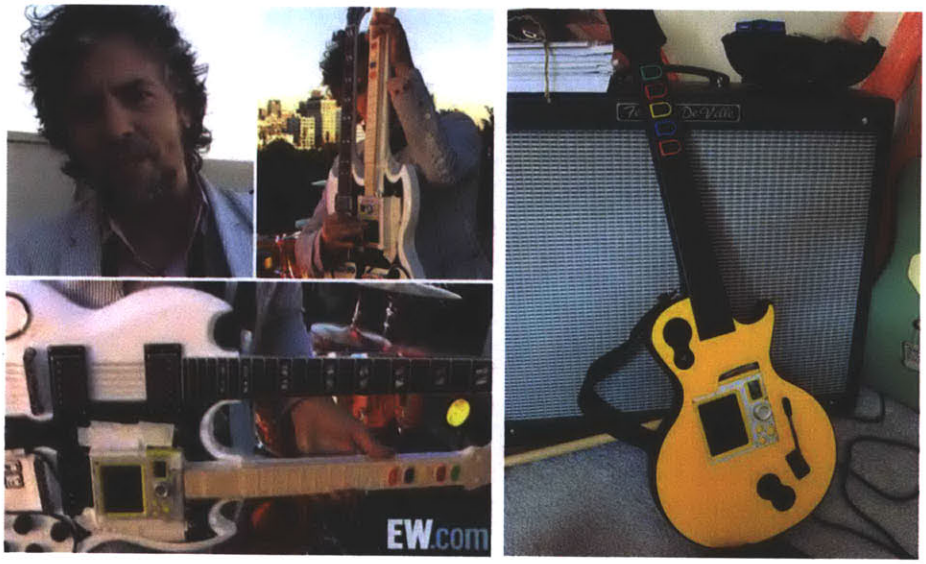

Figure 4.2 Left: Wayne Coyne of The Flaming Lips [65], and Right: DIY Korg Kaossilator guitar [66].

The goal of this approach is to extend a musician's prized instrument in an elegant way without changing its original shape and. Inspired by the Chameleon Guitar [67], a hybrid acoustic and digital instrument with a replaceable acoustic resonator that preserves the traditional acoustic values while capable of digital manipulation abilities, we attempt to create a printed sensate overlay that preserves the physical shape and properties of an established instrument. Because of its popularity, its accessible, relatively

flat and compact body, and the ability myself to play, I used an electric ukulele (Eleuke SC-100) as an example to demonstrate the possibility of adding more controlling capabilities to a relatively flat playing surface and explored its potential impact on future live performances. Figure 4.1(b) shows one of the implementations of our design.

Previous works on building pressure-sensitive surfaces with printed FSRs and capacitive sensing as a generic surface for musical expression include Koehly et al. [64], and Jones et al. [68]. In a recent example, Freed & Rowland made an aesthetic multi-electrode conductive pattern into a distributed speaker "browsed" with a handheld magnet [69]. These novel sensing surfaces were designed as new instruments for playing music. Our design, however, is not purposed for serving as a standalone musical instrument. Our surface is built specifically for increasing the expressiveness of an existing instrument. The interaction includes pressing, hovering and sliding. Technical details will be described in Chapter 7, where I summarize all the near-surface interaction techniques that I explored.

The next section includes two music controller surfaces that I built. The first example was in collaboration with fellow Responsive Environments Group RA, Nan Zhao. We designed three patterns with "blocks" as inputs, and the inputs are mapped as on-off buttons and sliders. The second example is the Zebra skin, in collaboration with fellow Responsive Environments Group RA, Amit Zoran, utilizing parametric design principles for creating an aesthetically-driven surface that allows the users to clearly see different control regions that will become more intuitive and nuanced via practice. Each user can develop their unique hand movement and gestures to perform expressively.

4.2 A Customizable Sensate Surface for Music Control

4.2.1 Functional patterns as inputs

We built a sensate surface controller prototype and provided three design examples on an electric ukulele for the reasons described above. The surface detects gestures, hovers and touches and transmits signal intensity and location via Serial communication to a software host on a connected computer, which then converts the signal into MIDI messages. These MIDI messages were mapped, based on the location of the gesture, to control signals such as tap tempo, pitch, distortion or simpler commands like volume change or record/stop.

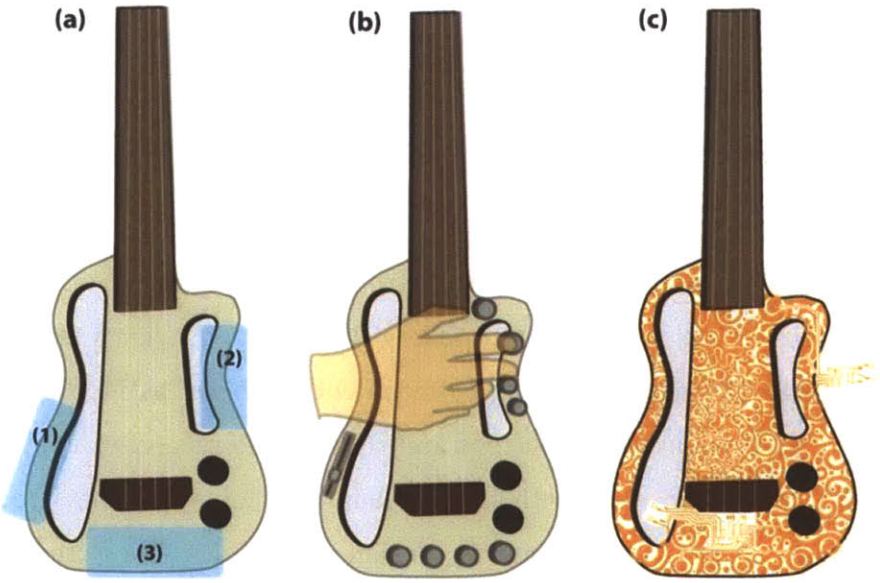

Figure 4.3. (a) Potential spaces (blue zones) for extra control inputs. (b) Illustration of traditional implementation of additional control inputs (c) Control surface design pattern with the same effect as (b) without physically changing the original instrument.

Our design principle is to embed extra control input ability in spaces that are normally too small or not suitable for implementing extra components, such as knobs and sliders. Figure 4.3(a) is an illustration of different potential

areas for adding control inputs onto our example instrument. Based on the gestures commonly used in playing this instrument, the three zones are mapped to different functionalities in our design. Figure 4.3(b) shows how extra control inputs could be implemented in a traditional design, and we demonstrate that the same functionality could be achieved with an aesthetic or decorative sensate surface input in figure 4.3(c).

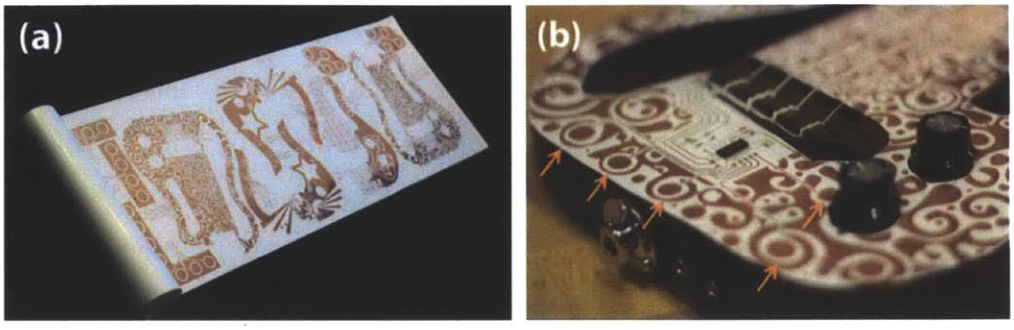

Figure 4.4. (a) Printout of our example designs. (b) Capacitive sensing buttons (indicated by orange arrows) and associated circuit with surface mount components (CY8C20) attached to the flexible surface.

There are two parts to the hardware design. First, we generate a flexible sensate surface printed with sensor patterns and limited components for capacitive sensing. And second, a PCB is needed for data processing and wireless communication. Our prototype sensate surface is based on printing copper patterns onto a thin plastic substrate using conductive inkjet printing technology [14]. With this technology, it is possible for us to print complex conductive patterns for electromagnetic field sensing [17]. The total cost for our design per ukulele is less than 10 US dollars (~$7 for the printing and ~$3 for components). The sensing method is capacitive sensing, which in this implementation relies on Loading Mode – measuring the capacitance change between a human hand and a metal electrode. By measuring the time between several charge and discharge cycles, the distance of a user's fingers from the surface can be inferred. While it is possible to attach surface-mount components directly to the surface with low temperature solder or conductive adhesive, this process takes more time and the mechanical

connection is not as strong as regular solder joints. Therefore, we minimized the components required for the flexible surface and only placed the critical parts, which are the capacitive sensing circuit and connections for communication with the microcontroller. Figure 4.4 (a) shows the printout of our example designs and figure 4.4(b) shows the surface mount components attached to the flexible surface.

We implemented a CY8C20x CapSense capacitive sensing IC from Cypress semiconductor, which is capable of supporting up to 28 CapSense I/O touch channels with two-wire communication (TWI) protocol and 16 bits of resolution. The device address of a CY8C20 can be changed manually, which allows multiple CapSense slave devices on the same bus. The device uses a seven bit addressing protocol where the last bit in a byte indicates read or write. This means there can be 27 addresses on the same TWI bus line – a total of 7168 (28 times 256) inputs, if designed properly. Also, this device supports two different filtering methods to reduce noise from different sources - the DTS (drop the sample) filter to discard samples acquired while data communication takes place, and the averaging filter to improve CapSense system noise immunity.

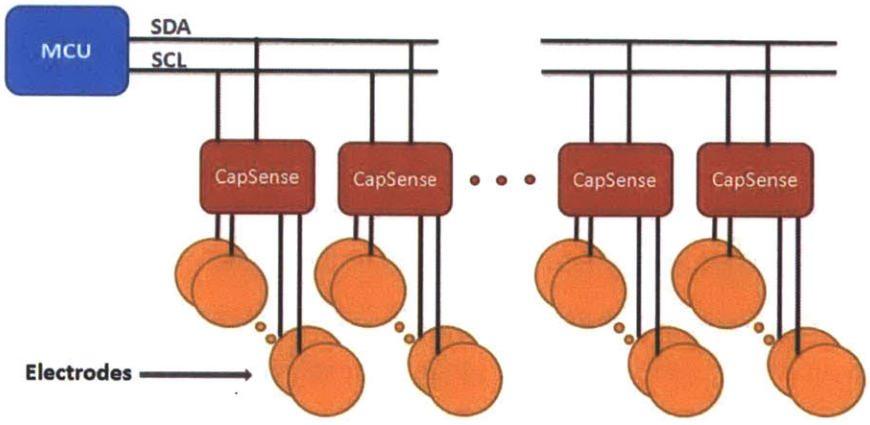

Figure 4.5. Connection details about the controller circuit. The microcontroller unit talks to the capacitive sensing chip with a two wire communication protocol, which allows many input devices to be communicating on the same bus.

For the PCB part, we used an off-the-shelf ATmega 328P (http://www.atmel.com/) development board with an 8 MHz external oscillator and Bluetooth radio chip (RN-42) from Roving Networks (http://www.rovingnetworks.com/). We wanted to design a modular and highly adaptive system that allows the sensate surface customization to be versatile yet intuitive for novices with minimum wiring. Therefore, we selected sensor ICs that support two-wire communication where only 4 connections were needed between the PCB and the flexible surface – power, ground, data (SDA) and clock (SCK). Once the capacitive inputs are triggered, data is transmitted to the host microcontroller, then processed locally and transmit to software, which converts sensor information into MIDI signals according to the mapping design. In our study, we used a MIDI library from Processing.org and sent MIDI commands to Propellerhead Reason 6.0, a digital music synthesizer platform, to generate sound and create a mapping to trigger effects and change the pitch and modulation of our instrumental input (Figure4.6).

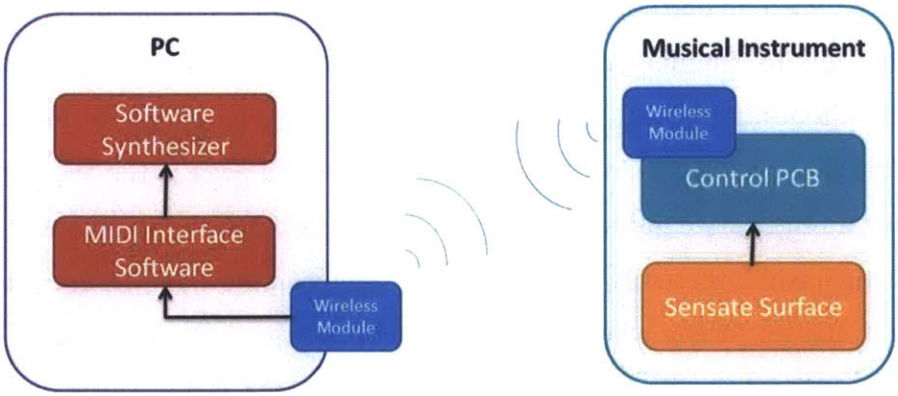

Figure 4.6. System block diagram – The main hardware is attached to a musical instrument or essentially any object. A sensate surface communicates with the control circuitry, which talks to a wireless module. The other end of the wireless data transmission sits on top of a computer, which parses and passes the information to MIDI interfacing software. The software then sends MIDI messages to a software synthesizer.

4.2 Mapping Strategies

The mapping strategies depend highly on the application and physical construction of each specific instrument and the location where sensor units are placed. Here, we discuss mapping strategies, both from the physical and signal point of view. Again, we used a ukulele as example to explain the relationship of sensor placement, hand gestures, and output mapping.

4.2.1 Mapping Strategies - Physical Mappings

Our mapping strategies are designed for demoing the variety of sound effects that can be achieved via on-body control surfaces for a stringed instrument such as a guitar or a ukulele. The pattern construction was built around three zones that have different impacts on gestures, such as finger picking or strumming. These three areas are termed trigger area, movement area and command area (Figure 4.7). The trigger area includes the most commonly covered right hand movement - ranging from strumming patterns by rhythm guitarists to fingerpicking from playing bluegrass-style banjo music (where clips are worn on one's thumb, middle & index fingers, and one or two fingers rest on the instrument). In this area, the sensor inputs are mapped to pitch and modulation control, so the player can either change the sound or add modulation while plucking the strings. The second area is the trigger area. During a finger style guitar performance, players pluck the strings with their fingertips, add fingernails, and rest their thumbs on the side. We use this area as the trigger area, where precise controls are made to trigger loops, instruments or pre-composed tracks. The last area is the command area, which is less likely to be triggered accidentally during a performance. In this area, we place inputs that have critical functions, such as "play", "record", "stop". In the mapping design, we also considered the possibility of detecting extended hand gestures during a performance and how to use that information to add expressiveness to the musical outputs. One of the advantages of capacitive sensing over pressure sensing is that we can detect

proximity. Therefore, it is possible to map non-contact gestures, such as strumming, to beat generation. In our first prototype, we did not design patterns specifically for sliders. Instead, we post-processed the data on the software end and were able to map a continuous motion trajectory from the button inputs to a slider motion. Besides sliders and buttons, inputs for continuous velocity or aftertouch (pressure sensitivity) control are also very important for musical expression. Therefore, a layer of elastic silicone was included on top of copper pads in our design as a way to generate continuous pressure-mapped control. The distance between one's finger and the copper pad (the distance between two conductors) is controlled by force applied on the silicone. A similar technique was applied in another musical example dating to the 70's; the Alles keyboard at Bell Labs [70] used capacitive proximity sensing to detect the height of each key continuously as it was pressed, and an elastomer at the bottom of the key's range turned the height measurement into pressure there.

More details about system setup and signal conditioning are provided in the evaluation section. In our experiment, we used one set of button arrays (as shown in the later section) and invited users to mount the sensors on their instrument based on their preferences with a preset mapping to our software synthesizer. The four buttons in the movement area are mapped to distortion, echo, reverb, and one bass note. This sensate surface can be applied to essentially any instrument, and our mappings are designed only for demoing one of the many possibilities. In the next section, we will describe the process of customization and the toolkit we created.

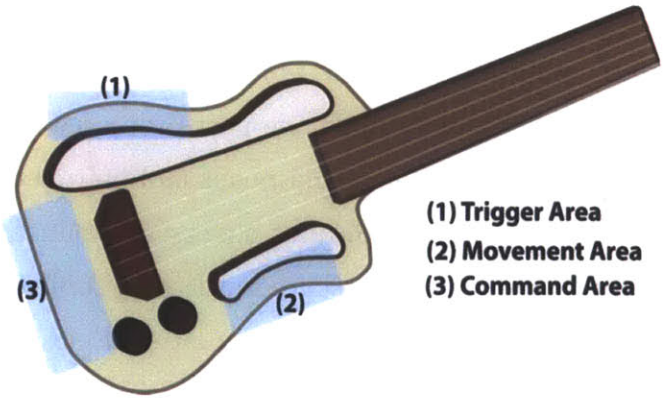

Figure 4.7. Potential mapping on a plucked string instrument based on gestures such as finger tapping, picking and strumming.

4.2.2 Mapping Strategies - Signal Mapping

The basic transduction principal of our design is capacitive sensing. With inputs from the capacitance variance between a user and the sensate surface, we were able to detect nuance of one's gestures. Our signal mapping experiment validates all the possibilities (button, sliders ...etc) of the uniform-shaped copper. Our attempts include push buttons, sliders, activity triggers, free gestural pattern recognition, and pressure sensing with a thin layer of elastic material placed on top of the sensor surface.

Proximity

There is a broad range of possible gestures, for example drawing gestures, waving, or other hand or finger gestures. We focused on one specific example, which is a finger near-far gesture based on proximity sensing in a close range above the sensor surface. Similar to the slider, the distance between the hand and the sensor surface could be mapped to velocity, aftertouch or other parameter to which a given audio effect responds to. The expressiveness of the gesture distinguishes the class of effects that are suitable for this type of control. The disadvantage of proximity control is the lack of haptic or tactile feedback and reproducible precision, but this is less of an issue for such basic expressive control.

The capacitive sensing surface in push button mode detects touch. A simple touch could trigger or toggle a preset effect. The control is simple and requires little attention from the player. Since the activation does not take any force, the player can gently tap the surface, swipe over it, or do any movement that is natural during a performance to make a contact. A software de-bounce was implemented in the capacitive sensing chip design in order to decrease the sensitivity and noise.

Pressure

As mentioned earlier, adding a layer of elastic material on top of the sensor surface creates an effective pressure sensor. In our experiment, we used silicone as an input pressure array. An advantage of this sensing method is the natural haptic feedback that the elastic material affords. It requires higher motor control attention compared to a simple pushbutton and therefore should be mapped to suitable effects or placed in an area where one finger is naturally resting.

Activity trigger

In this mode, capacitive sensors not only detect a simple touch but also take the duration or rate of change into account for more expressiveness and a higher degree of control. A leaky integrator model, most commonly used as a simple IIR low-pass filter or data smoother, for example, is an appropriate mathematical model compatible with an acoustic instrument, hence well-suited to controlling audio dynamic effects [71]. The more energy that is put into the system, the higher the value of the integrator, thus the higher the volume of an instrument or the more brittle the timbre. Hence, if no energy is added to the system, the value of the integrator will decrease to zero within a certain amount of time depending on the leak rate (k).

$$y(n) = k \cdot y(n-1) + x(n)$$

Where $0 < k \leq 1$ governs the decay of the integrator, n is the time index, y is the output and x is the input. The input value for the leaky integrator could be the duration of touch. In this case, the output value will increase linearly or follow any predefined function. As described in the button mode, a touch motion is easy and does not distract the player. If the rate of change is used as the input, small movements, tapping, or sliding motions will activate the sensing surface. The frequency and intensity of the motion defines the rate of increase of the integrator value. This value should be limited and a low pass filter could be used to smooth the signal.

In this case, the player has a higher freedom of control, but executes a more complicated movement, therefore the sensor should be placed in a convenient area where the control motion could integrate with the strumming or tap motion. The movement integral, for example, could be used in order to activate an effect during strumming, which increases with the strumming frequency or intensity.

Slider

A slider, in this environment, consists of multiple sensor pads placed next to each other, where we detect the transition of the finger between adjacent pads. Measurable parameters are finger swipe direction, position and speed. Pixelated capacitive sensing sliders are normally designed in a chevron shape (Figure 4.8), which produces a more continuous, accurate and robust sensory output then an array of simple buttons. In our case, we mapped a sliding motion to a series of evenly distributed input events taking place on an array of capacitive sensing pads. One can also make a continuous slider out of only two nested triangular electrodes [72].

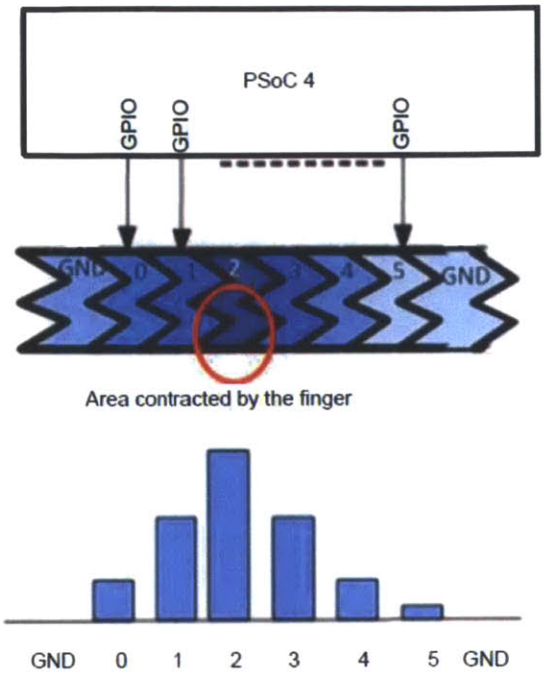

Figure 4.8 Design reference of a linear slider [73]. Top: sensor electronics. Middle: chevron-shaped input electrode array, Bottom: electrode signals for finger at red region above. The slider position is given by the distribution's centroid.

4.5 Customization

Since the process of printing flexible circuits is similar to using a printer, it is possible to draw the circuit the same way as drawing with any graphic editing tool that allows you to export a bitmap file. We invited users to design their control surface with the same process as creating an artwork with Adobe Illustrator. We provided design guidelines and several circuit layout images required to process capacitive sensing signals, control LEDs for indications and to connect to the PCB for data transmission. Our hope was to not only enable people to implement a sensor circuit on their instrument, but also to have them design an artwork that is aesthetically appealing.

Figure 4.9 shows the three different designs. Figure 4.9(a) is a design with whole body coverage and has sensor components covering all three interactive zones. Figure 4.9(b) and (c) are designs for partial coverage - (b) includes only the trigger and the movement area, while (c) covers the

command and trigger area. Two of the designs, (a) and (c), placed the circuit on top of the surface while (b) hid all the wiring and components in the back, by folding them on the Mylar sheet. The advantage of having shorter traces is to reduce the risk of broken connection due to folding, especially when some of the stress points were designed very close to surface mount components, which can easily cause connection issues. The disadvantage was having less space for touch inputs.

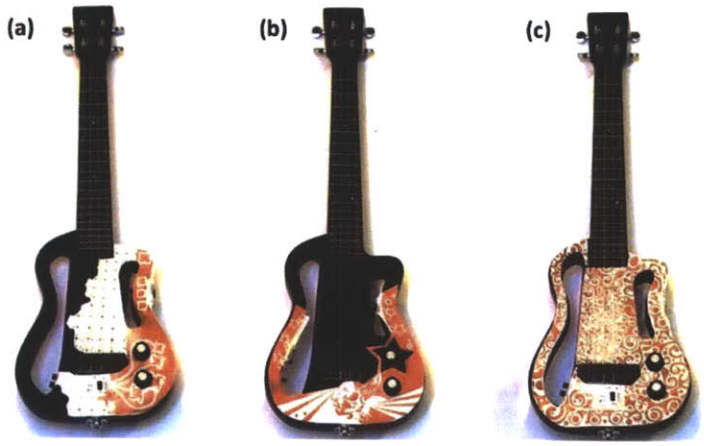

Figure 4.9. Three example designs for different coverage and input locations.

The combination of graphic design and circuit design creates a new art form that allows each sensate "skin" controller to represent the music genre that this controller is mapped to. We envision a musician with a "wardrobe" of different surface controllers that are interchangeable, similar to switching between effects or synthesizer racks or conversely, the manufacture can hard-glue an array of such skins onto the same "vanilla" instrument design, allowing user to pick an instrument with their style the way a consumer chooses a shirt in a different pattern.

In order to realize the idea of DIY music skin controller, I started the exploration of off-the-shelf inkjet printing with conductive silver ink. The manufacturing equipment setup is less than $100 USD for the printer, and we are able to design, iterate and modify patterns and manufacture things easily with the speed of normal inkjet color printing. The section below describes

the Zebra Skin, the first prototype I built in collaboration with fellow Responsive Environments Group RA, Amit Zoran. The cost of each Letter size print is ~$2 USD.

4.6 The Zebra Skin

Traditional music instruments are beautiful objects. Great effort is often put into both their aesthetic presentation as well as sound quality. Modern sensing technology, however, can enable the instrument's decoration to also serve as an expressive controller. For example, circular patterns can be rotary controllers, stripes can serve as multi-touch triggers, solid shapes can sense non-contact gesture and pressure, etc. What was only for beauty now becomes sensate. To explore the intersection between visual and auditory understanding and performance, we developed a music controller surface that covers an instrument with parametrically designed conductive patterns. The patterns function both as decoration and control inputs. A player learns to express through physically sliding, tapping, and pressing into the surface, or bridging patterns for more dynamic effects.

The development of the Zebra Skin started with the experimentation of conductive inkjet-printed patterns as sensor-input controller surfaces with off-the-shelf inkjet printers. By combining color pigment and silver nanoparticles in inkjet printing, we are able to create an aesthetically-driven sensing surface that is part of the music instrument itself, while also functioning as a controller. Adapting parametric design, the sensing patterns are generated computationally. We demonstrate the creation of a controller surface for an electric ukulele. One can learn to play it over time, as a user associates hand movements in different places with different kinds of effects and sounds. Each custom pattern allows players to "see" what they "hear" as they sculpt their timbre by touching and gliding, mix signals through touches with multiple fingers, and physically remap the properties of sonic interaction in the computer software.

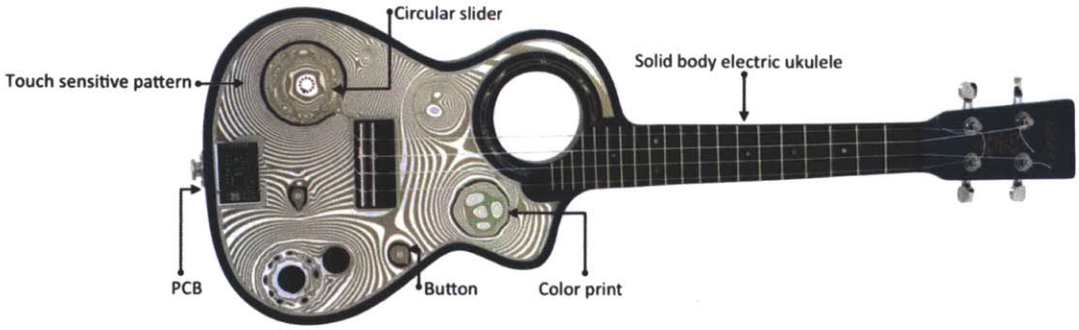

Figure 4.10. An example of inkjet-printed conductive patterns for physical manipulation of electric ukulele signals. All features on the surface can generate responsive control signals with touching, bridging, and hovering.

There are four components in this system: 1) parametric graphic design of patterns, 2) sensing interface printout through an inkjet printer (Brother DCP-J140w) with conductive silver ink, 3) a custom-made hardware interface for sensing communication with a computer, and 4) software (MAX/MSP) for computer music generation.

4.6.1 Parametric Pattern Design

The pattern is parametrically-designed in Grasshopper (a plug-in of Rhino). We defined surface boundaries and force vectors manually before using Grasshopper's Spatial Deform function to render a manifold for the visualization of a smooth field (maximal points and associated gradients were built into the field at the location of each significant controller nexus). This surface is then sliced using Level Set with a constant height (Z), generating a set of contour lines as shown in Figure 4.11. A few manual steps are further required to connect the traces to form control regions and define additional color prints. Once the regions and patterns were designed, we assigned regions of interest as functional inputs (buttons, sliders...etc) as shown in Figure 4.10. Another approach for parametric designed surfaces is, for example, auto-routing space filling curves with attraction-repulsion rules and predefined knots or centers to define particular controller locations.

To mark the regions visually, we add another layer of color printing to include graphic details and boundaries. We also excised several regions with a laser cutter to preserve and reveal the original instrument design, as well as designing sharp edges that can be naturally felt, hence help to guide touching fingers. The entire surface is a controller - even 'dead traces', such as decorative islands, can be bridged by one's fingers for dynamic performance effect.

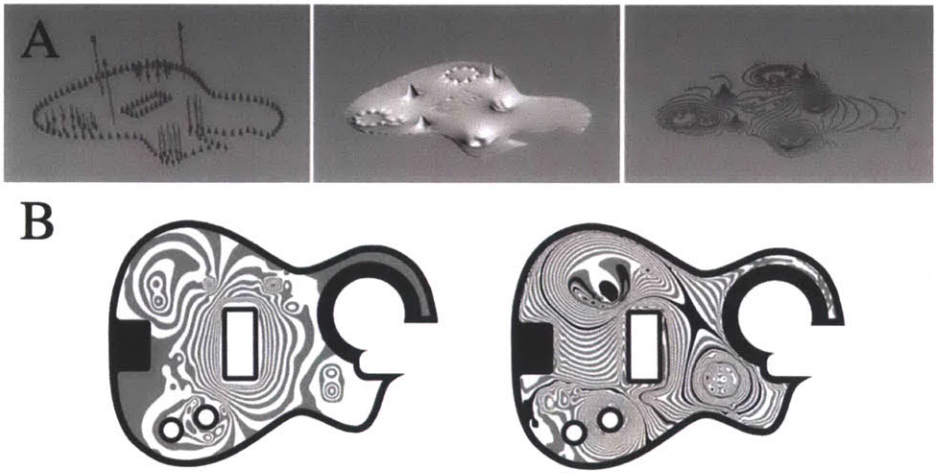

Figure 4.11. Design process: (A) from vectors to contours, (B) two examples of patterns designed with different force vectors.

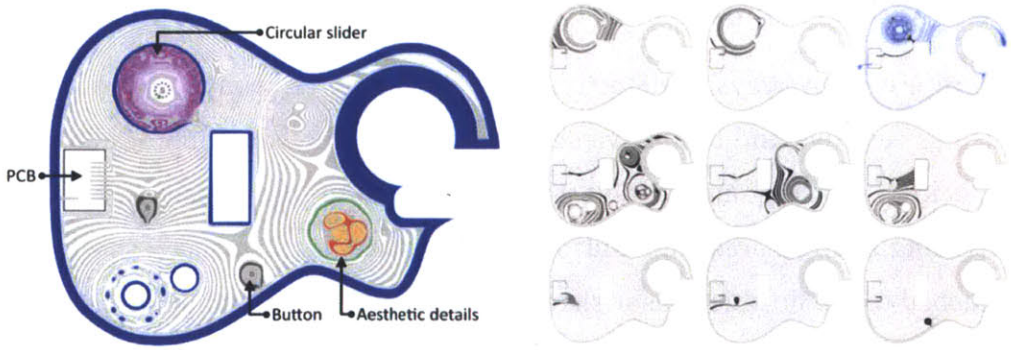

Figure 4.12. Different regions in the force vector field are defined as functional inputs such as buttons, sliders, etc. Left: complete design, combining with colored pigment. Right: Connected regions of each input.

4.6.2 Rapid Prototyping with Conductive Inkjet Printing

The process we explored is printing conductive traces with silver ink and an off-the-shelf inkjet printer (Figure 4.13(B)). We adapted conductive silver ink from Mitsubishi Paper Mill and printed conductive traces on photo paper or PET films. With this fabrication method, any iteration of the sensing surface only takes less than 5 minutes to construct. More details about the characteristics of conductive inkjet printing techniques will be covered in Chapter 7.

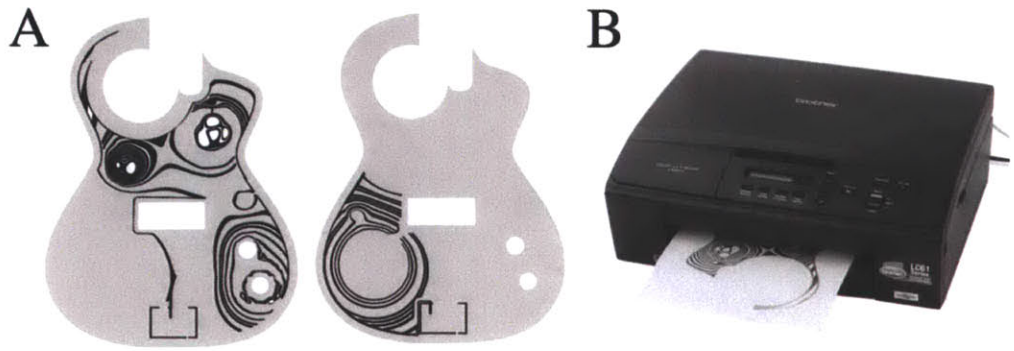

Figure 4.13. (A) Two examples of tracing continuity in sub-patterns, (B) the printing process.

4.6.3 Hardware Interface for Sensing and Communication

There are many ways to detect varying signals on the conductive patterns, such as resistive and capacitive sensing. In our implementation, we adopted capacitive sensing and added expressiveness to the music control by including sliding, pressing, and proximity to the performance. The PCB is attached to the flexible sensor sheet through signal pads at the bottom of the board with the 3M 9703 z-axis conductive tape. Nine separate input control channels are implemented across our current pattern.

4.6.4 Signal Mapping

The last component is the computer music software, which generates the sonic output of our sensing surfaces. We use Max/MSP as our experimental platform and implemented effects that are mapped to the patterns and buttons that control inputs such as echoing, overdrive, delay, and distortion.

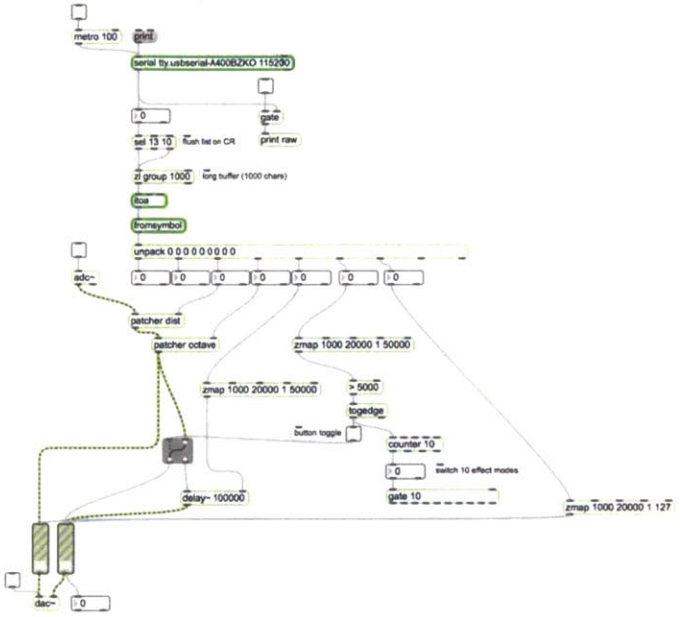

Figure 4.12. Example Max Patch for the Zebra Skin Interface.

Combining sensing-enabled objects and flexible conductive printing, our work serves as a platform for prototyping aesthetic graphic sensing input with high accuracy and reproducibility. Our platform explores the unification of compelling graphics and expressive input devices - a promising way of creating a new form of art that intimately combines graphics, interaction, and music.

4.7 Hardware toolkit for user customization

Although we envision a set of software tools to make this endeavor simpler, the complexity of drawing, mapping and routing these controller surfaces can now be difficult and time-consuming. Therefore, our future work is to

develop a software toolbox for optimizing the sensor design (such as trace proximity constructed for reducing extraneous pickup or crosstalk or eliminating short circuits), which allows any musician to draw out the basic shape and customize their desired patterns for their own control surfaces. The design should be able to be integrated with anything in one's environment or be laid on top of any object with a minimized signal to noise ratio (although noisy substrates such as LCD panels may require a rear gravel or driven shield, and conductive substrates can affect the sensing range, hence may need to be similarly adapted together with customized gain adjustment). To test the basic principle and generalize the design, we constructed two different patterns as a basic development kit, along with the circuit, for easy implementation and evaluation. As shown in figure 4.15, we printed out a series of buttons for touch inputs and the associated circuits.

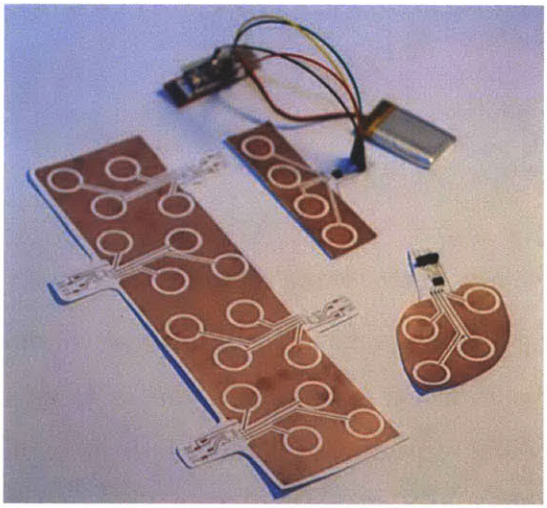

Figure 4.15. Toolkit for basic implementation. Two design patterns were made. Each battery-powered unit, as seen in the back, can transmit sensor data wirelessly though Bluetooth.

Users can cut out the desired number of buttons and sculpt the shape of their control surface, then reuse the rest for other applications. The sheet of circle patterns in the front Figure 4.15 is part of a continuous long sheet of sensors. Our vision is to build a library of sensor patterns and have them arranged on the same large sheet or surface, which can fit into essentially any design

requirements. We believe this technique can not only allow a user to reconstruct a controller panel for their software synthesizer, for example, but it also provides an opportunity for a user to physically reconfigure their software effect racks in a physical way through cutting and folding (see chapter 5).

Here, we report the capability of our system operating under various types of input conditions. We intended to explore the variation of finger touch input control that can be achieved with one generalized pattern design. In figure 4.16, we demonstrated four kinds of inputs - proximity, button, pressure sensing and activity triggering.

The first type of mapping strategy (Figure 4.16(a)) is for proximity sensing. Depending on the sensitivity settings of the capacitive sensing chip, we can modify the range from few millimeters to ~3 centimeters. Too much sensitivity, however, will induce noise and cross-talk between different input pads. Here, our setting is approximately 0.5 cm. Figure 4.16(b) illustrate inputs (directly touching the pads) that were mapped to button presses. Signals were clean with a steep slope and fast response. The detection range can be adjusted dynamically by changing the settings on the capacitive sensing IC (through sending I^2C commands from the microcontroller).

It is easy to create an on-off control like a button. However, for music performances, control inputs normally come with a dynamic range of adjustment. The method that is common for a software synthesizer rack is a re-purposable array of knobs, which provide a wide range of dynamic control. Hence, we use an array of pressure/proximity sensors. In order to produce a smooth input, we fabricated a silicone cover for our test button array. The addition of a layer of silicone on top of copper pads acts like a buffer and gives us information about pressure. We demonstrated improved signal range, with silicone cover, which was smooth and showed nice correlation with pressure in Figure 4.16(c). This input is ideal for mapping virtual knobs in a software synthesizer for expressive control.

Figure 4.16(d) shows raw signals from activity integration (red line) and output value (black line) after being processed by a leaky integrator. The output value was determined by activities on the sensor while playing, and had a variable decay rate based on the chosen k value (leakage rate, see equation 4.1). This control method provides similar output as a pressure sensor, but responds to dynamic motion with fast response time and more accurate control. The disadvantage of this method is the need to swipe one's finger on top of the sensor pad, unlike a pressure sensor where you can rest your finger on top of a certain point. Applications for finger style guitar performance would most likely have a pressure sensor input for the thumb location where one can adjust the sound easily by applying different pressure without moving the finger, and user integrated motion over some other parts of the guitar.

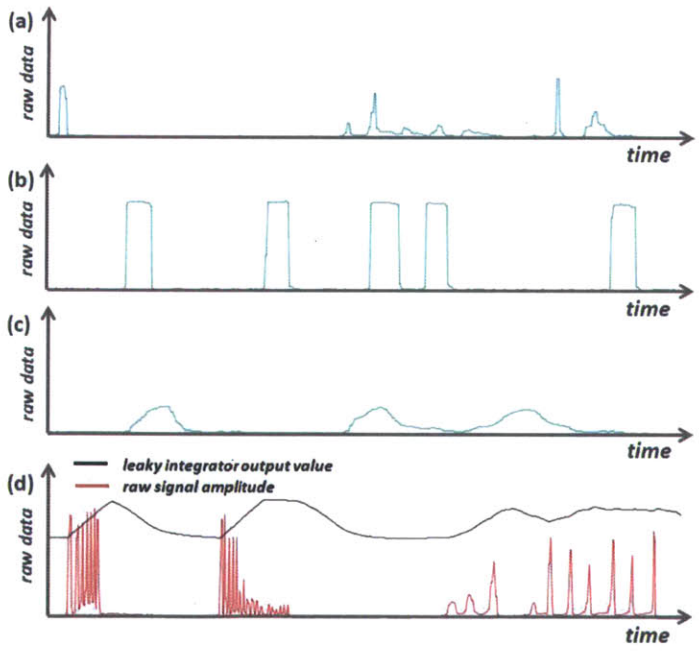

Figure 4.14. Data plots from four different signal mapping strategies – (a) proximity, (b) button, (c) pressure, (d) activity integration.

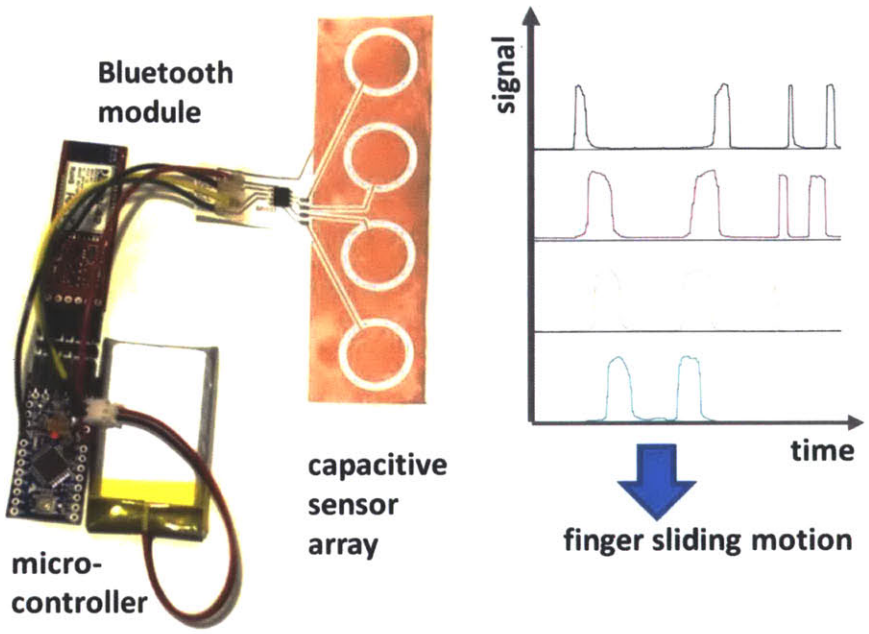

Figure 4.15. Our modular test setup – an array of buttons connected to a battery-powered microcontroller module that transmits data wirelessly. The figure on the right shows input signals from sliding one finger along the sensor array.

The last example in our signal mapping strategies is mapping for sliders. Figure 4.15 shows our test environment – a 4-pad sensor module attached to a battery-powered microcontroller and Bluetooth module to send the capacitive input signals wirelessly. One the right is the sensor data for those four input pads. In this test, we tried to use the four pads as a slider. Our user slid one finger across the surface back and forth from the top pad to the bottom pad. The signal that comes from the motion is clean and robust and can be easily mapped to software button presses or a slider when the four pads are grouped adjacently (without implementing the standard slider chevron shape), although that form could be also accommodated.

4.8 Conclusions

In this chapter, I presented two novel music control sensate surfaces based on different conductive inkjet printing technologies, which enable customizable integration to any musical instrument with a versatile and cost-

effective user interface. My goal is to provide design examples and corresponding physical mapping strategies for different finger techniques for plucked string instruments, with an aesthetic and functional conformal sensate skin adhered to the instrument body. To provide a more flexible way for fast implementation of a basic setup, I designed a DIY capacitive sensing toolkit and software interface for this system and provided five different signal mapping strategies– button, slider, activity trigger, proximity and pressure sensing, from the same pattern design. I demonstrated the usability and showed data from those five different modes and invited musicians to play and give us feedback on the mapping strategies.

My main interest lies in developing a system for producing new forms of performances and instruments through empowering musicians with the ability to improve, modify, and extend the capabilities of traditional instruments. Future work includes creating more sophisticated toolkits with multiple sensing modalities and better capacitive sensing capabilities (such as sensing for longer range or adaptive range), and program a software toolbox which will allow users to drag and drop sensor inputs to create the link to MIDI signals for software mapping and synthesizer manipulation. I used music controller surfaces as an example to demonstrate immediate control and sonic feedback. Many other areas can benefit from this principle, such as natural user interface design, interactive media and smart objects.

The next chapter is also about customization, but instead of using the software-driven, graphical design approach, we focus on different physical, tangible manual manipulation of sensate structures such as a linear sensor tape, or a planar structure for folding, cutting, and pasting.

Chapter 5

Sensing Fabrication:

Physical Manipulation

Chapter 4 describes examples of customizable sensate surfaces with emphases on their graphic design. The shape and pattern of the sensate surfaces are pre-defined in the computer to match the size and functionality of the instrument. The outcome is decided before the manufacturing process. In this chapter, I present two projects that focused on making sensate structures – a "smart sensate sheet" as a "functional material"- instead of an application specific input device. These "materials" are functionally specific and can be physically manipulated to match the desired shape and size. Based on the concept of digital fabrication, we explored what we termed "additive" and "subtractive" manufacturing approaches with linear "sensor tape" for adding, and "sensor sheets" with a redundant wiring design for subtracting. The following sections describe these two different approaches and our proof-of-concept prototypes.

5.1 The Making of Sensate Structures for User Customization – Cuttable Sensor Sheet and Sensor Tape

The purpose of designing our sensate "material" is to be able to provide users the freedom to physically manipulate the shape and structure of the sensate sheet through cutting, pasting or folding, without the need of pre-designing the shape or patterns beforehand. Such sensor sheets have an advantage in

custom, complex-shaped surfaces, since the sheet can be cut into the desired shape directly. Figure 5.1 (a) shows an example of a sensate surface. Figure 5.1(c) is an illustration of cutting a sensor sheet into another shape. To assure that all the electrodes are still connected, we developed two different types of wiring scheme and applied redundant wiring by combining different topologies, and increased robustness within each topology through forward error correction design [74]. However, the scalability of a pre-designed sensate sheet is constrained by the spacing between electrodes and the density of wiring. There is a limit to the size of the sheet and the ratio of electrode to wiring area needs to remain low for error free operation.

The other method that we explored is creating a linear structure as "sensor tape" and use an "additive" manufacturing approach to cover the surface area. Figure 5.1(b) shows the basic construction of a sensor tape. The green box indicates the circuit board, and the length can be as long as the roll-to-roll process permits. With this approach, users can "paste" different tape structures physically together to achieve the same final shape as cutting (Figure 5.1(d)). Although the associated circuitry may seem higher than the sensor sheet approach, the scalability is high when it comes to a large area-coverage sensing space.

Each input (indicated by squares) can be assigned or physically modified with specific sensing targets (e.g. sensing materials can be deposited atop the electrodes or sensors can be attached with conductive tape or low temperature solder). The basics are capacitive sensing and resistive sensing through interdigited patterns, which require no additional materials. The following sections describe details of each manufacturing approach, and discuss design approaches for the adaptability and scalability of those methods.

In conclusion, a sensor sheet subtractive approach has the advantage of fast prototyping, and perhaps, less "post-manufacturing" time, since the input space is pre-determined. In comparison, the additive approach of a sensor

tape requires more manual labor, components and time. In smaller-scaled production, it is more efficient to use the subtractive approach, but for a large-scaled application, an additive approach should be more scalable. Both work in most scenarios, and a mixed approach can support any complicated design.

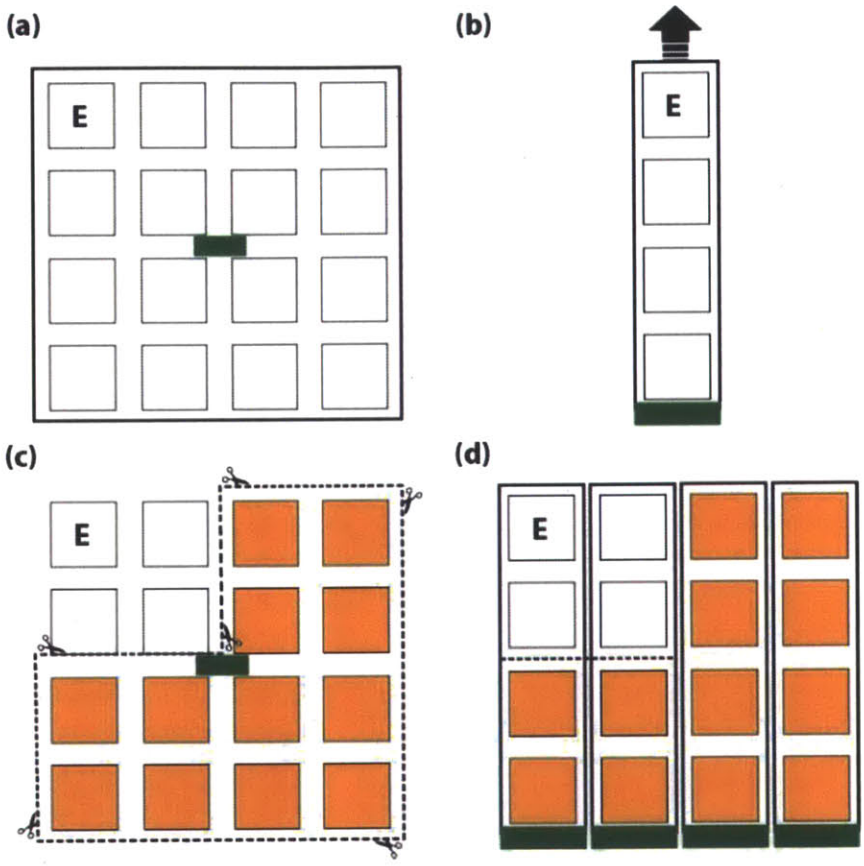

Figure 5.1. (a) Sensor sheet - the green block represents the connector or associated circuitry. (b) Sensor tape, which can be unlimited in length with repeated connectors, wired taps, or scalable Mux. (c) With the subtractive approach, one can cut out the desirable sensing area while in (d) one can paste, or add multiple linear tape sensors to make the same sensing surface. The dotted line in (c) and (d) indicates cutting lines.

5.2 Subtractive Manufacturing: Cuttable Multi-touch Sensor Sheet

To explore the design principal of subtractive sensor sheets, I started a collaboration with Simon Olberding and Dr. Jürgen Steimle from the Max Plank Institute of Informatics, Saarbrücken, Germany, about the development of a cuttable multi-touch sensor material [74]. This project focused on the technical principles for a printed capacitive multi-touch sensor, which the user can physically tailor by cutting to the desired size and shape. These principles make the circuit layout more robust against physical cuts and removed areas, taking inspiration from topology in biological systems and computer networks, as well as from coding theory.

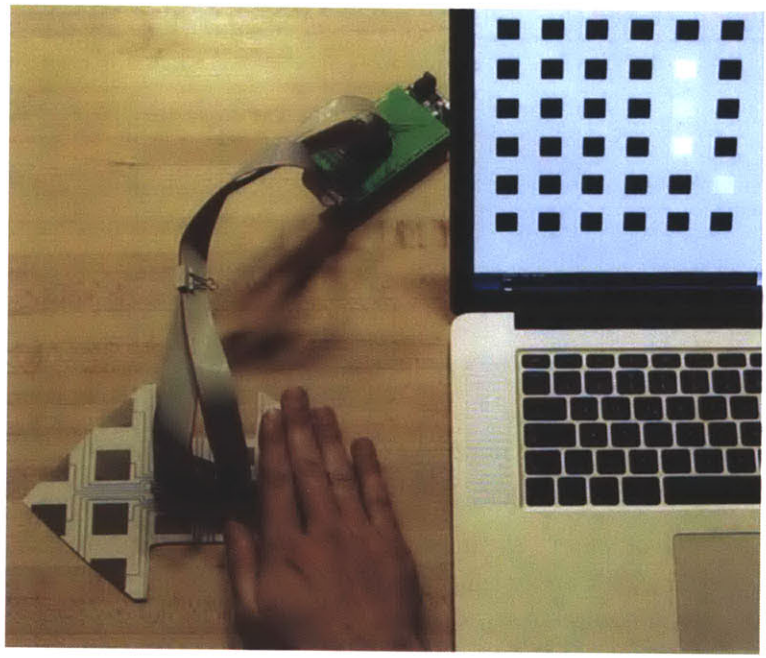

Figure 5.2. An example of sensor sheet being cut to a specific shape and the visualization its signal input readings.

In this project, we explored topologies for the circuit layout that are more robust against cuts, and a wide variety of cut-out shapes can be supported by combining several topologies in the same sensor sheet, adding various levels of redundancy within each topology and a physically-printed Forward Error Correction. The validation was done by a detailed simulation, an evaluation

of the electronic properties and sensing characteristics of several printed prototypes, and a proof-of-concept implementation of a letter-sized cuttable sensor sheet. Here, I will briefly introduce the topologies. More details about the redundancy scheme, FEC theory and our simulation can be found in [74].

The basic principal about increasing the robustness for subtractive methods is the design-redundant wiring schemes to resist the loss of information transmission channels (connecting wires) during the cutting. Two wiring schemes are introduced in our exploration – star topology and tree topology. In figure 5.4, we demonstrated the construction and implementation of a 4x4 multi-touch capacitive sensing sensor sheet, overlaying a tree topology and a star topology on top of each other. Overlaying different combinations of topologies can support different groups of cut shapes. From the simulation, we learned that that overlaying two tree topologies improves rotation invariance, while overlaying two star topologies allows for wider range of supported shapes. The limitation of this approach; however, is the spacing required and the potential cross-talking noise introduced by redundant wiring, and interference between sheet layers. Especially when the size of the networked electrodes grows, the trade-off between the resolution of each input will decrease due to the spacing and wiring constraints. This constraint only applies for a multi-touch sensor that requires dedicated signal line for each input.

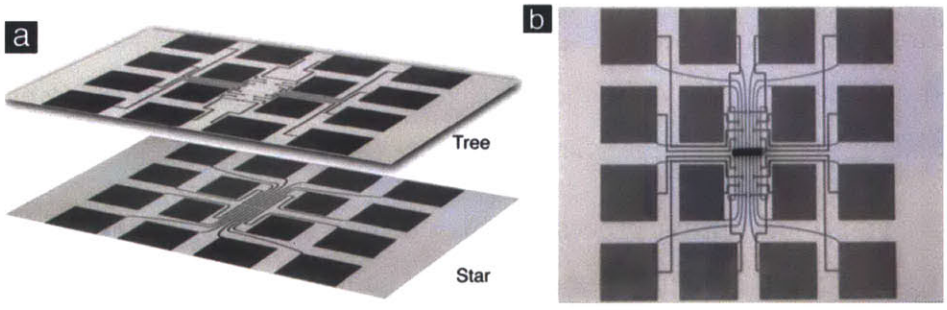

Figure 5.4: a) Prototype of a dual-layer sensor (b) with overlaid tree and star topologies (a) for a 4x4 sensor sheet. The tree topology is printed on a transparent PET film. Both layers are connected using 3M conductive z-Tape.

5.3 Additive Manufacturing – Sensor Tape

In this section, I will discuss manufacturing issues and an example application of sensor tape, which is made through a roll-to-roll process; we can produce long, linear sensing structures and also apply different chemicals on this surface for multi-modal sensing. The example I explored is humidity sensing for environmental monitoring. In this example, I demonstrate two aspects in additive manufacturing. First, as discussed in 5.1, sensor tape is useful for the addition in shape formation. Furthermore, I introduce the additive process of adding layers of chemicals to change the sensing target via printing, deposition or attachment as another form of the additive process.

Fine-grid sensing has always been a major challenge for the design and integration of large-area sensor systems. Deploying a dense sensor network nowadays involves implementing individual sensors and complex wiring between the processor and sensors. The cost of individual sensor manufacturing and system integration is high; hence, in most cases, engineers use interpolation to compensate the missing gaps. We envision a low-cost, large-area-coverage sensing tape based on roll-to-roll manufacturing, where the substrate, electronic circuitry, electrode, and sensing elements are implemented in the same process. Different sensing elements are introduced, either electromagnetic field sensing components that are embodied in the copper trace design or chemical sensing that is based on coating resistive or dielectric polymers, etc. on top of the copper trace "template" for multiple sensing targets.

This one-step fabrication process opens up the possibility for inexpensive dense sensor system deployment that could be unlimited in length and also enables different applications for large-area environmental sensing. In order to have the flexibility of grid compactness for both narrow and wide area coverage, we decided to experiment with a "tape" structured linear geometry with dense sensing capabilities. This shape enables the user to physically

manipulate and configure the sensing density for various measurements. The sensory units can be more precisely placed in a targeted location, like how the density and receptors' functionalities on our skin vary based on the location on the skin. Here, we present the possibility of creating sensing elements by adding a layer of conductive polymer, which can potentially be integrated into the same roll-to-roll manufacturing process as the circuitry printing process in the future. In this section, we show one example of the integration of printed sensor tape with humidity sensing capability. Similar approaches can be applied to other resistive sensors and we envision a sensor strip with multiple functionalities that can be used not only for electromagnetic field sensing, but also scenarios such as a smart material for building-scaled water leakage detection, for example.

5.3.1 Method and Experiment

We began our attempt of adding more sensing capabilities with coating polyimide films on our flexible electronics circuit layout. A polyimide film has a high water absorption property because of its imide bonds, which causes changes of space charge density under different humidity conditions. Also, it is stable and hence requires no extra packaging. We adapted spin-coating as our deposition method for testing different conditions.

Our material selection focused on finding a low-temperature curable polyimide (~150 C°) to match the melting point of our flexible electronics substrate, Polyester. In our experiment, we used a positive-tone photosensitive polyimide, Photoneece® (PW-1500), which is commonly used for buffer and insulation layers in semiconductors and electronic components, and as a humidity sensing material. We experimented with a 9 mm * 12 mm film with 20 μm thickness (figure 5.5(a)) of polyimide coating. The film was produced with spin coating.

The polyimide material was first applied on top of the flexible electronics substrate and then spin coated at 700 rpm for 10 seconds and then 2750 rpm

for 30 seconds (figure 5.5(b-c)). The samples were then prebaked at 120 °C for 3 minutes on a hot plate. The last step was to cure the polymer on a hot plate at 150 °C for 180 minutes. The I-V curve was measured with a two-point probe system. The I-V curve for all samples was consistent with a forward bias diode characteristic for the 0.8 cm^2, 20 μm thick polyimide films under 58 % RH, as shown in Figure 5.6.

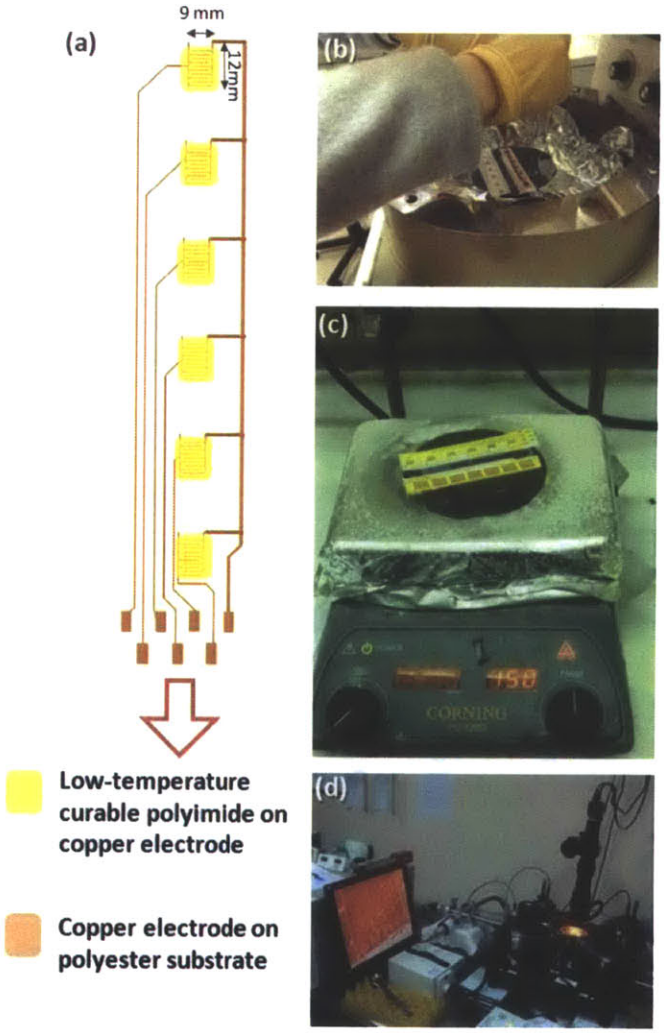

Figure 5.5 (a) Sensor design – copper electrode on polyester substrate coated with low-temperature curable polyimide. (b) Spin coating 20 μm thick polyimide onto conductive inkjet-printed substrate. (c) Pre-bake and curing on a hot plate. (d) Apparatus for IV sweep measurements with 2 point probe.

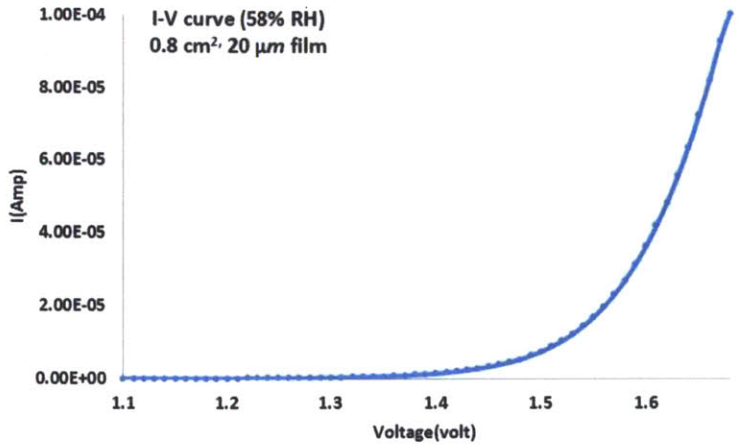

Figure 5.6 I-V curve of a 0.8 cm2, 20 μm thick film at 58 % relative humidity.

Typical polyimides as Langmulr-Blodgett Films exhibit an exponential I-V curve. The tunneling effect can be explained with Simmons tunneling theory [75]. Since the I-V curve was consistent with a forward bias, to test the sensitivity of this material with humidity, we designed a current-to-voltage converter circuit to measure and amplify the signal. Figure 5.7(a) is our circuit design – the operational amplifier (TLV2371) provides a constant voltage for the humidity sensor, while R1 in the negative feedback loop amplifies the signal a factor of $R1/R_{sensor}$. Figure 5.7(b) is the picture of an example circuit implementation. The four output leads were connected to the analog-to-digital input of a microcontroller. A main concern about having a long cascaded line of sensing elements is the line impedance and signal drop. In our implementation, we measured 6 Ω of impedance caused by the copper traces in a 0.3 meter line, which would cause less than 1% of variation in the sensor reading. Induced pickup is another factor for long lines, especially at high impedance. With multiplexing at the end of each sensor tape, we could read the humidity measurement of each sensing element with minimum components, as shown attached to one reel of tape. To test the response time of our humidity sensing element, we started by placing our sensor under 99 % RH and then moving back to 58 % RH, which was the ambient humidity. Figure 5.8 shows an impedance variance of 30 kΩ from 99% to 58% RH

within 300 seconds under constant 1.4 volts. Although the response time was not as fast as most polymer-based capacitive humidity sensors [76], the value is repeatable and responsive to humidity changes. Response time could be improved by increasing film thickness or using a polymer with higher water absorption ability (for PW-1500, the water absorption rate is 4%). The time-dependent ripple in Figure 5.8 shows the polymer thin film system reaching diffusion equilibrium state.

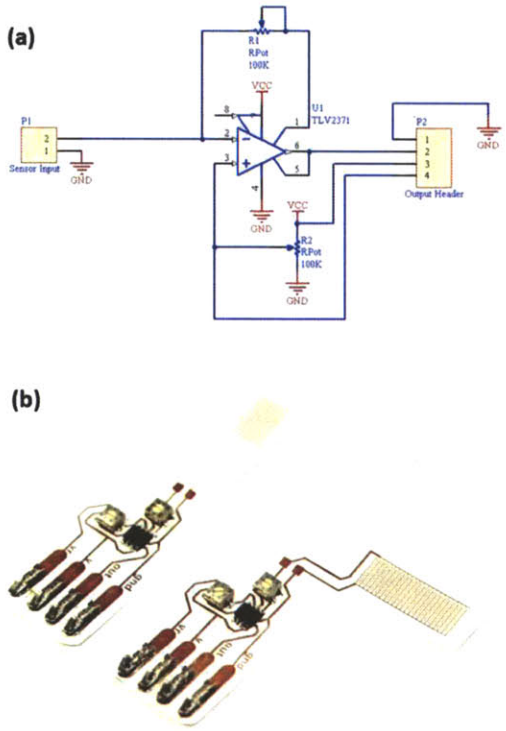

Figure 5.7 (a) Circuit diagram for measuring resistance change at a fixed voltage. (b) Picture of the actual circuit and components. The four pins are connected to power, ground, reference voltage and amplifier voltage output linked to the analog-to-digital input of a microprocessor.

In conclusion, we describe the concept and provide an example of fabricating low-cost humidity sensing tape for fine-grid environmental sensing based on a roll-to-roll manufacturing process. We experimented with the possibility of constructing sensors and sensor templates with a low-cost conductive inkjet printing copper circuitry.

Our first attempt was to fabricate humidity sensors by spin-coating low-temperature curable, high water absorption, conductive polymer (polyimide) onto our sensor substrate and integrate the design with an embedded system for data collection and power management. The humidity sensor was tested in a two-point probe and exhibits the I-V profile of a diode. We utilized the property and designed a current-to-voltage converter circuit to measure and amplify the signal. We demonstrate a working humidity sensor prototype with an impedance variance of 30 k Ω from 99% to 58% relative humidity (RH) within 300 seconds under 1.4 volts.

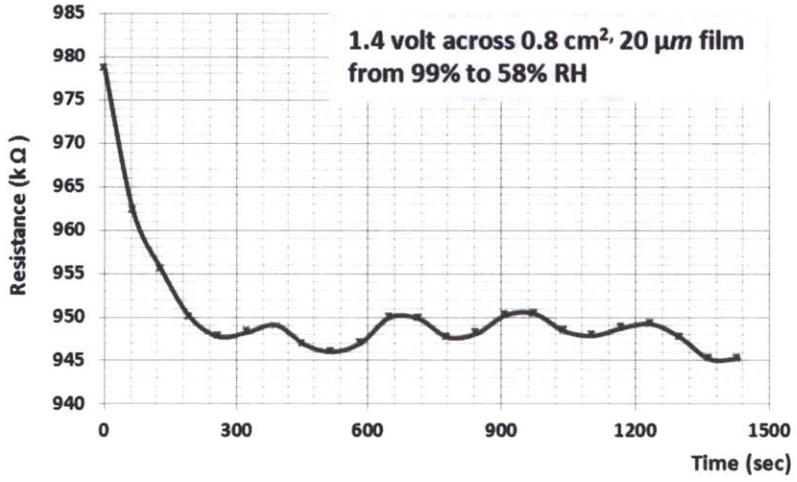

Figure 5.8 Impedance variance of 30 k Ω from 99% to 58% RH within 300 seconds under 1.4 volts.

Future work includes developing multiple sensing modalities, such as temperature and light on the same template for the production of a linear sensor tape with an assortment of sensing abilities, and also better ways to apply different chemicals on the tape substrate, such as drawing with a pen loaded with a sensor "ink" [77]. Research about mechanical drawing of gas sensors on paper [77] has been done in Prof. Tim Swager's lab at the Chemistry department at MIT (Figure 5.9) and other methods such as spinning coating, piezo-electric based inkjet printing and drop casting can also be used as a fast way to apply different chemicals on the sensor tape template.

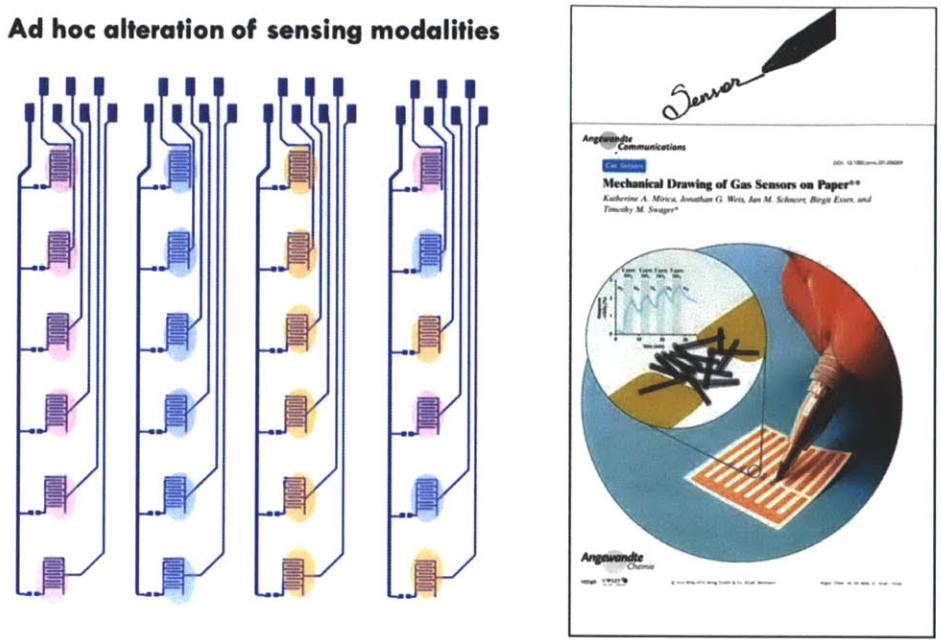

Figure 5.9 (a) Illustration of sensor tape as a template for different sensor coating, while (b) changing the sensing target through mechanical drawing, or drop casting.

We envision a flexible, inexpensive, low power sensor tape system that can be embedded into or adhere to the construction materials as building blocks of smart structures in the future. As mentioned at the beginning of this chapter, sensor tape is a way of constructing a complex sensing surface with an additive approach and can have great scalability for large-area, environmental sensing applications.

This sensor tape can be served as a template for various sensing targets, which can be changed ad-hoc based on the application, environment and hardware platform associated with immediate needs, and charged wirelessly or through energy harvesting as mentioned in the related work section. Besides the "addition" in shape, adding different materials for expanding sensing targets is also one of the aspects of the additive manufacturing approach, which can support more scalable and versatile sensing applications.

Although more and more materials can be printed in the near future, additional chemical layers often require specialized equipment for reproducible manufacturing results; therefore, as covered in the following chapters, I started to explore multimodal sensing techniques for near surface interaction, without any additional layer of deposited chemicals. Each input capacitive or resistive sensing element connects to an analog multiplexer and cycles through different filtering circuitry that is targeted to the most common interaction inputs – hovering, touching and pressure, without any additional complication.

Chapter 6

Multi-modal Sensing:

Target Specific Shapes

6.1 Sensor floor –background and related work

To demonstrate the scalability in power, data transmission and versatility of multi-target sensing on a printed flexible sensor network, we use a roll-to-roll process to create a sensor floor for activity sensing. Our prior work has explored dense networks of hardwired sensor modules (termed *Sensate Media*) as a scalable sensor substrate [22] [19] [20]. Many research groups explored low-cost and dense sensing environments, mostly as floors, for multi-media applications. Unlike computer vision based tracking, this approach requires minimal computing power, can be quite low cost, and can also provide good range-independent resolution, depending on the sensor density. A flexible sensor floor can be quickly rolled out and hooked up anywhere without constraints on lighting or issues of camera occlusion. One of the methods is to use load cells at the corners of a surface that can estimate the changes in weight and position of an object and further identify people based on their footstep force profiles [78] [79]. Other projects, including the Magic Carpet (piezoelectric wires) [80] , Litefoot (optical proximity sensors) [81] and ISA floor (FSR) [82], create pixilated surfaces using larger numbers of sensors. The Z-tiles used Force sensing resistors (FSRs) in networked modular sensing units for easy installation and reconfiguration [83]. Ada's floor [84] is a networked tactile-sensing luminous floor that was constructed and used as the skin of the playful interactive

space Ada. Recent projects in the area of floor sensing evolved quickly in the direction of multi-modal sensor fusion, especially those combining vision tracking for off-floor three-dimensional movement and interaction [85].

6.2 Overall Architecture and Construction

Our prototype sensate surface [16] is based on a matrix of sensing 'tiles' that is formed by printing a specific copper pattern onto a thin, flexible plastic substrate using conductive inkjet technology. Each sensing tile is around 0.3m x 0.3m and contains four printed electrodes of approximately 0.12m x 0.12m for capacitive sensing and two additional printed RF antennas – one for detection of cellular GSM UHF electromagnetic radiation and another for Near Field Communication (NFC) pickup in the HF band.

Whilst it is possible to attach surface-mount electronic components directly to the printed substrate, using either low-temperature solder or conductive adhesive, this process is not straightforward and does not yield high enough performance to support the circuitry needed to process the signals picked up by the printed electrodes and antennas. For this reason, we decided to implement the required circuitry on a small but separate conventional FR4 glass fiber printed circuit board (PCB). This is reminiscent of the architecture proposed by Wagner et al. [86] for an elastomeric skin that carried rigid islands housing active sub-circuits. In our case, the PCB forms a signal conditioning and processing module, which is itself attached to the flexible substrate. One such module is attached per tile, in the center of the four capacitive electrodes. Figure 6.1 shows photos of these components. Details about the operation of the various sensing modes supported by the electronic hardware are described in the following section.

In addition to performing the necessary signal processing, the PCB modules also contain a microcontroller unit (MCU), which is able to sample the detected waveforms and communicate this information with a PC over a shared I^2C bus that runs along the length of the substrate. In order to

minimize any cross coupling between the data lines, each is separated by a grounded trace. The MCU can also be instructed to excite the electrodes with a predefined waveform – for this, synchronization between the adjacent squares is required, and this is achieved using one additional line that distributes a global clock to all tiles and their associated MCUs.

Power is distributed to each PCB using dedicated power and ground lines running along the left and right edges of the substrate. Wider tracks are used for this to lower trace impedance and hence power drop. The conductive inkjet printing process results in a sheet resistance of 200 mΩ per square, and the resulting power drop across each sensing tile was measured at ~0.18V with all sensing modules fully powered on. The power rails run at 18V nominally (for 8 units), and a smoothed linear regulator fitted to each PCB is used to generate a 5V supply locally.

Figure 6.2 shows what the sensing floor looks like when the PCB modules are attached to the flexible substrate. Our test-bed is based on a 2.4 m length of 0.3m wide printed film, which has 8 tiles along its length. It works under regular carpet tiles. In our prototypes, the width of the substrate was limited to a single tile because the conductive inkjet process was only available to us on a 30 cm wide roll at the time of manufacture, although our supplier's manufacturing facility is theoretically capable of printing on substrate up to around 2 m wide. The length of substrate is only constrained by the size of the roll; a single piece tens of meters long is entirely feasible. The PCB modules are soldered to the substrate with low temperature solder (we used $Sn_{42}Bi_{58}$ tin-bismuth solder: melting point 138°C, tensile strength 55.2 MPa). We also attached a piezoelectric pickup element directly to the substrate.

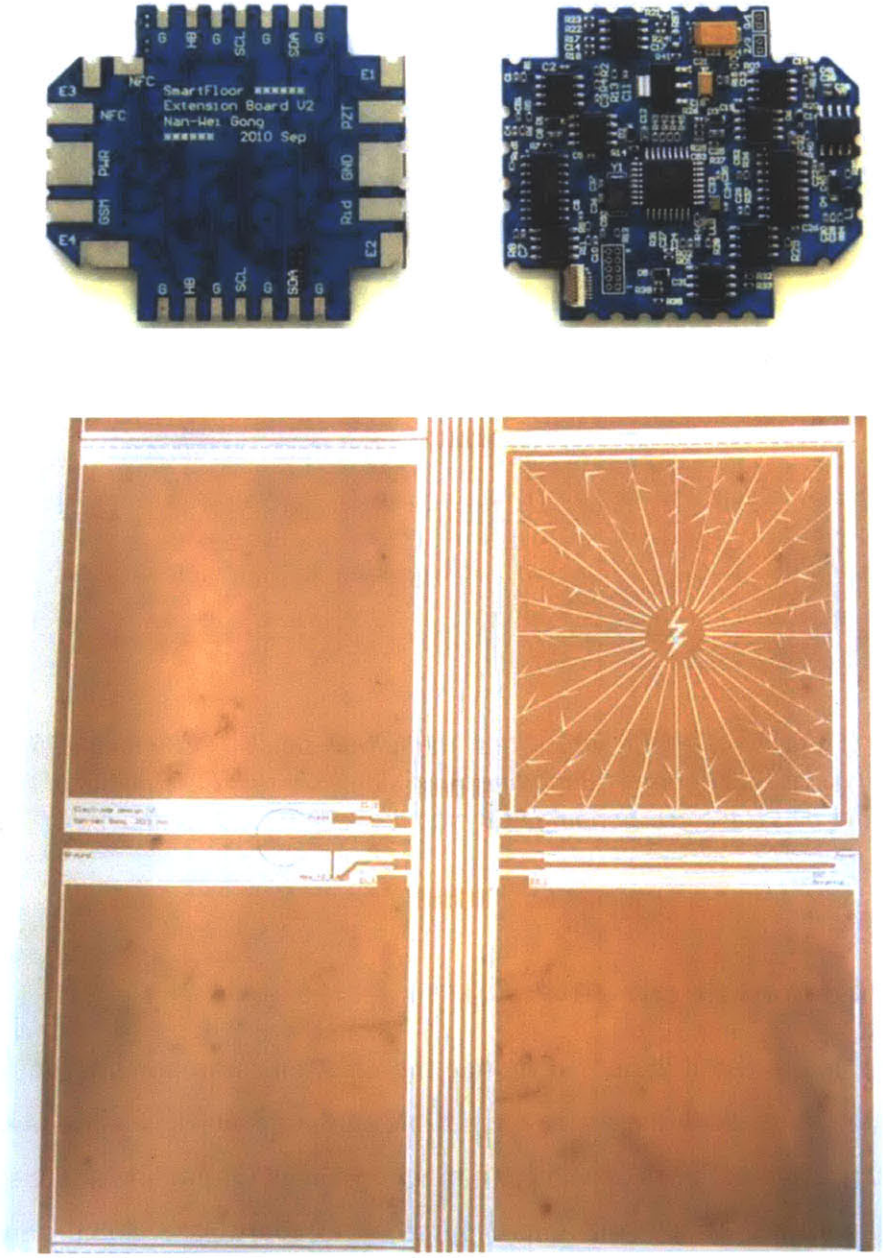

Figure 6.1. Top left: The top view of the signal processing PCB module shows the electronic components. Top right: The surface-mount pads on the underside of the PCB module, which are used to connect with the substrate below. Bottom: The substrate is made up from sensing tiles like the one shown. The 2x2 matrix of printed electrodes is clearly visible; note that the top-right electrode incorporates a pattern of breaks in the copper designed to minimize Eddy currents because the NFC HF antenna is printed around it (just visible in the photo). The GSM UHF antenna is just above the bottom-right hand capacitive electrode.

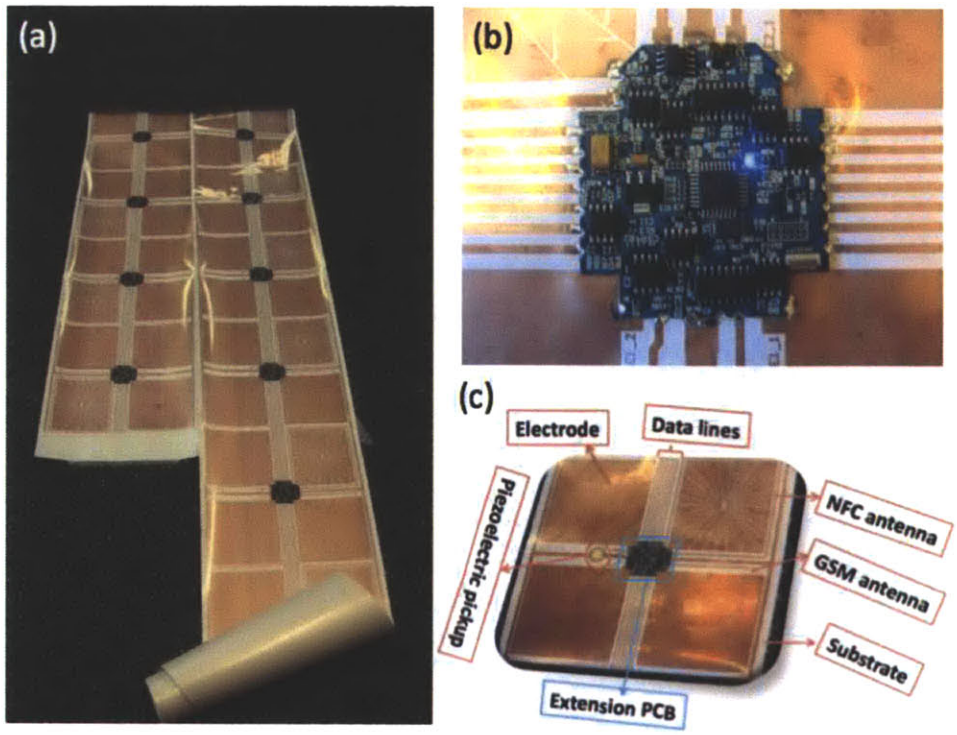

Figure 6.2. (a) A roll of the substrate with multiple sensing PCB modules fitted and (b) a close-up of one PCB module. (c) A single sensing tile consists of the substrate plus the corresponding PCB module.

6.3 PCB module circuitry

Having made the decision to mount the electronic components on a 'PCB module' rather than directly to the flexible substrate, we decided to make the circuitry as versatile as possible. To that end, each PCB module in the system uses an Atmel Atmega368 microcontroller to coordinate global and local communication, manage sensor I/O and perform basic data processing. Global communication is achieved by a two-wire I^2C protocol that is coordinated by a master microcontroller, which interfaces between the end of the substrate and a PC.

Figure 6.3 shows a block diagram of the sensing operation of each unit. There are five major modalities: passive capacitive sensing, active capacitive sensing, GSM UHF detection, NFC HF detection, and vibration/pressure

sensing from the piezoelectric sensor. This wide range of approaches was chosen to allow us to explore the use of printed conductors for sensing as extensively as possible. The raw signal from each printed detector is passed through some signal conditioning circuitry and then into a multiplexer (CD4052) for selective analog to digital conversion (ADC) sampling on the microcontroller. The sampling rate was set to fast mode (400 kHz) with 6 channels of 10-bit ADC. The electrode size in our design (~12cm x 12cm) seems to work well for resolving detail down to the size of a human foot. It would be possible to design a higher or lower resolution floor to match different needs for tracking and localization.

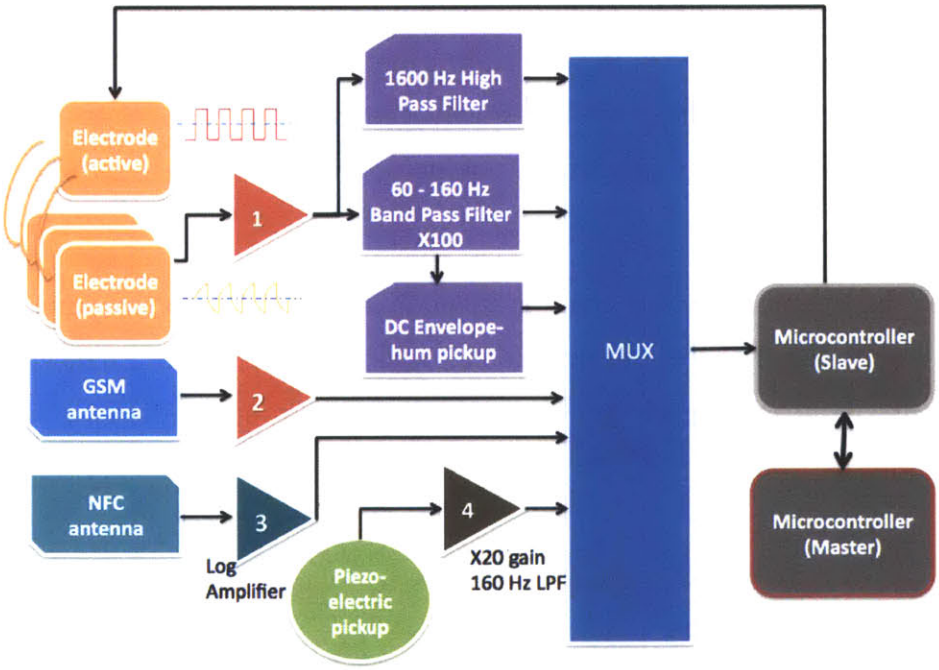

Figure 6.3. Block diagram of operation for each sensing tile. From left to right, signals picked up by the electrodes/ antennae are then filtered by analog circuits and finally sampled by the microcontroller. Each microcontroller acts as a slave device to a master microcontroller, which controlled the entire floor via a two-wire communication protocol.

Figure 6.4 below illustrates the basic operation of the firmware for power management on each slave sensor unit. Each operation starts after receiving a "start" command from the master MCU and then enters idle mode after it successfully joins the I^2C network. Idle mode is the low power mode where

the MCU stays in sleep state and the most power-hungry analog circuits (e.g. the NFC log amp) are disabled to save power. The slave units will wake on interrupts from the passive sensor signals, piezo pickup (or optionally on the passive capacitive or GSM/NFC signals), indicating nearby activity. If verified, every unit in proximity wakes up and enters passive capacitive sensing mode.

In the passive capacitive sensing mode, we can easily locate the presence of a person and start the active (interaction) mode. If nothing is detected (event completion), passive mode will eventually time out in favor of idle mode. However, if presence is detected, the operation enters active sensing mode. In this stage, the slave MCU repeatedly excites one of the electrodes with a 5V square wave pattern and samples adjacent electrodes for coupled pick-up, transmitting signal strength information back to the master node. It also samples for signals that are potentially generated by mobile devices the detected user may be carrying or interacting with, namely GSM and NFC signals.

After the interaction stops, the master node sends out a stop command, and slave units return to low power mode until further movements are picked up. Details about how each sensing modality works are described in the following section.

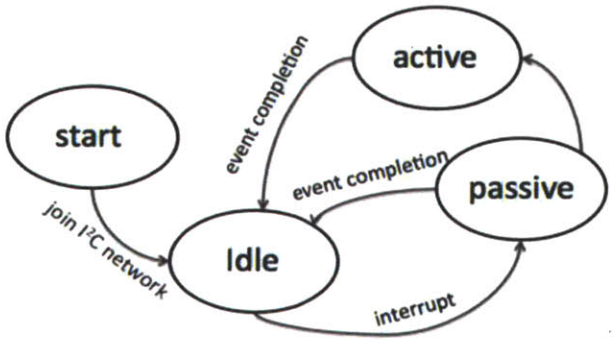

Figure 6.4. Basic operation of each slave sensor unit. Once an unit joins the I^2c network, it enters a low-power idle mode and can be interrupted by piezo pickup, RF signals, or the network (signal detected from adjacent units) and enters presence sensing, interaction and recognition mode.

6.4 Physical topology

As mentioned above, our prototype is based on a relatively narrow roll of substrate due to current limitations of the production process we used, as shown in Figure 6.2(a). In order to cover a wider area with a single strip of sensing substrate, we explored the use of folding – which is possible given the flexible nature of our prototype. In this way, it is possible to cover large areas and also non-flat geometries without the need to cut or re-connect different pieces of the substrate. Examples of this are shown in Figure 6.5.

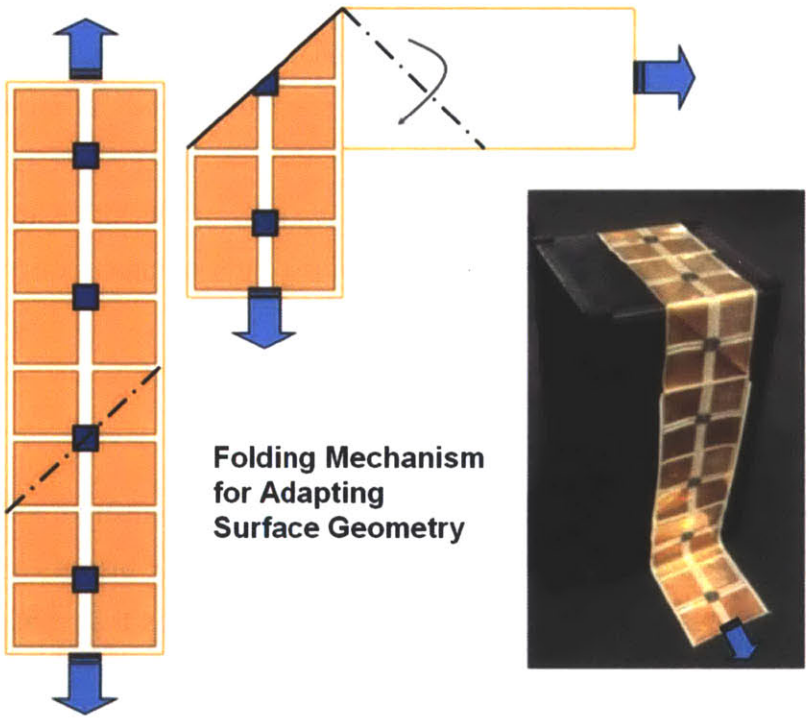

Figure 6.5. Example folding schemes that allow wider and non-flat areas to be covered using a single piece of the substrate without any cutting or joining. Blue arrows indicate the direction of connecting units.

6.5 Sensing Modalities

Analog active filtering circuits were designed to detect all of the supported signal types mentioned previously. Each is described in more detail here.

6.5.1 Passive Mode Capacitive Sensing

Passive mode turns out to be both the simplest and the most power-efficient mode for tracking people moving across the surface. In passive mode, the floor detects signals from the environment, such as power line hum (usually 50 or 60 Hz). These signals are coupled into electrodes much more strongly when a person stands on them. We implemented circuits for detecting and sampling this electric hum. The raw signal was first fed into a band-limit filter, made from a pair of first-order filters - a 50Hz high-pass followed by 160 Hz low-pass with x100 gain. The filter output can be selected for ADC sampling by the microcontroller, or alternatively it is also passed through a DC envelope- detector that gives an easily-sampled smooth output reflecting hum amplitude. Because there was a 2.5 V offset on the electrodes, they worked as condenser microphones, and were very sensitive to impacts. Although this was mainly filtered out by our conditioning circuitry, it could be used as another sensing modality as well.

6.5.2 Active Mode Capacitive Sensing

In active mode, one of the floor electrodes on each tile transmits a signal that is detected by adjacent electrodes when a person's body bridges any two of those electrodes. Any of the four electrodes can serve as the transmitter by emitting a 0V to 5V square wave. The other three electrodes are set up as receivers via trans-impedance front-end current-voltage converters that amplify coupled transmit signals. This process is illustrated in Figure 6.6.

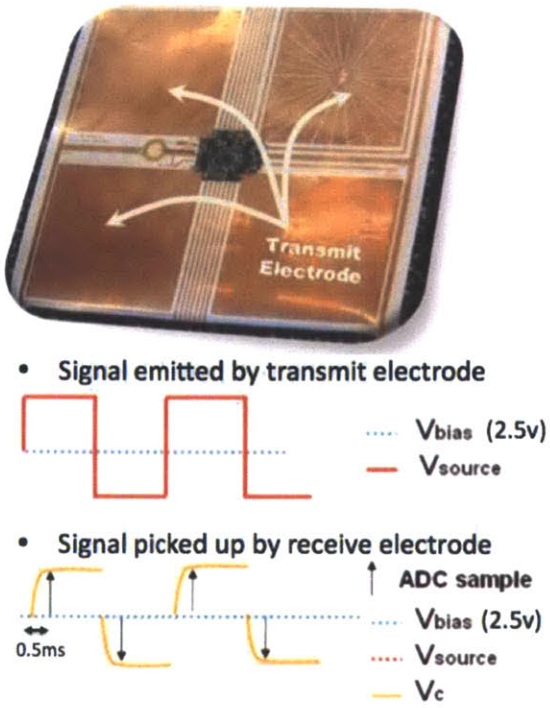

Figure 6.6. Active capacitive sensing: one of the electrodes serves as a transmitter by way of a series of rising and falling edges that act as an excitation waveform (Vsource). The neighboring electrodes pick up this signal (Vc). The amplitude of Vc is proportional to the capacitive coupling between transmit and receive electrodes.

Signals from the receive electrodes were connected to a high pass filter (1600 Hz cut-off frequency) with 10x gain and then sampled by the built-in microcontroller ADC after each changing edge of the transmit electrode (ADC sampling rate ~9600 Hz), once the receive signal stabilized (around 0.5 ms in our case). As seen in Figure 6.6, we sampled the charging and discharging amplitude change (voltage) for 32 cycles and averaged their difference.

It is important to note that with a tiled setup like our floor system, there is very likely to be crosstalk between tiles during active mode. This means the transmit electrode of any one tile is likely to generate a signal that is picked up by electrodes on neighboring tiles. In our prototype, we alleviate this issue by ensuring all tiles operate in sync when running in active capacitive sensing mode. We do this by running a global clock synchronization line to each tile. Accordingly, with proper synchronization, sensing between a

transmitter attached to one microcontroller and receiver on an adjacent microcontroller is possible.

There are two possible scenarios when a user's body comes into the electric field between transmit and receive electrodes – these are known as transmit mode and shunt mode [87]. In transmit mode, the signal is coupled through the person, effectively increasing the amplitude of the signal on receive electrodes. The user or object has to be very close to the transmit conductor, hence is acting like an extension of the transmit electrode. Conversely, in shunt mode, the object or body of the user is not connected to the transmit electrode. Instead, it blocks the electrical field between electrodes, i.e., the coupling between the person and the room ground dominates.

The relative dominance of transmit and shunt modes depends on aspects of the physical configuration of the floor and the user walking across it – things like the position of the user's foot relative to the transmit electrode and the distance between the somewhat dielectric floor surface and the capacitive electrodes below it. In transmit mode, the strength of the detected signal will increase as the foot approaches the floor, and in shunt mode it will drop. Nonetheless, it is possible to use either to detect the user's presence.

In addition to localization and identifying people, an active capacitive sensing floor can be further used as a platform for communication between different devices or users by transmitting signals through the user's body. For example, we have demonstrated this with a small circuit clipped on a shoe with inner side electrode to local ground (against the body) and outer electrode transmitting/receiving a digital signal to and from the floor.

6.5.3 UHF and HF Sensing

We implemented two antenna designs to pick up signals from a cellular phone. The first type is a ¼ wave GSM antenna, which is designed to pick up both 900 MHz and 1800 MHz emissions from a GSM cellular handset. The

design is a simple 8 cm by 0.3 cm trace on the flexible substrate that feeds a Schottky diode detector followed by a low-pass filter with gain.

NFC signal detection was achieved by constructing a square loop antenna designed to be resonant at 13.56 MHz around one electrode. The electrode was cut into sectors as shown in Figure 6.1(c) in order to eliminate Eddy currents that would decrease performance. The signal is amplified and detected with an AD8307 log amp in order to produce an easily sampled output response.

6.5.4 Piezoelectric pickup

In addition to printing electromagnetic pick-ups on the substrate in the form of capacitive sensing electrodes and UHF/HF antennas, we also integrated flat contact piezoelectric pick-up sensing elements onto the substrate, adjacent to each PCB as shown in Figure 6.2(c). Each sensor was soldered onto the ground line of the substrate and was also glued in place to ensure it would be physically coupled to any vibration around the area, as well as responding to dynamic pressure applied from above. Signals were conditioned with a 160 Hz active x20 gain low pass filter.

6.6 Evaluation

Here, we report the capability of our system operating under various types of inputs and conditions. We seek to demonstrate the potential of printed conductive technology as a basis for sensing the presence and location of users in a low-cost, highly flexible sensing system.

6.6.1 Detecting users with passive mode

First, we evaluate the ability of our system to sense users via the electric hum, which is coupled into the electrodes using the passive capacitive sensing circuit outlined above. Without any stimulus, the output from the signal

conditioning circuitry is centered at the bias voltage of just under 2.5V. When a user steps on the sensing surface, different intensities of electric hum coupled via the body were picked up based on the contact area and proximity.

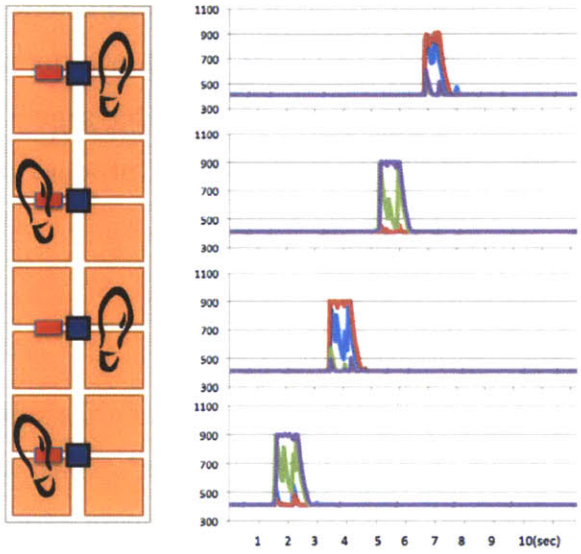

Figure 6.7. Footstep patterns detected by electrodes embedded in the floor in passive capacitive sensing mode. The four different colors in the right-hand figures represent the signals from the different electrodes in one sensing tile.

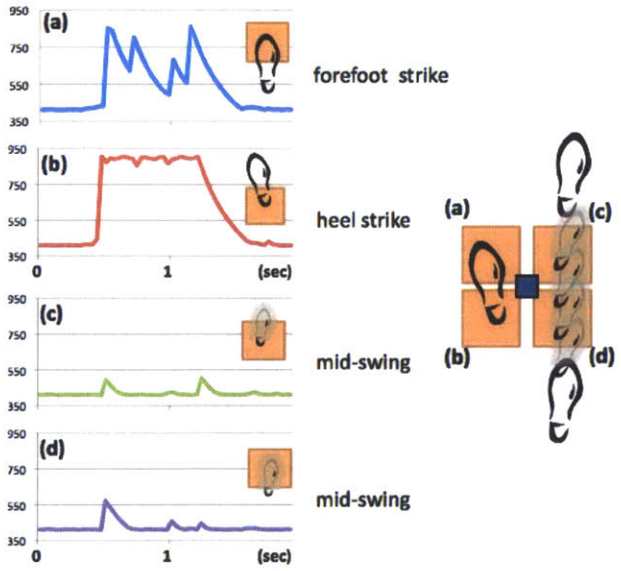

Figure 6.8. Different signatures typically detected with the passive capacitive sensing method. (a) Forefoot strike, (b) heel strike pattern (left feet), (c) and (d) mid-swing between steps (right feet), detected by adjacent electrodes. The decay time is from the RC response of the envelope detector.

In Figure 6.7, we demonstrate footstep detection over time on 4 individual sensing units. As we can see from these traces, the interaction patterns are clean and consistent. It is also worth observing that we can detect the user's foot approaching from a range of 15-20 cm in passive mode. In Figure 3.8, signals from each of the electrodes in a single tile are plotted separately. Three major signatures of the three typical signal patterns – heel strikes, forefoot strikes and mid-swings between steps – can be differentiated.

6.6.2 Sensing with active mode

As mentioned above, depending on the distance between users' body and the transmit electrode, two possible effects can be observed during active capacitive sensing, namely transmit mode and shunt mode. We therefore tested the active mode in these two conditions.

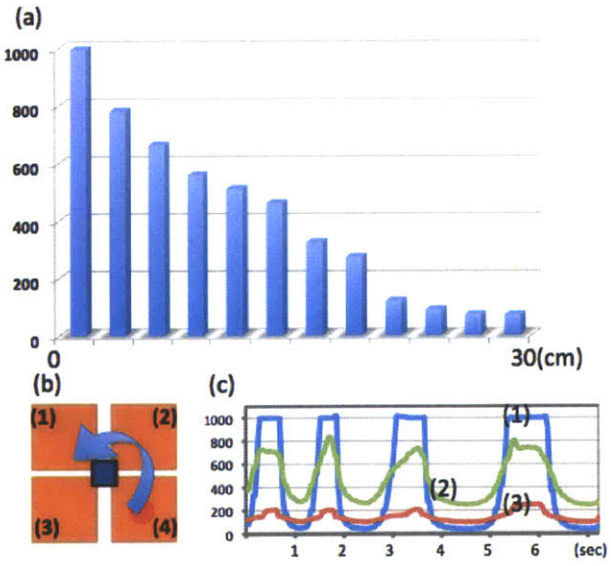

Figure 6.9. (a) The effectiveness of active capacitive sensing mode. (b) Shows the electrode pattern of a single tile, where the electrode marked by the red dot served as the transmitter. The user was bridging two electrodes, namely transmit electrode (4) and receive electrode (1). (a) The user was touching the transmit electrode and moved from towards electrode (1). The strength of the signal pick-up is plotted as a function of distance. (c) Signal pickup on all the receive electrodes as a function of time, as the user repeatedly bridges electrodes (4) and (1) – significant signals are picked up by adjacent electrodes (2) and (3) as well as electrode (1).

Firstly, a user interacted with one unit by directly touching the transmit electrode (4) and approaching the receive electrode (1), see Figure 6.9(b). From the resulting signal distribution in Figure 6.9(c), it can be seen that adjacent electrodes picked up the signals as well. To demonstrate the range versus signal response of transmit mode, we tested and plotted signal strength based on 5 sets of interactions per sensing distance. The result shown in figure 6.9(a) indicates that signal strength decays smoothly with distance. This not only demonstrates transmit mode, but also suggests that signals can be easily capacitively coupled into and out of the body, enabling the body to be used as a conduit for electronic messaging via touch.

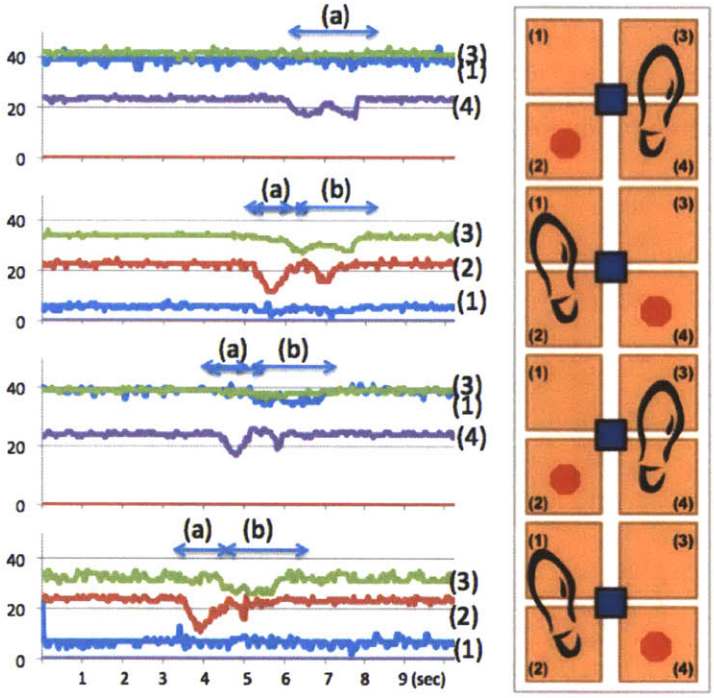

Figure 6.10. Walking patterns detected by shunt mode. During each step, the user effectively blocks the electromagnetic field flux, hence the signal drop: (a) heel strikes and (b) mid-swing. The red dots mark the transmit electrodes.

The second condition involves detecting walking signals on the floor in shunt mode. The testing environment was set up on the floor, with ~4 cm of high-dielectric constant foam on top of the sensors. The test subject walked over the receive electrodes as indicated in Figure 6.10, thereby avoiding transmit mode. Again, the red dots in the figure represent the transmit electrodes, and

the results plotted show how the signal picked up by the electrodes adjacent to the transmit electrode demonstrate a noticeable attenuation through the shunt effect. Although this effect is less marked than the passive sensing results, it none-the-less shows around 4 bits of resolution. Signals from each electrode are marked with numbers – patterns from the steps were consistent across four units: (a) heel strikes and (b) mid-swings. Better shunt-mode response can be attained by lifting the electrodes a few cm above a conducting floor (e.g. by putting a piece of wood below the sensing strip).

6.6.3 Piezoelectric sensor

We integrated piezoelectric sensors into our system for a several reasons. First, like passive capacitive sensing mode, piezoelectric sensors do not require active pulsing, and can therefore be operated with relatively low power consumption. Additionally, a piezoelectric sensor can sense vibration and strain on the surface, so activity at distance can be detected as well as dynamic pressure applied directly to the sensor. In this way, we can easily use the signal from a piezoelectric element to trigger wake up of the microcontroller from a low power sleep mode. The piezo signal also yields dynamics that might roughly infer the weight of a person and provide insight into gait dynamics [88].

We evaluated the effectiveness of vibration and pressure detection in a similar manner to the previously reported tests of capacitive sensing. Figure 6.11 shows the signals picked up by our system. When a user walks along the floor, vibrations that match their footsteps are detected by the nearest sensor; smaller amplitude vibrations are also detected by adjacent sensors.

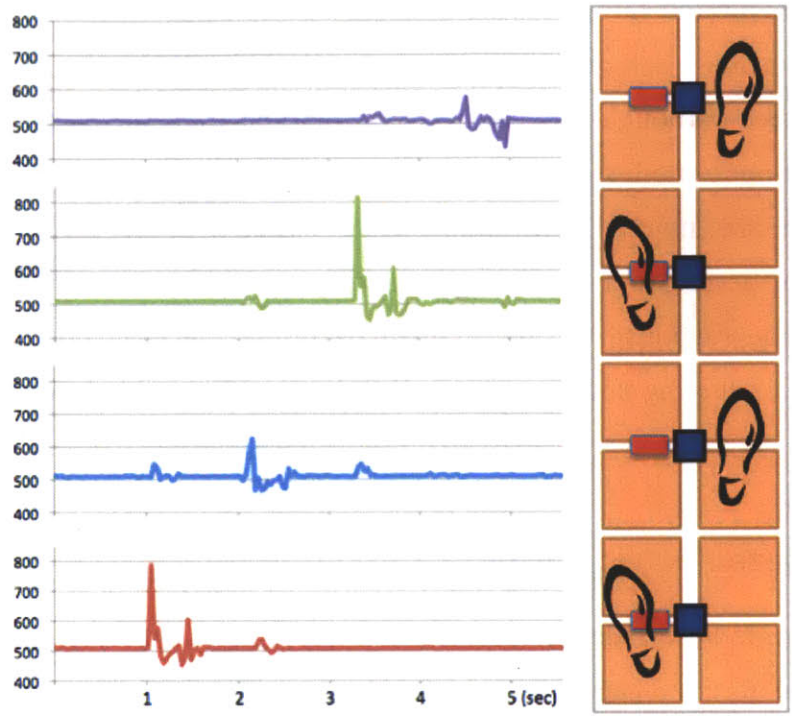

Figure 6.11. Signals picked up from the piezoelectric sensors. Red rectangles mark the location of each sensor within the sensing surface. Walking patterns were consistent with the other experiments reported in this paper. Note that vibration from adjacent units is also perceptible.

6.6.4 Cellular signals versus localization and identification

In our system, we included two types of RF antennas, namely 13.56MHz NFC and 900/1800 MHz GSM. We used a Nokia 6212 phone to test the signal strength of both NFC and GSM emissions across the platform. Figure 6.12 shows the typical signal patterns picked up by our system.

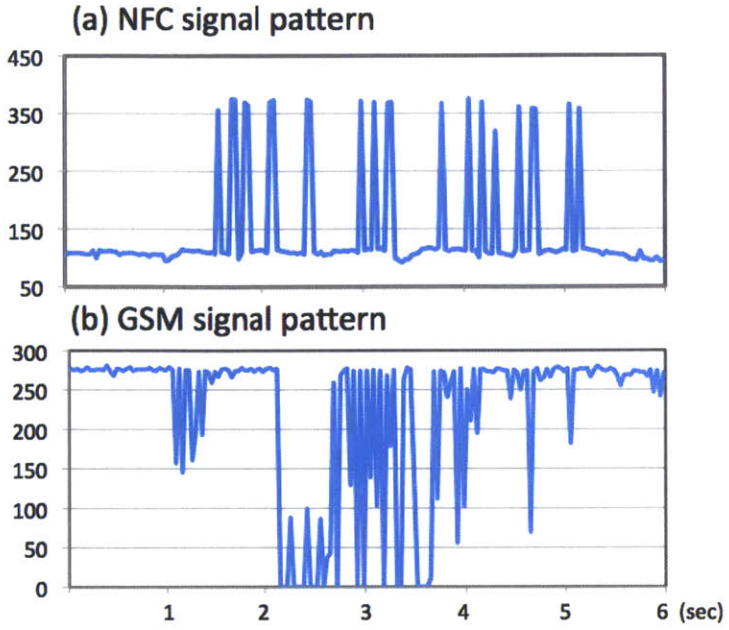

Figure 6.12. Signals picked up by antennas printed on the sensing substrate. (a) NFC signal pattern. The pattern and signal strength of NFC are consistent and can easily be used to determine range by measuring peak thresholds. (b) GSM signals have stronger signal response that can infer longer distance tracking by integrating and averaging the signal patterns.

The signal response from the NFC output of our logarithmic amplifier circuit is consistent and can be mapped to the distance – Figure 6.13(d) shows this. GSM signals are both stronger and more complex. The signal versus distance relationship can be seen more easily by filtering and averaging the signal patterns. Figures 6.13(b) and 6.14(b) show the experimental setup. We tried to evaluate the effectiveness of our platform in terms of identifying the exact unit the user was standing on or near, and the detection range over which cellular signals could be used. Each data point was taken and averaged according to five measurements.

To demonstrate signal propagation across the whole floor system, we plotted the signal response across the tiles in Figure 6.13(a) when the NFC device was held 30 cm away from the surface. The peak value was reported from the tile directly under the NFC reader as expected, and the signal strength drops off in all directions, enabling the location of the handset to be

determined via the NFC signal. We further tested range versus signal strength by taking data from only one tile, recording measurements at various distances. The red circle in figure 6.13(b) indicates the location of NFC antenna used for this. Results are shown in Figure 6.13(d). The NFC signal is good for detecting short-range signal emissions, up to around 90 cm in our tests.

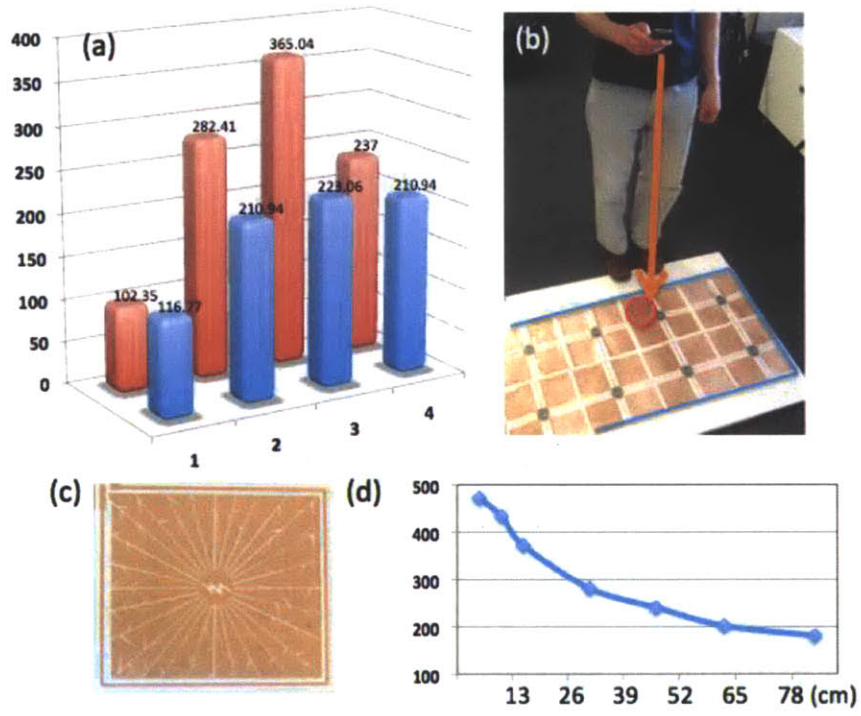

Figure 6.13. (a) Signal response versus sensing unit location when a NFC device is held 30cm from the surface. (b) Illustration of the experimental setup. (c) Close up of the NFC square loop antenna printed on each tile. (d) NFC signal strength versus distance.

We performed a similar experiment with GSM signal detection. When communicating with the cell tower, a cellphone generates a strong signal in the GSM band, which turns out to be readily detectable by the floor tiles from significant distance via our simple circuit. Figure 6.14(a) shows the signal strength distribution across our platform when the mobile device is held about 1m away from the sensing surface as shown in Figure 6.14(b). The signal strength was integrated and averaged from a 6-second long GSM connection. As seen in Figure 6.14(a), the peak value fell off in adjacent tiles

in a similar manner to the NFC signal. We again recorded signal strength versus range as described above, and illustrated the result in Figure 6.14(d). This shows that the GSM signal strength drops off with distance in a similar manner to NFC and it is apparent that either could be used as a basis for determining range.

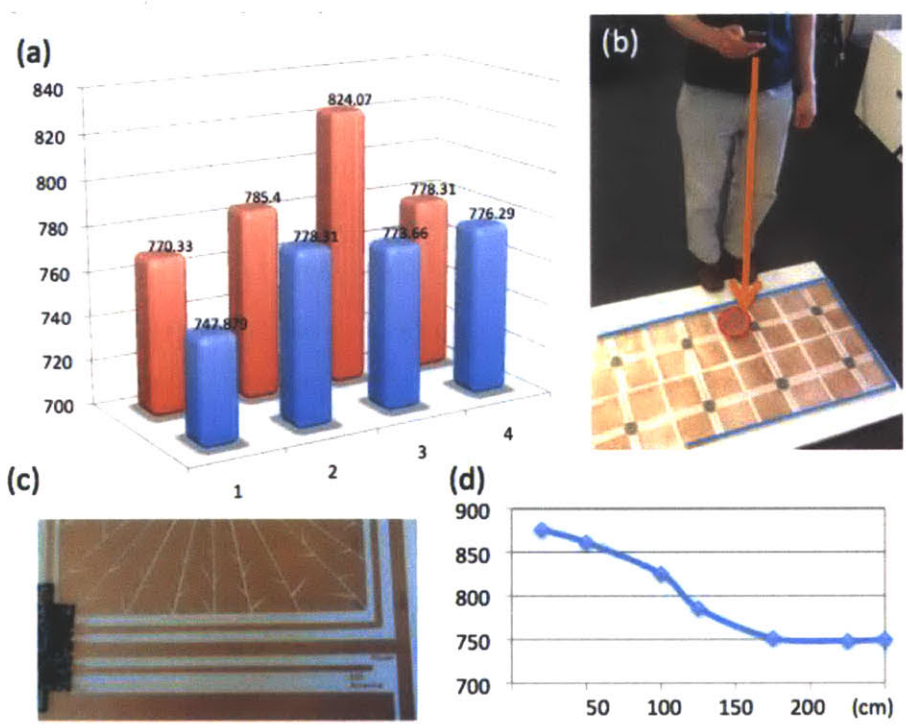

Figure 6.14. (a) Signal response versus sensing unit location when a GSM device is held 1m from the surface. (b) Illustration of the experimental setup. (c) Close up of the tile GSM antenna. (d) GSM signal strength versus distance.

Both NFC and GSM signal strengths are directionally sensitive and could be affected by the way a user holds the mobile device. We have seen the GSM pickup to be fairly resilient, however, and the NFC detection range has been over a meter when the NFC antennae on the floor are isolated from magnetic material below – e.g., by putting a piece of magnetic shielding under the antenna or raising the floor up by a cm or two atop a nonconductor (e.g., piece of wood).

6.7 Conclusions

Passive mode is the simplest sensing method to integrate and implement with minimum electronic components, and it is yet one of the most powerful modes for localization. Crosstalk between different electrodes was unnoticeable. The received signal patterns could be used to distinguish walking direction, strikes and mid-swing – all useful information for gait analysis.

In order to minimize system power consumption (in our full system deployment, each unit consumes ~25 mA when it's actively scanning for each sensor input), we combined both active and passive modes as a low power hybrid mode. The floor defaults to sleep mode and interrupted only when a vibration occurred at the nearby surface and immediately entered passive mode. Upon confirmation from the passive mode, the floor switches to active mode (see Figure 6.5). Interrupts can also be triggered by the passive capacitive sensing mode or GSM or NFC pickups. It is possible to form a larger network if the current drain is managed properly to avoid excessively loading the power bus lines.

Whilst the sensate floor described in this paper can detect and locate users, it is not intrinsically capable of identifying specific users. However, substantial studies of locomotion and especially gait structure analyses [89] suggest that it is possible to use the difference in a person's unique walking motion for identification. Given the gait data presented in Figures 6.7, 6.8 and 6.10 we believe these techniques may be applicable here. It may also be possible to combine additional sensing and identification modalities. For example, if a user is positively identified when they are logged into a desktop computer or when they make use of an electronic access control system, it may be possible to track them subsequently using the floor and maintain the correct association between identity and current location.

Besides localizing and identifying people, it may also be possible to use this technology to sense hands interacting with a surface such as a desktop or

wall, and to associate these with the corresponding feet using active transmit mode coupling between the two surfaces through the user's body in a DiamondTouch-like manner [90]. It may also be possible to instrument more complex surface structures by folding or forming a conductive printed substrate in more sophisticated ways than we have presented here. In active capacitive sensing mode, the signal strength is strong enough to be used as a way of transmitting digital information from a body-worn device to the floor sensing system. For example, it would be possible put small tags on users' shoes that transmit unique identification signals for each person with a transmit electrode outside and local ground electrode inside against one's sock and sending the ID of a user (see Figure 6.15).

The future work will focus on integrating this system into a building environment to form a ubiquitous computing platform. To minimize the wiring and power drop across long power line, printing flexible batteries with power harvesting and charging circuit, as well as connect the data transmission wirelessly are two directions that can truly make each floor tile standalone and scalable.

In addition to evaluating and extending the system further, this gives us an opportunity to investigate potential applications, including smart floor sensing for motion tracking, localization, identification, gesture recognition, gait analysis and a variety of human-computer interaction and ubiquitous computing scenarios. These technologies can also be used in other applications off the floor, as described in the next chapter, which describes a multi-modal sensing platform especially designed for human-computer interaction design with two conductive inkjet printing technologies.

Figure 6.15. Illustration of transmitting/receiving into the floor – from clip on shoe attachment to the sensor floor tiles.

Chapter 7

Multi-modal HCI Sensing: Multiplexing Inputs

In this chapter, we describe the design of multimodal sensing techniques for near surface interaction based on only one electrode input. The signal is multiplexed with three analog circuits and can infer hovering, touch and pressure. By combining multi-touch, pressure and proximity inputs, the sensor detects rich variations of grasp, plus on-surface and near-surface interactions. The sensor is so inexpensive that a large number of everyday objects can be instrumented with it, such as tools and controllers, training devices, wearable accessories, furniture, home appliances, and smart packages. We illustrate these unique capabilities with the following examples:

7.1 Example Scenarios

Our design supports a wide range of applications in tangible wearable, mobile, and desktop computing. To illustrate the unique capabilities of the sensor and the innovative interactions it enables, we provide several usage scenarios.

7.1.1 Enabling rich input on and above smart objects

The vision of ubiquitous computing is becoming a reality, and everyday objects are increasingly getting "computerized" [1]. It is obvious that this development requires novel interaction styles that go significantly beyond those known from desktop computing and today's mobile computing devices.

Detecting grasp and reacting to how a user holds an object is a promising new interaction method [33] [34]. The way a person grasps and manipulates an object not only tells a lot about its current or intended use, but also implicitly conveys information about the user.

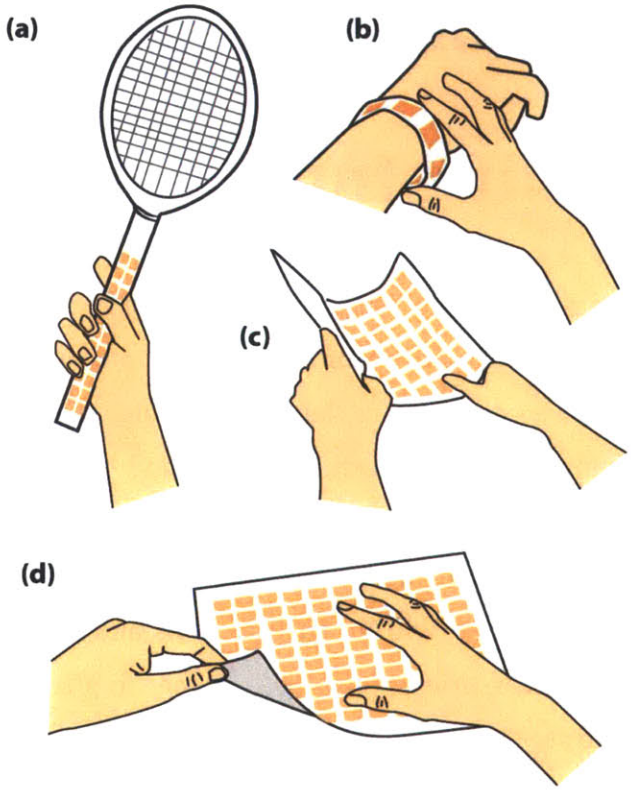

Figure 7.1. Motivating scenarios.

The ability of capturing the detail of a grasp can be used to extend a device's functionality, such as enhancing game controllers and as a learning tool and data logger for repetitive gestures. Many activities require a user to hold and move an object in a very precise way; examples comprise sports (especially racquet sports and bat-and-ball games), playing an instrument (holding the bow of a stringed instrument), a worker or artist using a tool (such as calligraphy). Our sensor enables low-cost tangible control for computer applications that provide a more realistic capture of the user's movement. A controller in the shape of a tennis racket with a sensor sheet on its handle (Fig. 7.1 (a)) could enable more realistic tennis games by capturing where the user holds the handle and infer what forces are applied. Moreover, a

sensor sheet could be added to a real tennis racket and used to capture detailed information about a player's grip, which could be used to provide personalized feedback to improve the player's form.

Another class of smart objects makes use of the sensor for inferring knowledge about its user. For instance, a smart handle of an oven door could lock the door automatically if the user's hand is smaller than a certain limit, preventing young children from opening the door. Additionally, a "secret" movement, hardly visible to an observer, allows parents to lock and unlock a door for anybody, to allow or prevent young children from using it [91].

Smart accessories could be used as body-worn controllers. For instance, the sensor could be integrated into a bracelet (Fig. 7.1 (b)) or a watchstrap (even sharp folding around a thin object is possible). The inner side could be biometric data for healthcare [92]. For instance, galvanic skin resistance correlates with the user's stress level [93]; knowing about the stress level can either be used in health care applications or as a direct feedback for entertainment services. The outer side could be used to provide an interactive surface for touch, pressure and proximity gestures.

7.1.2 Interactions with, on and above flexible surfaces

Computer interfaces are becoming physically flexible, thanks to recent advances in flexible electronics and e-textiles as mentioned in Chapter 2. Flexible materials that can sense how people interact with them and how they are touched and deformed are crucial for the implementation goals of such interfaces. We offer a lightweight and robust way of sensing such input on very thin and flexible surfaces, such as paper, thin plastic film and non-stretchable fabric.

For instance, the flexible cover of a tablet can become an input device (Fig. 7.1(c,d)). It detects not only multi-touch/pressure/proximity input, but also curving at the same time. This enables novel interactions for navigation

within a document by bending the left or the right edge, similarly to flipping pages in a book [94]. The sensor differentiates various ways of bending, which can be mapped to different speeds of navigation. Simultaneous multi-touch gestures allow the user to perform activities like copy/paste and moving contents while navigating through the pages of the document. When the sensor is printed transparently onto a flexible display using ITO or conductive polymer, for example, these interactions become also possible with flexible tablets and smart phones.

7.2 Design and Fabrication Principals of PrintSense

In this section, we will describe the design rules and techniques that we developed for our infrastructure, which we call PrintSense. Our first approach is simple – print single-layer patterns and traces, then use flexible printed circuit connectors to interface the rigid circuit board with the flexible sensor sheets. This approach works well as a basic platform for near-surface sensing.

Our purpose is not to create a 3D controller, but instead a 2.5D user interface (e.g., inferring particular 3D actions as opposed to tracking 3D position) that is low-cost, customizable and malleable. The uniqueness of our approach is that the sensor inputs can be constructed with the same *material* and *pattern design*, which could greatly increase the reusability and adaptiveness for user customization.

Figure 7.2 is an illustration of the basic architecture of the system. The first component is the flexible circuit printout from either a conductive inkjet printer or regular printing cartridges with conductive particles [21]. With roll-to-roll printing, it is possible to create flexible sensor stripes or sheets that are unlimited in length. The sensor printout can be customized as any shape (long stripes conform to the shape of an object such as the surface of a guitar, or even a pattern for origami). The impedance, noise and the power drop across a long signal line are the major constraints on the sensor size.

However, this is not an issue for smaller scale applications within a few meters square. The second component is the sensor board electronics for filtering, amplifying, multiplexing and communication with a computer. Although it is possible to implement all of the circuitry on the flexible sensor pattern design, we designed a traditional printed circuit board (PCB) since our approach is to create reusable PCB hardware for interfacing with different interchangeable PrintSense sensors. Spatial and temporal multiplexing and data conditioning for all three input modes are processed in the hardware and a microprocessor transmits the data through serial communication to a computer. Further gestural recognition and mappings are implemented in the computer software.

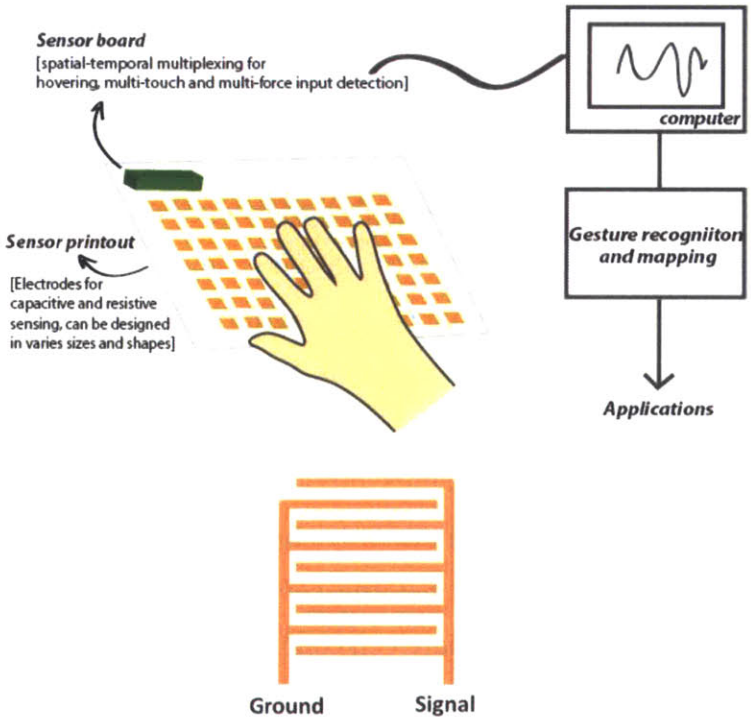

Figure 7.2. Top: System architecture of PrintSense. Down: The design of an input element. One side of the IDT pattern is always connected to ground.

Our implementation (figure 7.3(a)) demonstrated a sensor array with an element size of 1 cm^2 and distance of 0.5 cm between inputs. The advantage of this approach over the following methods is the one-step prototyping

ability. Flexible Printed Circuit connectors (FPC) are used to interface the sensor sheets and the PCB. However, strain mismatch may cause tear damage and breakage at the connector if not handled properly. It also makes the sensing density slightly lower due to the need for extra wiring in between electrodes.

To explore the possibility of multi-layer sensor construction, and also different connections between microprocessors (or PCBs) and sensor sheets, we experimented with the pressure sensitive adhesive (PSA) transfer tape from 3M with anisotropic electrical conductivity – the "Z tape" that only conducts on the Z-axis. The Z tape matrix is filled with conductive particles, which allow interconnection between layers through micro vias. The conductive channels are spaced far enough apart for insulating adequately in the plane of the adhesive (X and Y). The contact resistance is <0.3 ohms and the minimum gap is 15 mils between conductors [33].

Figure 7.3 (b, c) shows design examples; utilizing the unique properties of the Z-tape, we can route the traces on a second printed layer, and also connect the signal IO to a printed circuit board (PCB). This approach allows maximized sensing density and also makes it possible to interface flexible sensor sheets with rigid PCBs in a more robust and compact form factor. It is also possible to "tape" components directly on top of the circuit design printout, which is a convenient way for prototyping surface mount components. The only drawback is the constraint in feature size, and the weaker physical bonding force between components and the circuitry.

The last fabrication possibility follows the design principles of either single or multi-layer construction, but prints double-sided conductive traces. For electromagnetic field sensing that requires proper shielding or a power plane, an extra layer is critical for an adequate signal-to-noise ratio.

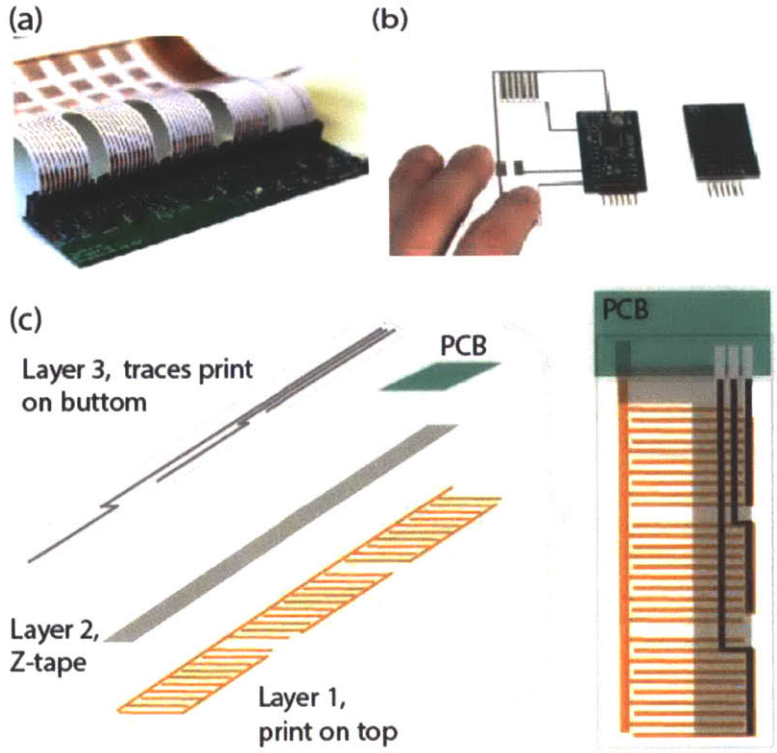

Figure 7.3. (a) Example implementation of single layer sensing matrix (copper traces), interfacing with FPC (Flexible Printed Circuit) Connectors. (b) Connecting sensor sheet (silver ink on paper) to PCBs using the Z-tape; on the right is the bottom view of the PCB design, with pads connecting the sensor inputs and IO of the microcontroller. (b) Illustration of multi-layer construction of the dense capacitive sensing matrix. The tape (middle gray layer) only conducts in the Z direction, which connects the top traces to the bottom traces. It can also be used for connection between pads on PCBs.

7.3 Sensing Principles of PrintSense

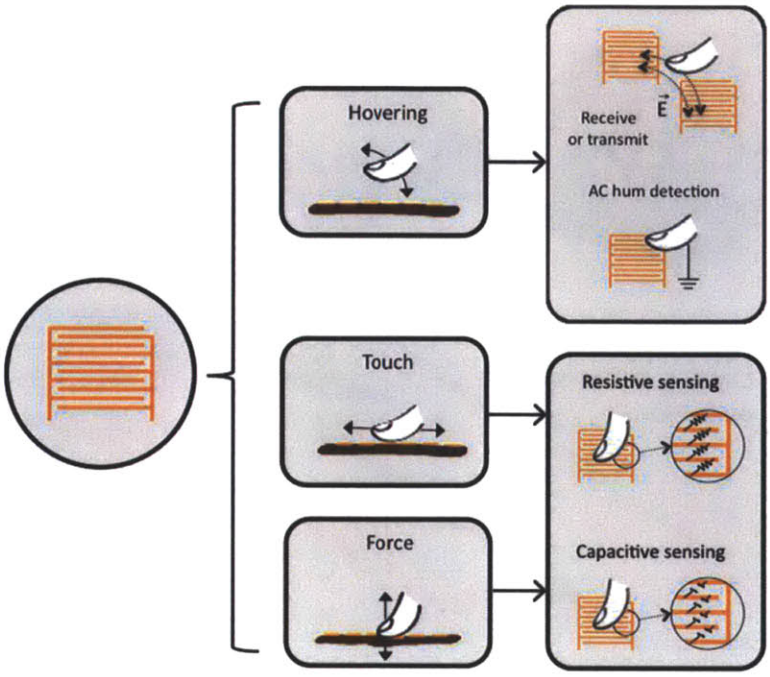

Figure 7.4. Four different sensing modalities supported by PrintSense, in conjunction with inter-digitated electrodes. Illustrated from top to bottom: Close proximity active transmit-and-receive capacitive sensing, AC hum detection (passive capacitive proximity sensing), traditional capacitive sensing and resistive pressure sensing. Note that fold detection is not illustrated.

There are four different sensing modalities we explored with single layer printing without adding extra layers of materials. Figure 7.4 summarizes the various sensing modalities. The four modalities are close proximity, active transmit-and-receive capacitive sensing, induced AC hum detection, resistive pressure sensing and capacitive surface sensing, as illustrated in figure 7.4. Details about the operation principles are described in the following sections.

7.3.1 Capacitive Touch Sensing

The operating principle of the majority of simple, single-layer electrode capacitive touch systems is based on repeatedly charging up an electrode and then timing how long it takes to discharge. When a finger, hand or other

body-part is close to the electrode, the capacitive loading will change, as will its rate of discharge, since as more charge can be stored at the larger capacitance when the body approaches the electrode. This can be detected and inferred as touch. PrintSense supports this mode of touch sensing, which we refer to as *load sensing*.

7.3.2 Capacitive Proximity Sensing

PrintSense also supports a completely passive capacitive sensing mode, which we call *AC hum detection*. In this condition, each electrode is connected to an analog sensing circuit, which is simply detecting any mains electricity noise coupled into it. Just as touching an audio cable that is attached to an amplifier causes noise to be picked up, so proximity to a sensing electrode can be detected. More specifically, we implement a band pass filter centered at a frequency of 50 to 60 Hz to match the power line alternating current (AC). After the band pass filter, a peak detector holds the AC signal amplitude, outputting a DC voltage equal to the peak value of the AC signal. This mode provides hover detection with a range of around 10 cm.

An alternative approach to proximity detection is an active *transmit-and-receive* scheme similar to that used in SmartSkin. In this mode of operation, each sensing electrode must consist of two interleaved sets of conductive 'fingers', as shown on the left of Figure 7.4. We refer to this configuration as an inter-digitated electrode.

When one set of fingers (the 'transmitter') is stimulated with an AC signal, the second set (the 'receiver') will naturally tend to pick up the same signal. If part of a user's hand is in contact with the transmitting electrode, it will act as an extension to the transmitting electrode and increase the signal transfer to the receiving electrode. Conversely, when a hand is in-between the transmit-receive electrode pair, it tends to blocks the electric field, and creates a signal drop [19, 25]. These effects can be used for proximity detection. Increased range can be attained by driving blocks of proximate

electrodes together and summing adjacent blocks of receive electrodes, thereby creating larger effective electrode areas.

Although only the resistive sensing requires an interdigitated (IDT) electrode configuration, capacitive and resistive modalities are all compatible with that configuration – either by using just one of the sets of fingers for sensing or by using them both connected together (switching the second electrode from ground to the transmit or reverse function). Interestingly, as we show later, in some cases performance is improved with inter-digitated fingers.

7.3.3 Other sensing modalities

As mentioned earlier, in addition to capacitive touch sensing, it is also possible to support additional sensing modalities. As well as its use for proximity sensing, the active transmit-and-receive capacitive technique may be used in a slightly different way to detect folding of an array of electrodes. In this case, one electrode acts as a transmitter and is detected by other 'receiving' electrodes on the sensing substrate if it is brought close to them. So if the corner electrode on the substrate is folded over, this can be detected. This process works best with a transmit electrode that is a little larger than the 'finger-sized' capacitive sensing electrodes we have considered so far.

One final sensing modality which we can readily support is resistive pressure inference. This exploits the fact that when a fingertip comes in contact with a bare inter-digitated electrode it will allow current to pass between the two sets of electrode fingers. Although there is a considerable variation in baseline skin resistance between different users due to a number of factors, in all cases applying pressure increases the contact area and density of conducting ionic physiologic fluids in the finger, which decreases resistance. This can be measured to give an indication of applied pressure.

7.4 Electrode substrate

For the purpose of testing and evaluating the techniques described in this chapter, we designed a single versatile conductive pattern shown in Figure 7.5. It is roughly 24 x 12 cm with a 14 x 12 cm central area, which contains a grid of 42 inter-digitated sensing electrodes. Each electrode is around 1.5 x 1.5cm and there is a roughly 0.5cm separation between adjacent electrodes. Two much larger 3 x 6cm electrodes designed to be used as transmitters are included on the left- and right-hand edges of the substrate. These provide more range for proximity detection and are not needed for close range interaction. Similar range can be attained by electronically ganging proximate groups of small electrodes as described earlier.

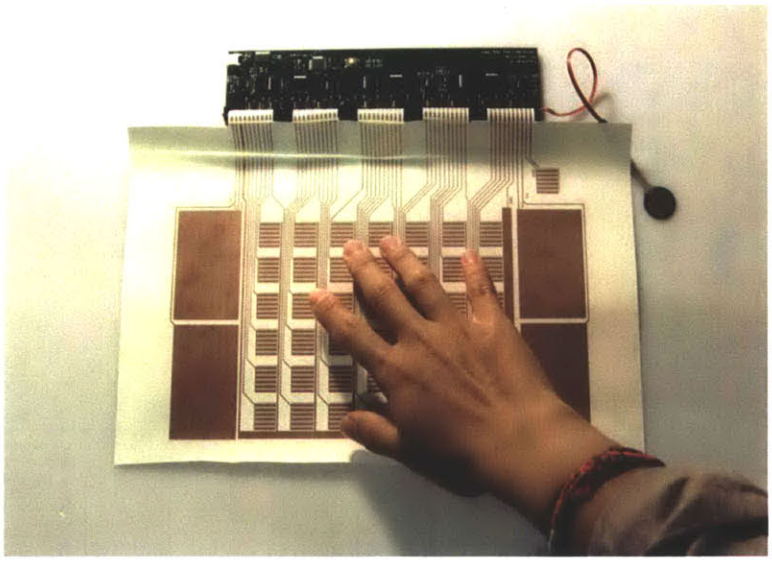

Figure 7.5 PrintSense Implementation, 12 x 24 cm2, 6 by 7 sensor arrays for multimodal near-surface gesture contact sensing. Four large electrodes at each corner are for longer range hovering and folding detection. The FSR at upper right is for GSR pressure calibration.

The design is single-sided, i.e. it requires just one conductive layer – all the traces which connect inter-digitated fingers to the PrintSense controller run in between the electrodes. Flexible printed circuit (FPC) connectors are used to interface the sensor substrate to the PrintSense controller board.

7.5 Hardware implementation

Our PrintSense controller (shown in Figure 7.6) is based on a 16 MHz ATmega328 microprocessor, which can support 46 inter-digitated electrodes through the control of three 16:1 MUXes (CD74HC4067) in order to switch each input between sensing modes. Each input electrode is first fed into an amplification stage for the current to voltage conversion in the resistive sensing before the analog MUX scans through each input and transmits the voltage level to a 10-bit analog-to-digital converter (ADC). A second MUX that is connected to the same output of the amplifier switches on after the first MUX switches off. Output of the second MUX is connected to an analog active filter circuit that processes the capacitive sensing information.

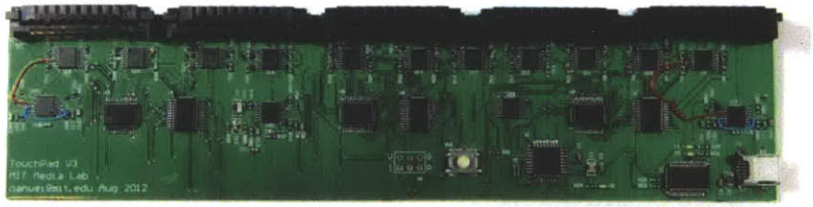

Figure 7.6. PrintSense hardware.

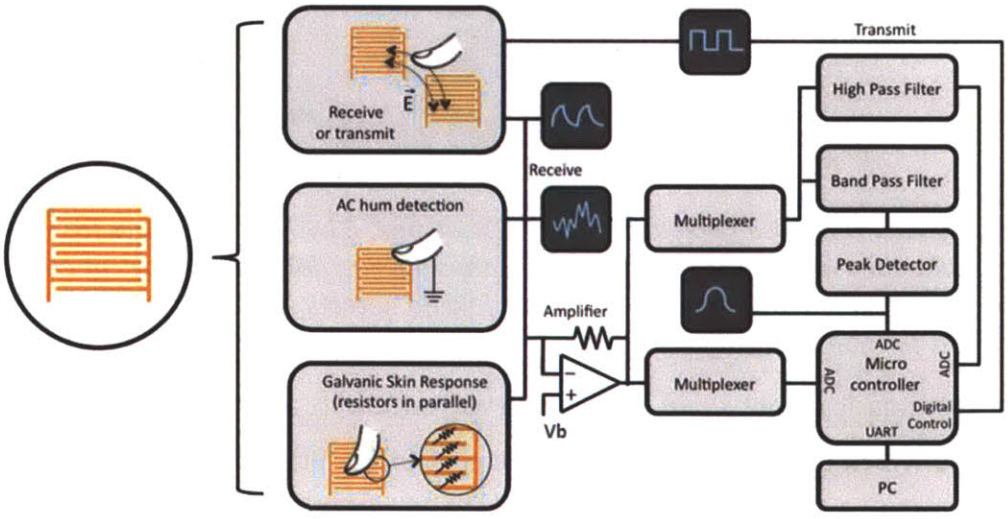

Figure 7.7. PrintSense Sensing Block Diagram.

The geometry of the controller and the associated sensing substrate was chosen to support fullhand interactions. The connection between the flexible substrate we used and the controller board was made with flex circuit connectors (JST-10FDZ).

For the AC hum detection, we designed a band-pass filter, 50-160 Hz with gain of 100. For the receiving electrode of transmit-receive pair, the high pass filter has a cut-off frequency around 1.6kHz. The ADC sampling with our microprocessor is approximately 10kHz.

The whole system samples 46 channels with two modalities at 84 Hz. The raw data is low pass filtered on the hardware before sending it to the computer. The sensor board is USB powered, and a FTDI USB-Serial chip is used for the serial communication between the microcontroller and a PC (Figure 7.7).

7.6 Characterization of operation

To demonstrate and characterize the performance of our platform side-by-side between different sensing methods, we compared the resistive pressure input with a commercialized force sensitive resistor, utilizing a different printing technology [95], and demonstrated the continuous behavior of near surface sensing starting from hovering, to touch and pressure input on the same electrode.

7.6.1 Resistive Sensing

To evaluate the resistive sensing characteristics of PrintSense, we used an Interlink Electronics force sensing resistor (FSR 402) with continuous force resolution and a sensitivity range from 0.2 - 20.0 N for comparison. Our experiment was performed with one a user touching the inter-digitated patterns with an FSR under the pattern for pressure calibration. The blue and red graphs in Figure 7.8 show how closely the two signals track each other.

We used the voltage divider front end circuit shown in Figure 7.10 for these tests, which gives an asymptotic response.

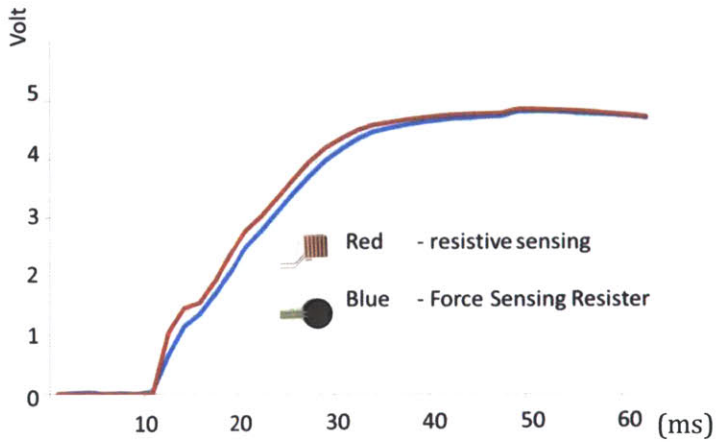

Figure 7.8. Comparison of touch and pressure detection using different sensing techniques. Notice how closely the resistive sensing tracks the force sensitive resistor.

We investigated this in more detail, however, to be able to better understand the sensor characteristics across a population of users and over time – see below.

To evaluate the quality of the force measurement inferred by our proposed resistive sensing (galvanic skin response, GSR) method on the interdigitated electrodes, I conducted a user study to compare the average response, stability, and drift over time of two sensors: a Force Sensitive Resistor (FSR) glued under an interdigitated electrode for GSR measurement. FSRs are an established technique for measuring pressure in HCI implementations. Typically, the part-to-part repeatability tolerance held during manufacturing ranges from ± 15% to ± 25% of an established nominal resistance [96] and it also depends on particular implementation. In the comparison presented in the following section, I will term the two sensors as FSR and GSR. Many researchers have conducted experiments on the GSR signal over a long period of time to infer blood pressure and emotion, comparing conditions such as before and after exercise, before and after emotional events and stress [97]. It is known that skin conductance can be used for simple "input",

but was never studied quantitatively for inferring force. The purpose of this evaluation is to demonstrate the utility and calibration needed for GSR as a force sensor and its variance across users and over time. Figure 7.9 is a typical simultaneous touch response over time using our setup with FSR and GSR electrode. A 10-bit ADC was used for data collection, and both sensors were not saturated, either in the linear signal conditioning electronic, or the ADC measurement. The FSR is from Interlink Electronics, Part No. 402 (0.5" Circle), with a 10K measuring resistor [96] that determines the pressure sensitivity, see Figure 7.10, this circuit was used for GSR measurement as well but with a 2M Ohm measuring resistor (hence the higher pickup noise in the GSR signal of Figure 7.9, which is easily filtered out).

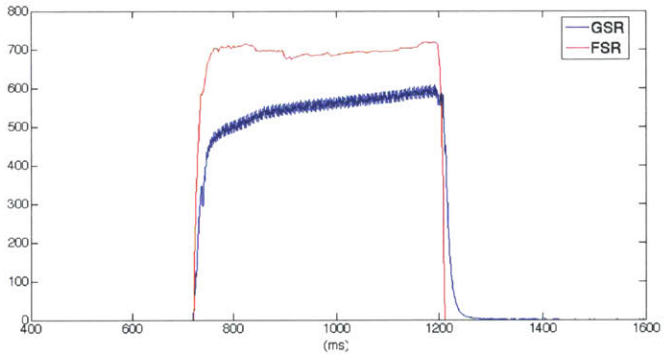

Figure 7.9 A typical touch input over time on a FSR and a GSR electrode. Y-axis is the reading from a 10-bit ADC.

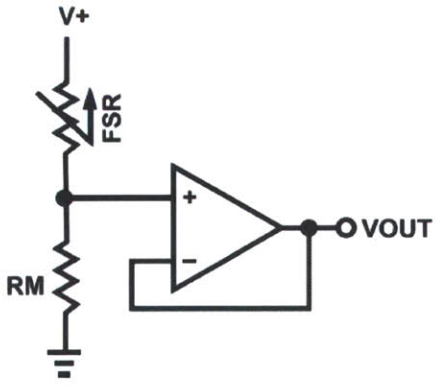

Figure 7.10 FSR voltage divider circuit used in our setup. RM stands for the measuring resistor.

5 users were recruited and asked to "touch" the GSR/FSR input stack 10 times for 5 seconds, each with an interval of 5 seconds between touches. The same experiment was repeated three times every 4 hours during the same day. To get the most stable measurement, I selected the middle 5 of the 10 touches for analysis, and only used the first second of data (1000 samples) in each touch, windowed to remove the applied pressure transient. Figure 7.11 is the relative pressure ratio (GSR/FSR) across users and time. Although there may be some skew due to differential non-linearity, this relative pressure is effectively calibrated by the FSR measurement. The author calibrated the electronics to average at a GSR/FSR ratio to unity for her touches. Figure 7.11(a-c) shows 5 touch inputs across 5 users, at 10am, 2pm and 6 pm.

User 3 has the most consistent input response, while user 5 has some fluctuation in the morning. In order to determine whether the fluctuation comes from GSR, instead of from the fluctuation of the FSR or force inputs, the relative standard deviation (standard deviation divided by mean value) of each group of FSR and GSR readings for each user is plotted as shown in Figure 7.12. The significantly smaller relative standard deviation for most of the FSR data indicates that the noise and variation in the ratio plot (Figure 7.11) comes mainly from the GSR, as we expected. The composite standard deviation of User 1 is 5.5388 for FSR inputs and 14.3325 for GSR inputs. And for User 2, composite STD_{FSR} = 11.5373, STD_{GSR}= 13.8052; User 3 composite STD_{FSR} = 3.2757, STD_{GSR}= 6.3888; User 4 composite STD_{FSR} = 4.6115, STD_{GSR} = 10.4574; User 5 composite STD_{FSR} = 10.947, STD_{GSR} = 9.4832. In general, the standard deviation is much higher for GSR inputs.

Figure 7.13 shows the mean values of the GSR/FSR ratio across all presses for each user at each testing time, with error bars representing the standard deviation of that mean. This plot shows how the temporal variation changes over longer timescales. Each user exhibits slightly different trends, which are

independent of the room humidity and temperature; this essentially reflects their dynamic perspiration changing the skin resistance.

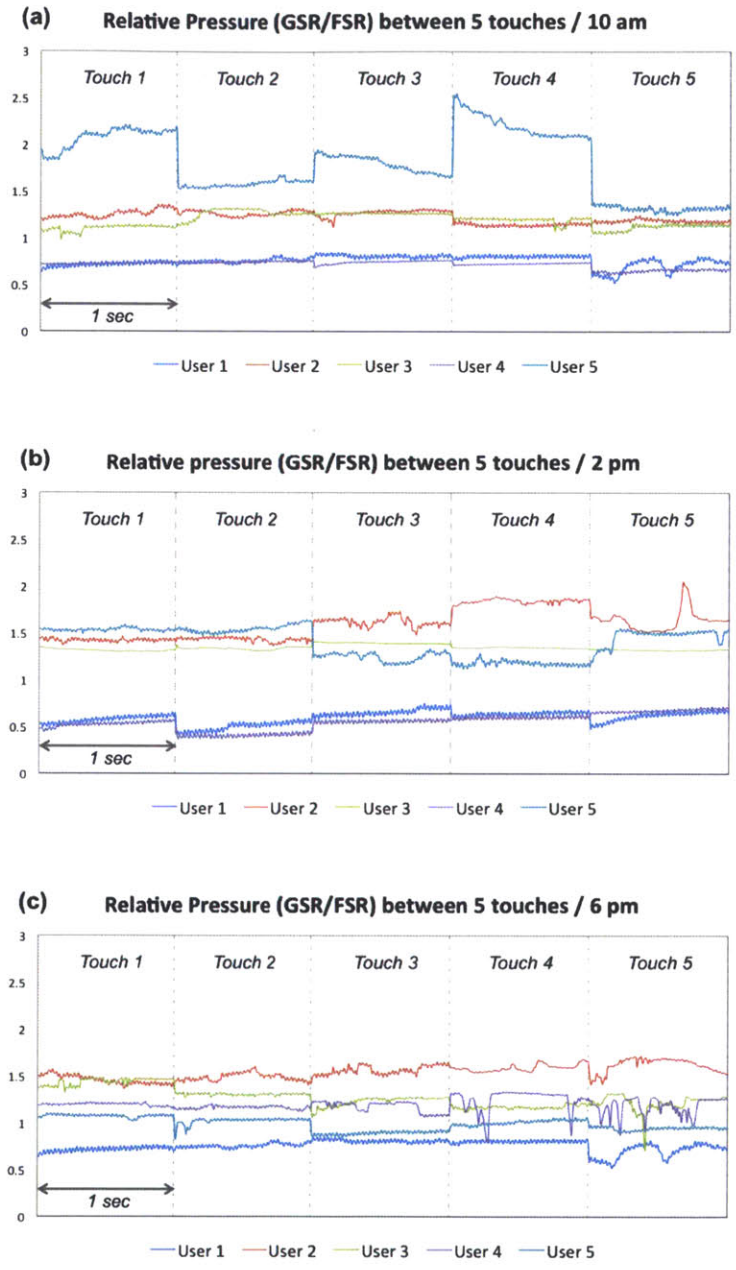

Figure 7.11 Relative Pressure between 5 touch inputs among 5 users across time. Each incontiguous input is 1000 samples with duration of 1 second.

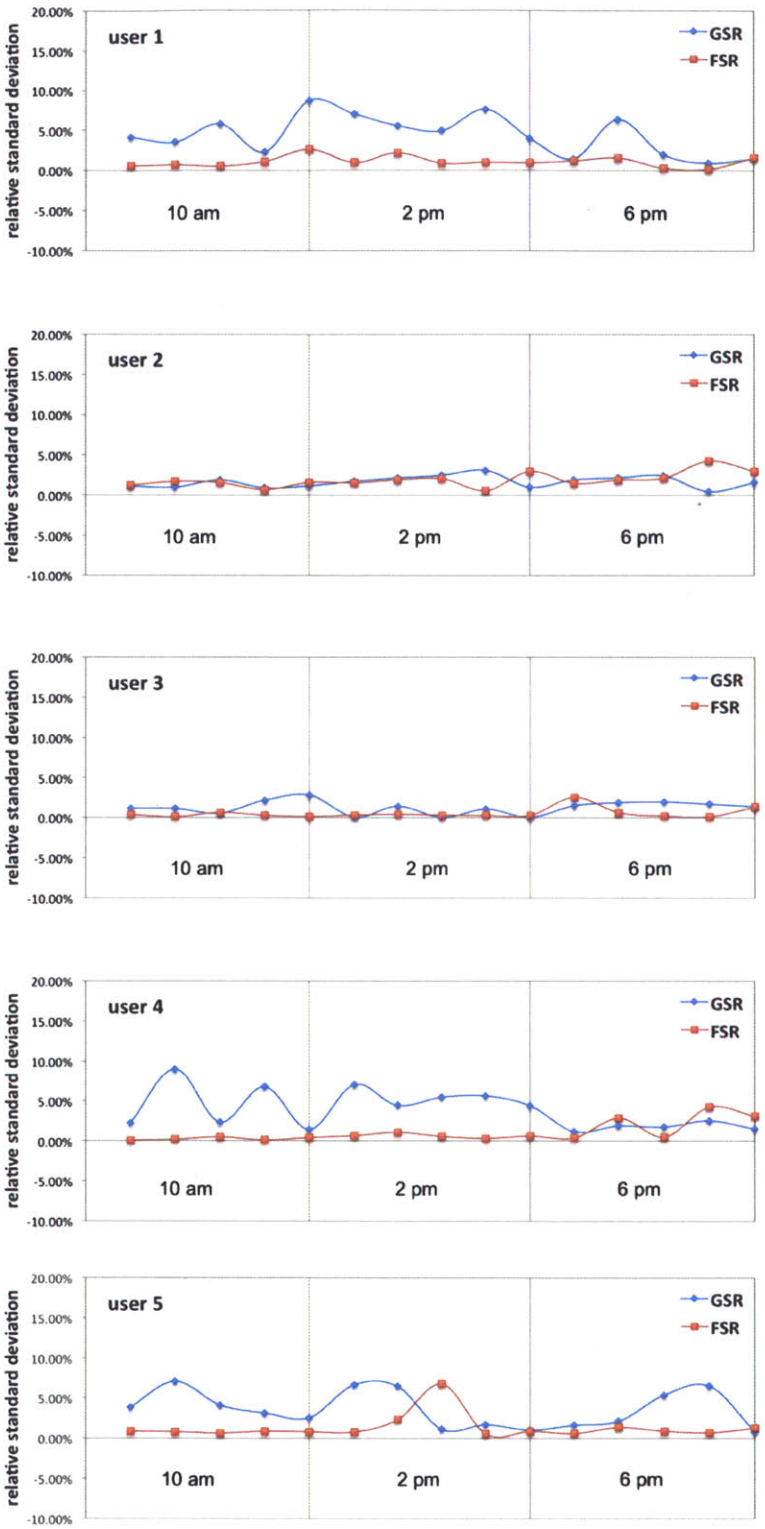

Figure 7.12 Relative standard deviation of FSR and GSR inputs over time for each user. Each point represents the relative standard deviation of a touch input within 1 second, 1000 samples.

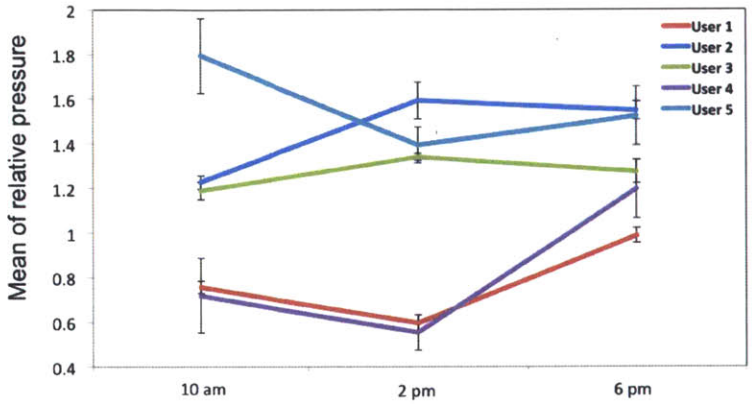

Figure 7.13 Mean values of the GSR/FSR ratio for each user across time, with error bars representing the standard deviation of that mean.

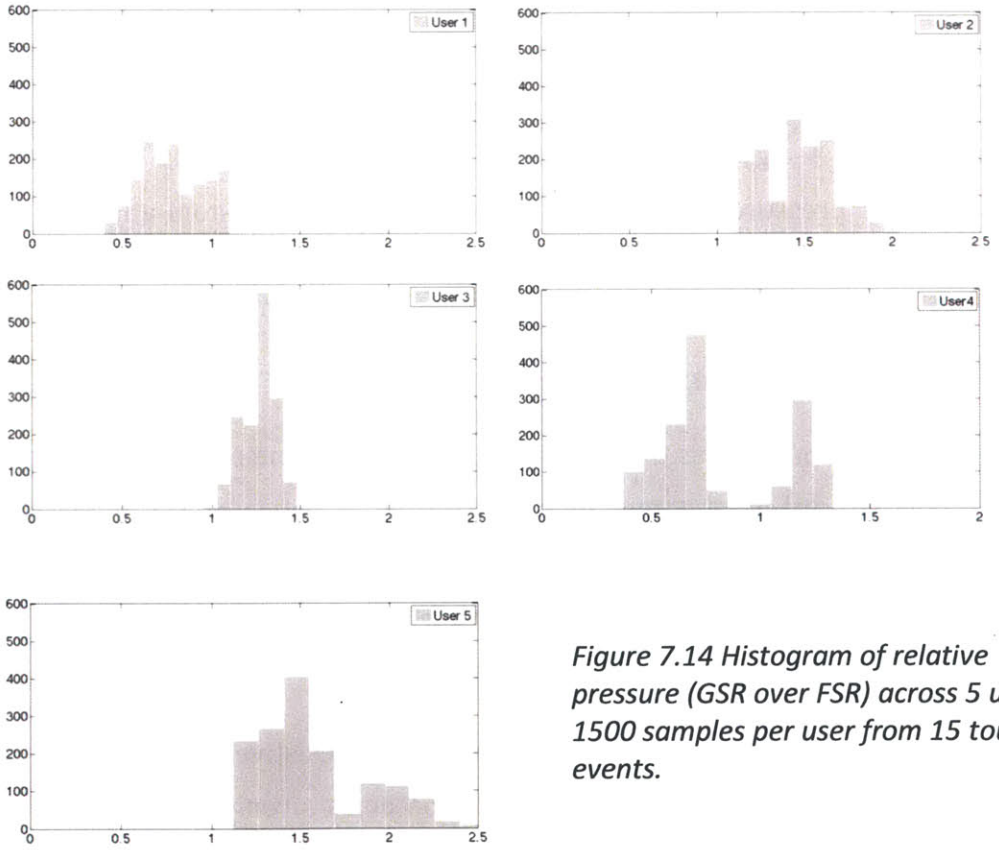

Figure 7.14 Histogram of relative pressure (GSR over FSR) across 5 users. 1500 samples per user from 15 touch events.

To get a clear view about the characteristics of GSR/FSR performance of each user, a histogram of each user's relative pressure response is plotted in Figure 7.14. We can observe a distinctive characteristic within each user. For user 3, a somewhat ideal case, the spread in relative pressure is minimal, and all the inputs are within 1 to 1.5 relative pressure reading. To unify the inferred "force" reading of GSR, we can use such a histogram and try to shift the peak in the distribution to "1", which indicates a similar reading of the FSR and GSR values in the ADC. That said, Figure 7.13 and Figure 7.14 show what a poor pressure sensor the GSR modality provides, as it generally varies greatly across users, time, and touches. As seen in Figure 7.14, user 5's pressure calibration could vary by over 100% and user 4's calibration looks to be bi-modal. Figure 7.11 also shows a noisy time response for some users, indicating perhaps, a spatially inconsistent finger conduction profile due to patches of dry skin or calloused/scarred areas on the finger tip, indicating that GSR finger-touch data should be heavily filtered to avoid "glitching", and that the overall use of GSR data for pressure needs to be very approximate and relative – e.g., the system gives some signal when it thinks the appropriate pressure target is met so users can each custom-adjust their force inputs.

7.6.2 Capacitive proximity sensing

Figure 7.15 demonstrates the raw signal responses of one electrode using AC hum passive capacitive detection and also using resistive pressure sensing. The X-axis is time and Y-axis signal amplitude. The user pointed one finger at a single electrode, approached it, touched it and pressed into the electrode before slowly moving away.

The blue line inferred pressure level from the GSR resistive sensing signal; as the user presses the electrode, the signal becomes stronger. With AC hum detection, we are able to detect fingers and hands around 10 cm above the surface. The red line shows how this signal increases as the finger

approaches until the finger touches the inter-digitated electrode and shunts the capacitive signal to ground, whereupon the signal immediately drops to the 2.5V bias voltage.

More dynamic range can be achieved with active capacitive sensing (shown as the transmit-receive pair in Figure 7.7), which can attain a range up to 20cm.

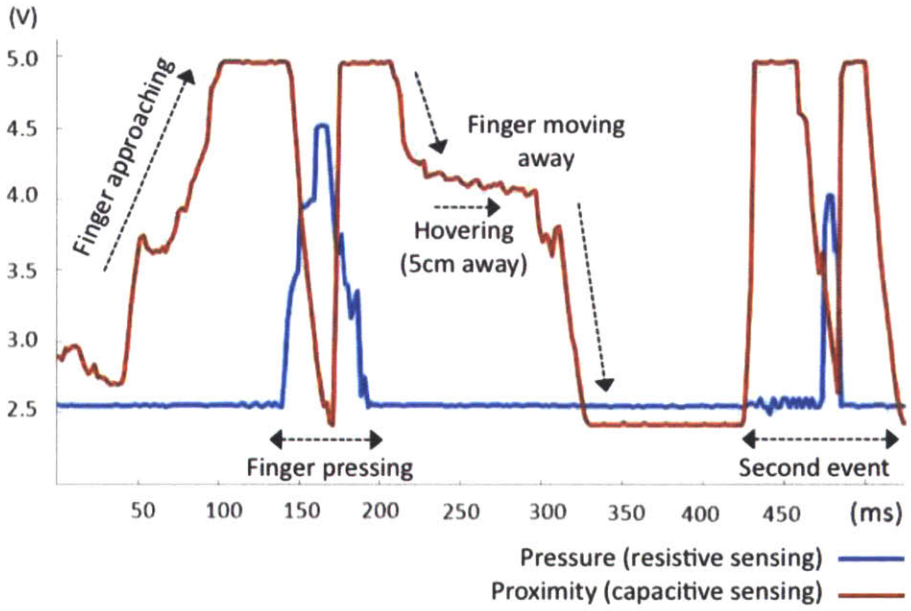

Figure 7.15. Near surface sensing signal responses of one electrode.

7.7 Example use cases

In order to demonstrate application scenarios for PrintSense, we picked two examples that require different configurations of our system, which we present here.

7.7.1 Use Case 1: Grasp Detection on Curved Objects

The first use case is grasp detection for curved objects, in which the main sensing method is resistive sensing. Our example object is an insulated coffee beaker (as shown in Figure 7.16), which is wrapped with a substrate of printed electrodes. A set of six gestures were performed: *no touch, one finger,*

pinch, three fingers, four fingers and whole hand grasp. Although further machine learning implementation would need to be done to ascertain how well actual grasp detection works, these results indicated that this array can separate the various stages of grasps.

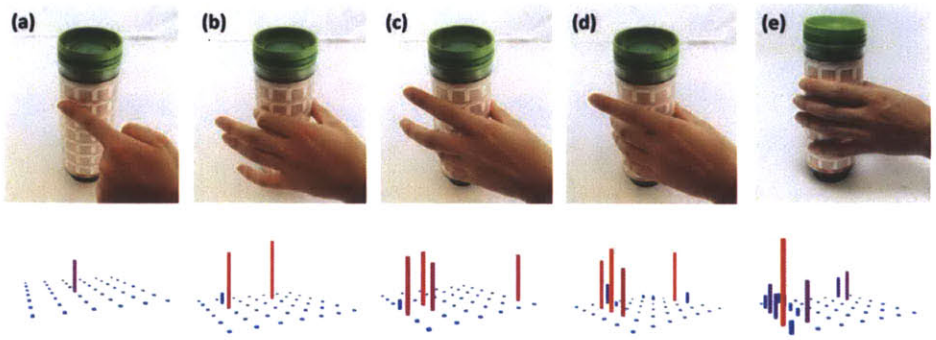

Figure 7.16. Grasp detection and raw data on curved objects. (a) One finger touch. (b) Pinch – two fingers input. (c) Three fingers touch. (d) Four fingers touch. (e) Whole hand grasp. Raw data visualization below each image is from resistive sensing and capacitive pressure sensing. The length and color both represent the level of pressure.

7.7.2 Use Case 2: Manipulation of Flexible Surfaces

In our second use case, I demonstrate detection of the manipulation of a flexible surface, more specifically bending and folding the corners of this surface. An example application would be e-book navigation using a flexible display. A set of gestures were evaluated: *no touch, folding with left hand, folding with right hand.* As demonstrated in Figure 7.17, clear distinguishable results were observed for different folding motions. Note that two of the corner electrodes ((1) and (3) in the figure 7.17) are transmitting a signal in alternation, which is picked up by the closest inter-digitated electrodes. When the hand is touching the transmitting electrode directly, the signals are similar in character, but uniformly bigger, providing a longer detection range.

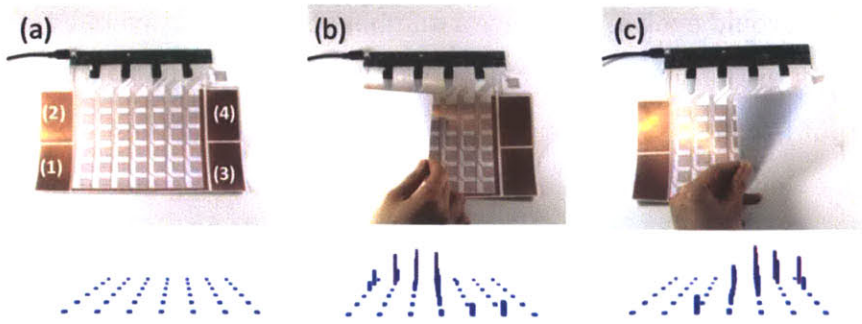

Figure 7.17. Using PrintSense to detect folding. (a) The basic setup; electrodes 1 and 3 are active transmitters. (b) Folding over the left-hand corner. (c) Folding the right side. The raw capacitive receiver data from each electrode is shown in the bottom row.

7.8 Discussion and conclusion

In this chapter, I presented PrintSense, an architecture for utilizing single-layer flexible printed conductive electrode arrays to support a range of sensing modalities and associated interactions such as touch, proximity, pressure and folding. The advantage of our approach over previous research that supports low-cost single-layer flexible sensing surfaces is the use of multi-modal sensing.

This implementation was designed for simulating a flexible display or e-paper display. For other applications, such as swing training on a tennis racket, the associated circuitry will be designed with wireless and low-power capabilities. Of course, there are a number of limitations with this system. For example, resistive sensing relies on a good electrical contact, which in turn requires reasonably clean electrodes and bare skin. The resistive response can also vary between users and change or stop entirely when the patterned metal tarnishes (which accelerates from skin oils), suggesting that a non-tarnishing material be printed or that the touch-exposed electrode be plated. I acknowledge that these requirements might be impractical for some commercial applications, but none-the-less believe that resistive pressure sensing is interesting in a prototyping scenario and that sufficiently robust

approaches could evolve. There are a number of interesting avenues for future work. I am exploring the use of machine learning techniques to characterize the output from PrintSense sensor arrays in order to detect gestures, different types of object manipulation and so on. Additional sensing modalities such as light, humidity and chemical sensing could in theory be incorporated through the addition of suitable polymer layers to the substrate, as outlined in Section 5.3. To conclude, my overall aim has been to highlight a spectrum of sensing techniques for flexible conductive surfaces and to illustrate when and why they might be valuable.

Chapter 8

Conclusion

This dissertation has presented a series of research platforms for exploring the design and applications of inkjet-printed sensate surfaces, and demonstrated its potential through a collection of work that covers the following four areas: manufacturing, sensing design, sensing fabrication and sensing applications.

In the *"Manufacturing"* area, two types of printed electronics manufacturing methods are investigated - conductive inkjet-flex printing [14] and conductive Silver nanoparticle ink [15] with an off-the-shelf inkjet printer. The first method has great scalability and bendability, and these advantages are demonstrated with the sensor floor project in Chapter 6 (Multi-modal Sensing: Target Specific Shapes). The second method can support small-scaled manufacturing at home and rapid prototyping for customization. This aspect is presented with two music controller projects in Chapter 4 (Sensing Design: Computer Aided Design for Customization). The two platforms work well for rapid prototyping, but there is still room for improvement. One of the disadvantages of Conductive Inkjet Technology is the substrate material, which has always has to be Mylar. New technologies such as T-Ink, Inc [98] or conductive silver ink that can each print on essentially any kind of surface are promising for broader applications.

User customization was discussed from two approaches – 1) Sensing Design and 2) Sensing Fabrication.

In the *"Sensing Design"* area, I explored designing sensors in a computer-aided design (CAD) environment. In Chapter 4, two example principles are provided – designing on top of existing patterns with the addition of sensing

elements, and designing with parametrically-defined patterns. Combined with customized color patterns, and other digital fabrication tools such as a laser cutter or a 3D printer, users can design their aesthetically-driven interactive surfaces in an integrated, rapid-prototyping environment.

A further goal in digital sensing design is to create software tools with design references and rules for computer-aided sensate surface construction. In this graphic editing environment, users can drag and drop "sensor" templates and modify the vector graphs in order to integrate physical inputs with graphic designs; the associated circuitry and electronics are auto-routed and generated based on an assumed set of design rules.

In the *"Sensing Fabrication"* area, users customize sensate surfaces with physical manipulation without the need of pre-defined graphic design. This concept is demonstrated with two physical geometry designs – linear-shaped sensor tapes, and planar-shaped sensor sheets. Unlike the former digital design method, the surface is pre-manufactured with built-in sensing capabilities, shapes and sizes, and the shapes and sensing targets are processed post-manufacturing. The first example is a multi-touch cuttable sensor sheet. This sensor sheet has a varied redundant wiring design and physically-embedded error correction capabilities. The second example is a humidity sensor tape, which demonstrates both the "additive" aspect of the shape formation, and overlaying additional layers of chemicals to change the sensing targets through printing, or other deposition. Adding an extra layer of chemical for ad-hoc sensing target alteration is also part of the bigger concept of broad multi-modal sensing. However, extra materials are required in this approach, making it less applicable for rapid prototyping before deposition techniques are supported for a wide range of functional materials with a user-friendly machine, such as an inkjet printer.

Lastly, Chapter 6: Multi-modal Sensing: Target Specific Shapes, and Chapter 7: Multi-modal Sensing: Multiplexing Inputs, both describe the *"Sensing Applications"* area, with techniques for the design of multi-modal sensing

with target specific shapes and multiplexing independent inputs for inferring near-surface interactions. A sensor floor-tile network is presented to demonstrate "target specific shapes" for different sensing targets. Examples include special patterns for specific electromagnetic sensing modalities, such as electrodes for capacitive sensing, antennas for Near Field Communication (NFC) and Global System for Mobile Communications (GSM) signal pickup [16]. This example opens the possibility of easily deploying a large-area surface sensing system. The deployment includes peer-to-peer communication through a network of tiles. To make this a practical and truly scalable system, I envision combining printed, flexible batteries and wireless modules for communication and charging the batteries though slow current trickle across long resistive traces or (in the case of very low power demand) environmental energy harvesting as described in Chapter 2.4.

Lastly, for facilitating the rapid prototyping of smart, interactive objects, I present a single-layer printed surface for multi-modal, near surface sensing (pressure, touch, folding, proximity sensing) that is based on multiplexing an input electrode with various analog circuits.

In this thesis, I strove to combine emerging technologies in manufacturing of low-cost flexible electronics with advances in sensing and industrial design for human computer interaction. This work points to a fundamental framework for the future of rapid sensor array prototyping and interactive design.

I envision that in the future, every printer will come with cartridges beyond just different colors, but also dispensing conductive ink and sensing materials. Furthermore, there will be software frameworks that can support users to not only design graphics with clipart templates, but also to intuitively design circuitry and sensors that are integrated with the printout as a "design-for-manufacturing" process.

Appendices

The appendices chapter contains the schematics and designs that are included in this dissertation.

A.1 Sensor Floor schematics

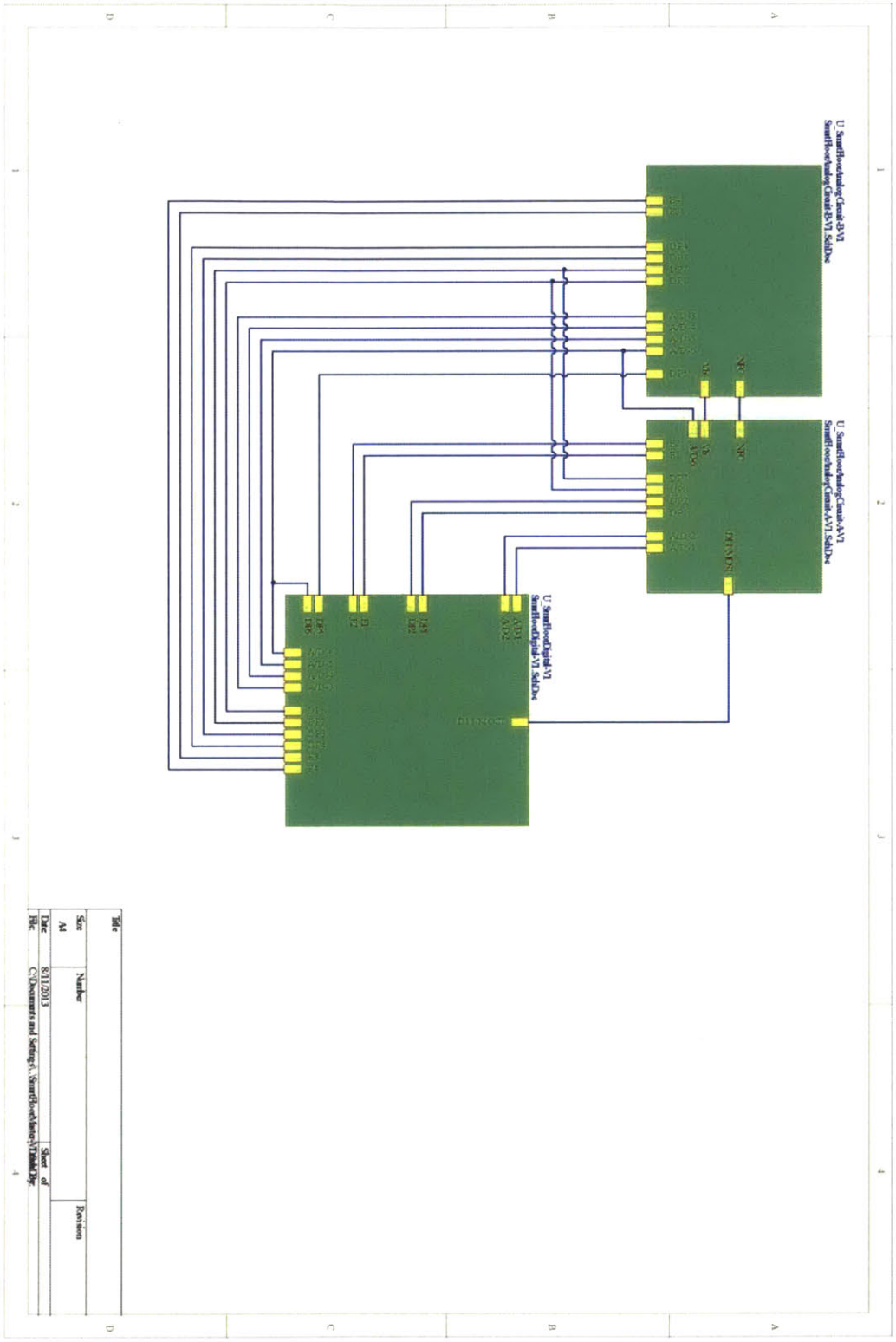

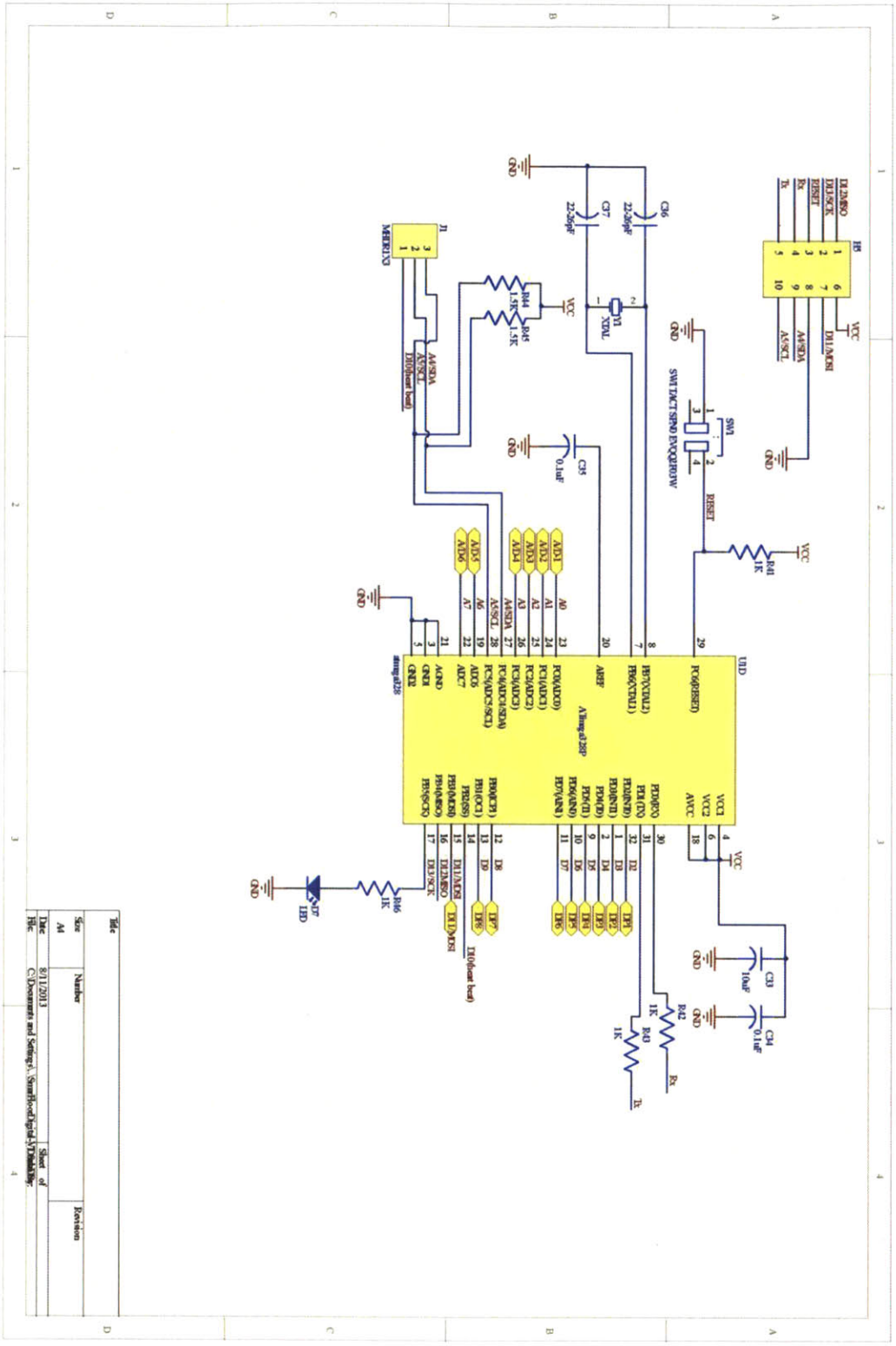

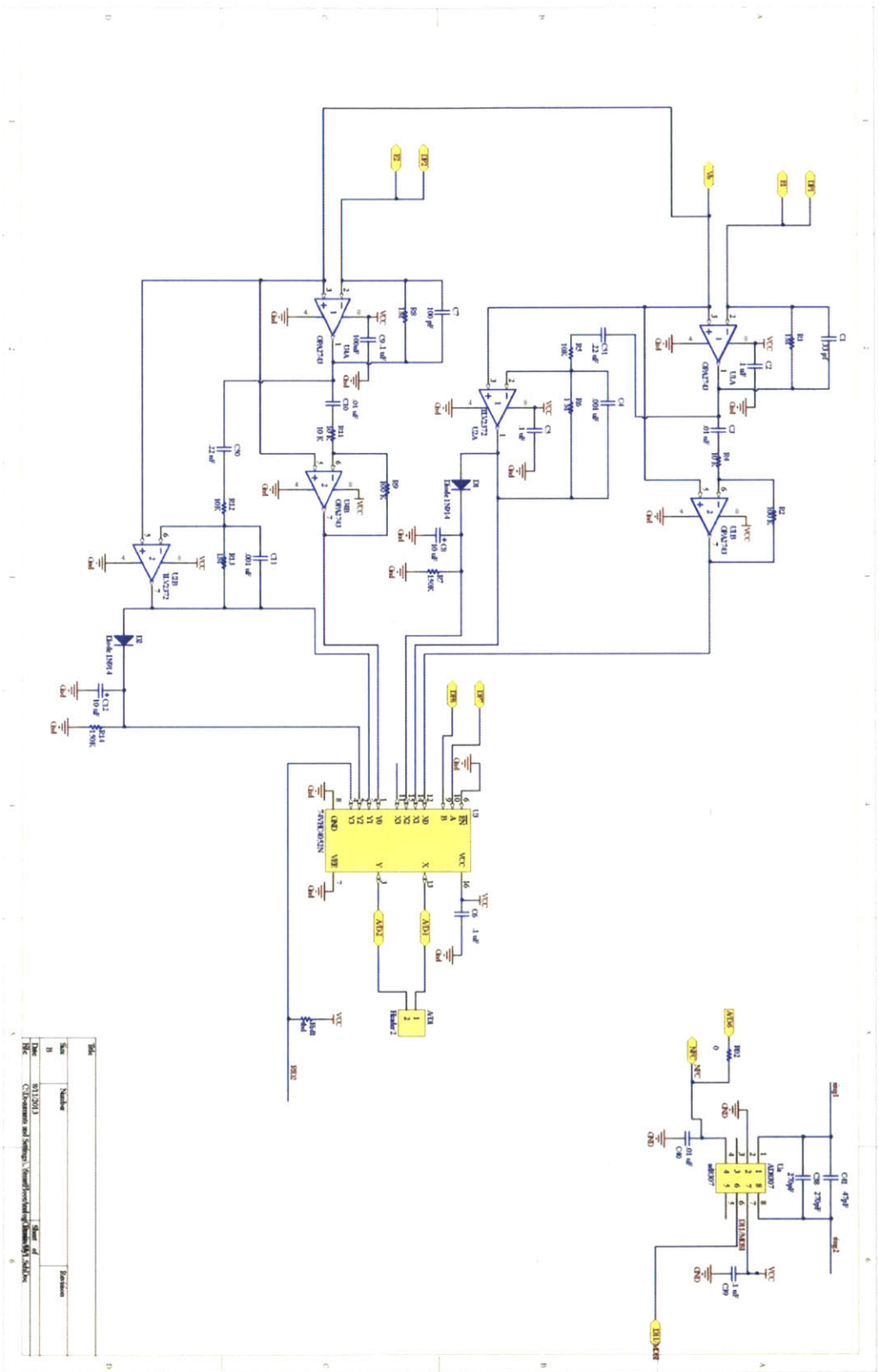

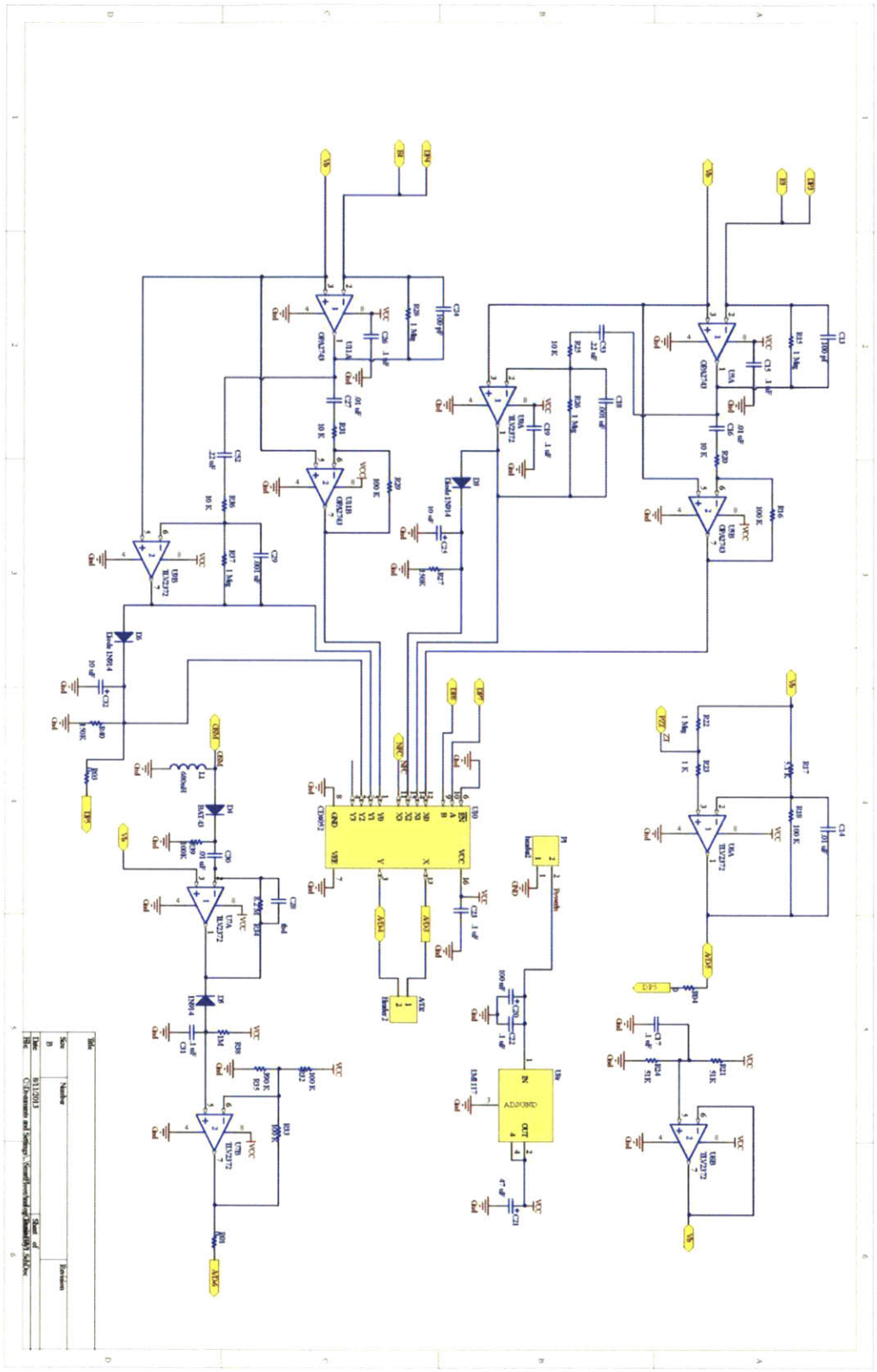

A.2 PrintSense schematics

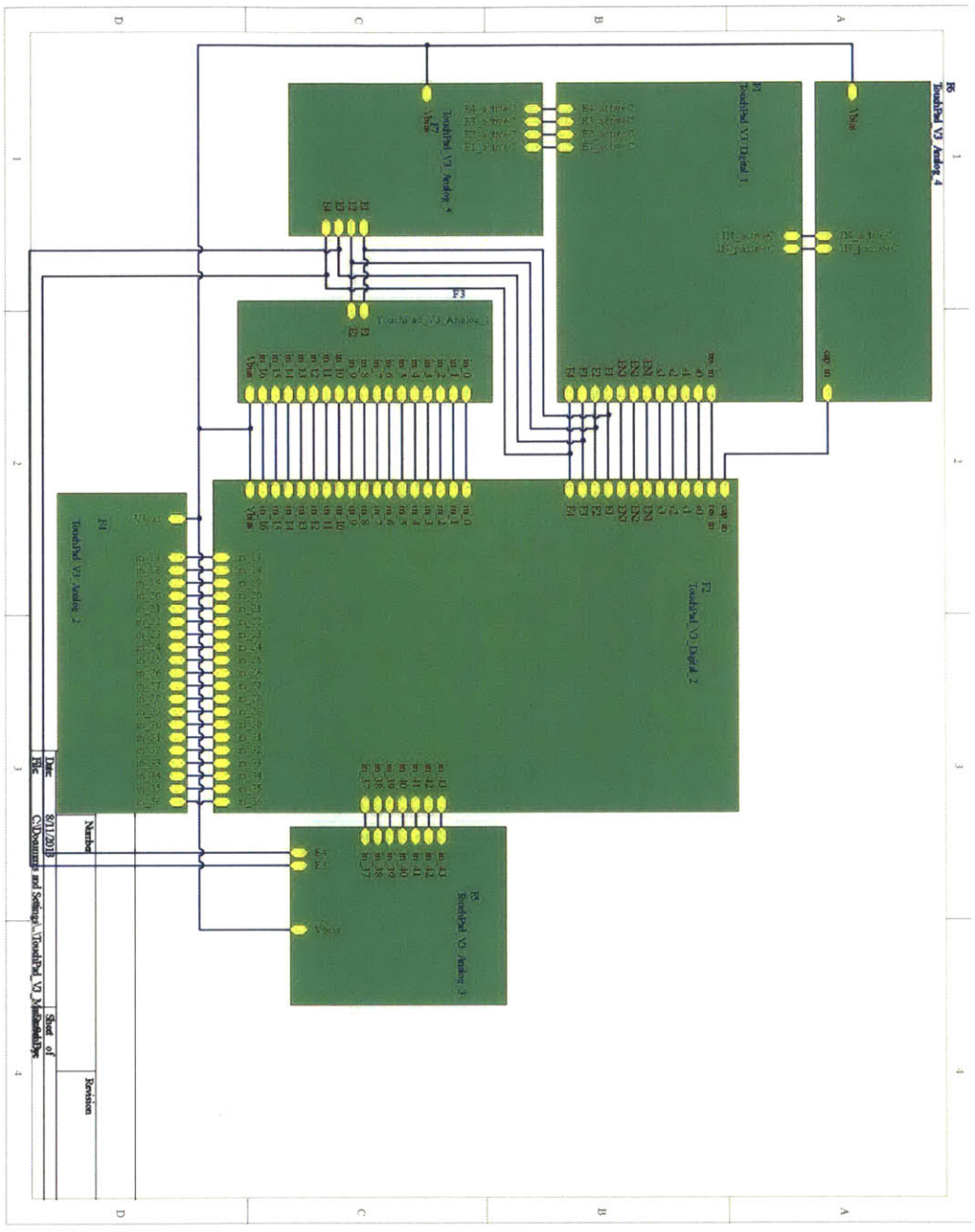

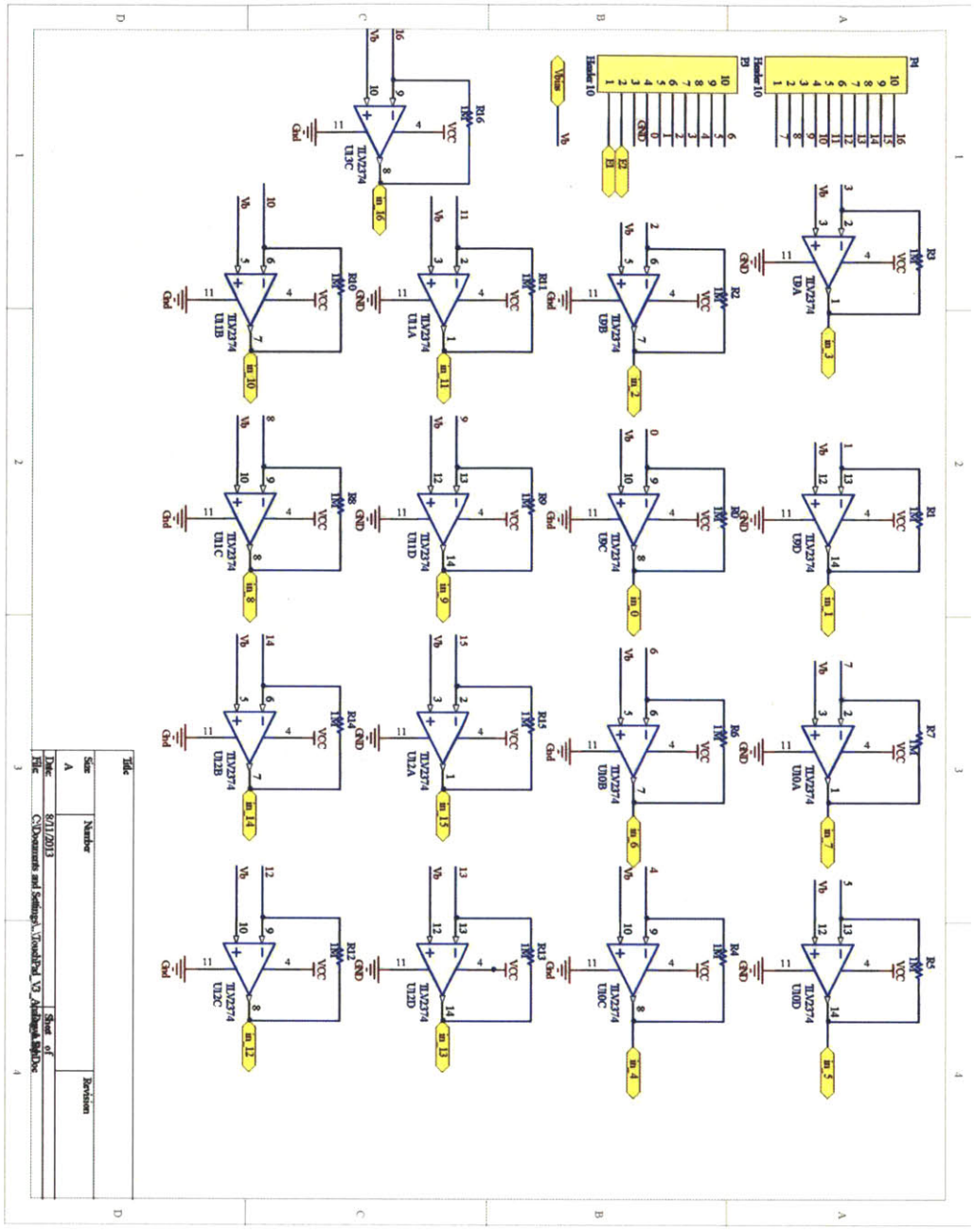

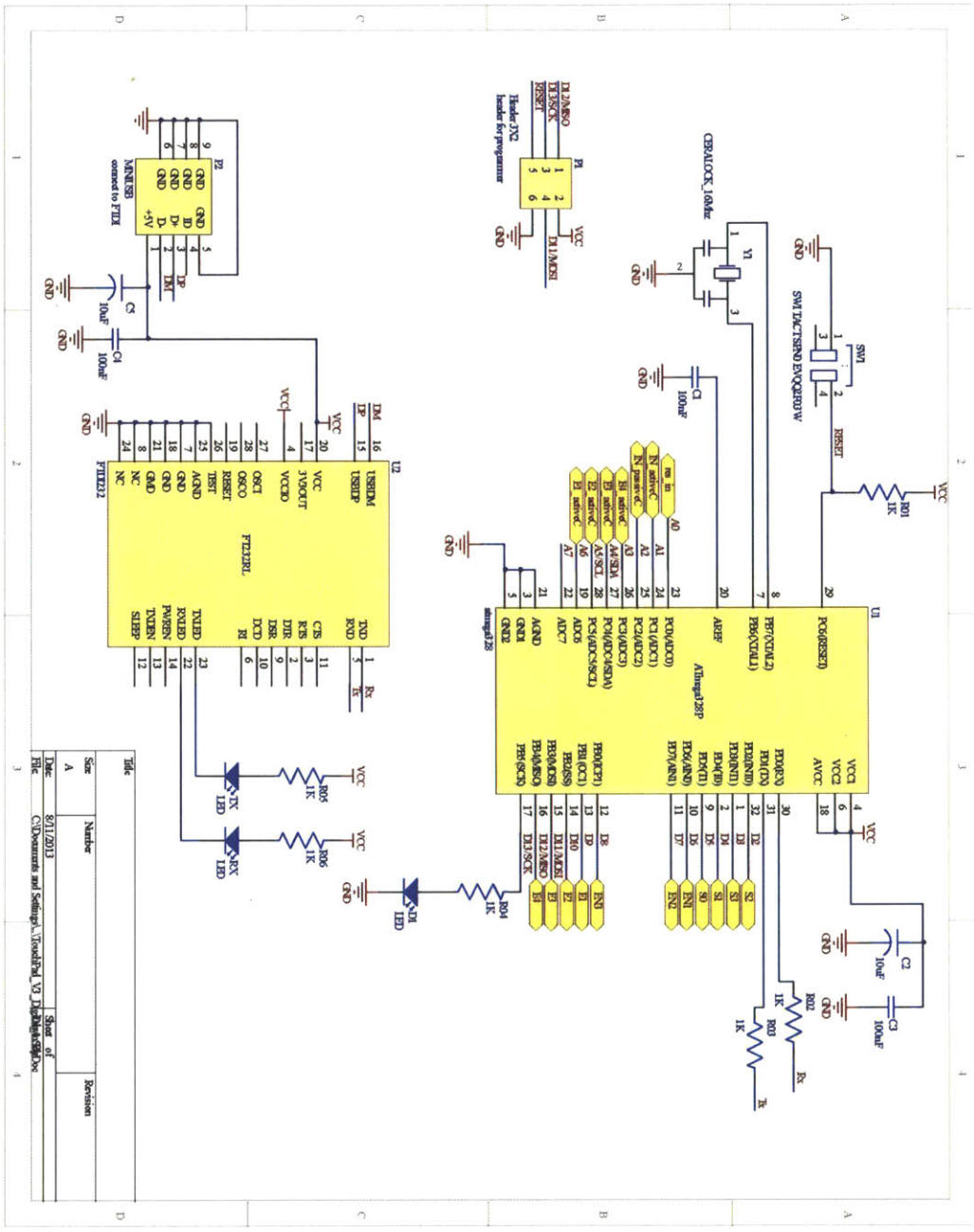

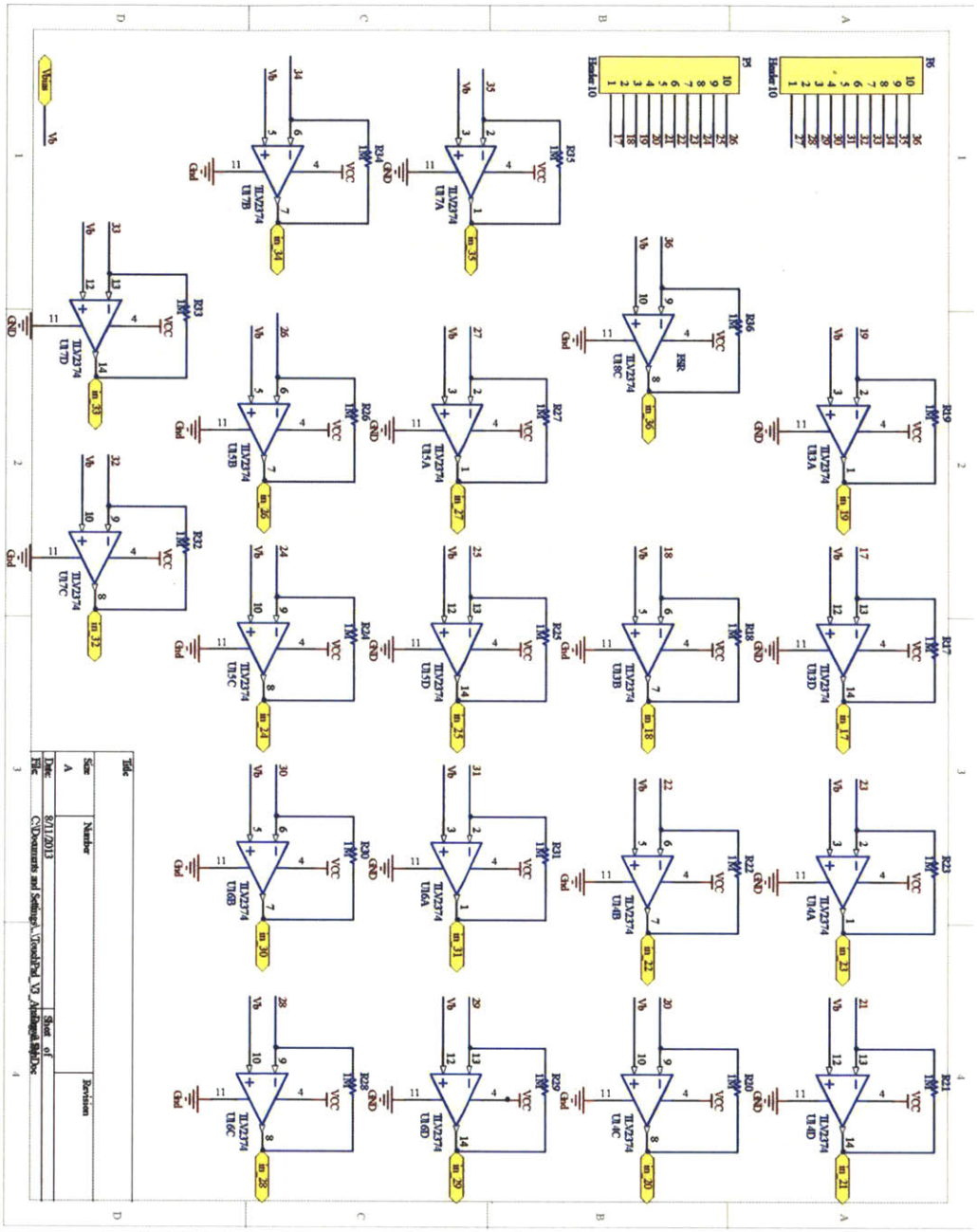

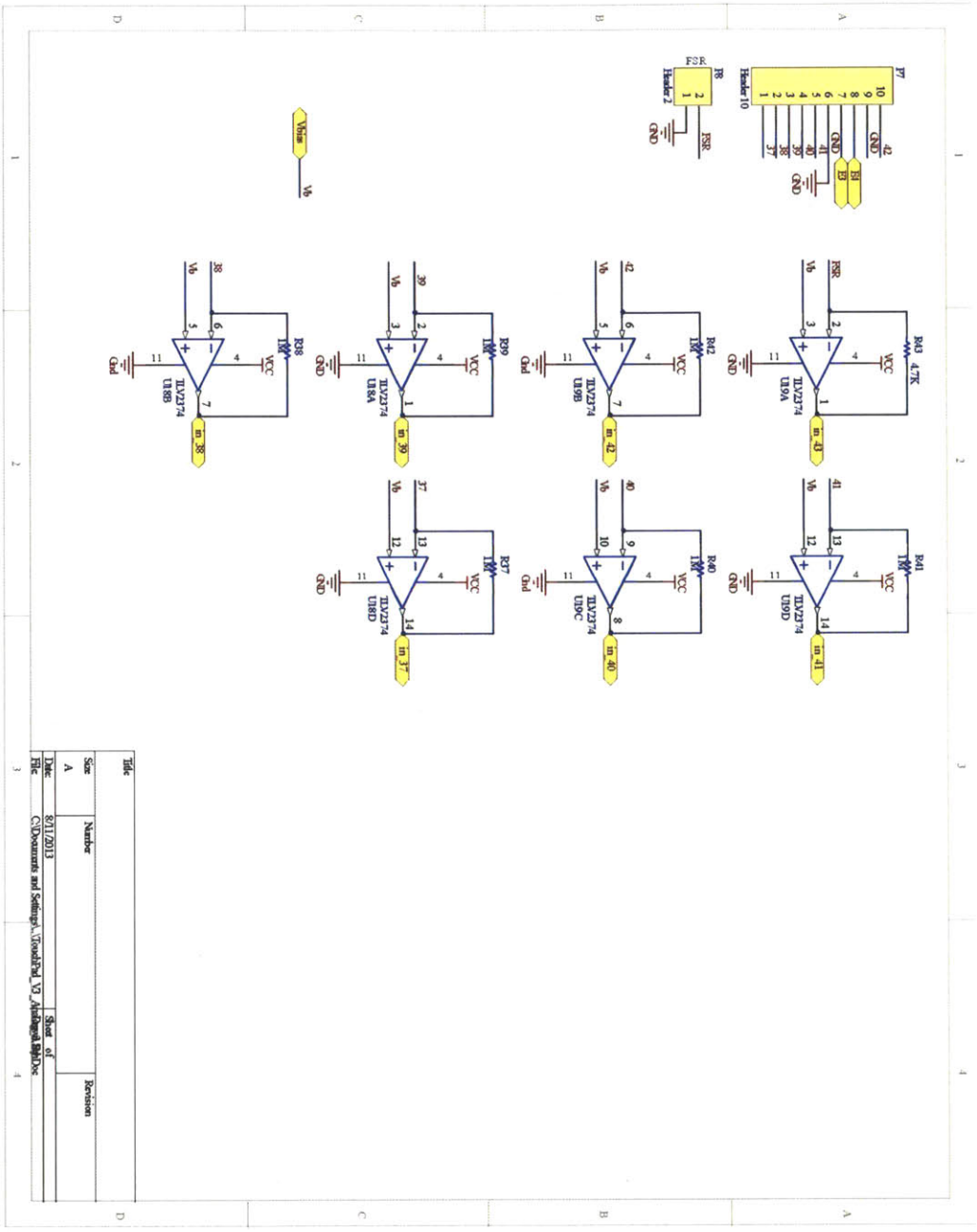
P7
Header 10
GND
P8
Header 2
FSR
Vb
R43 4.7K
R42 1M
R41 1M
R40 1M
R39 1M
R38 1M
R37 1M
TLV2374
U19A
U19B
U19C
U19D
U18A
U18B
U18D
in_43
in_42
in_41
in_40
in_39
in_38
in_37
Gnd
VCC

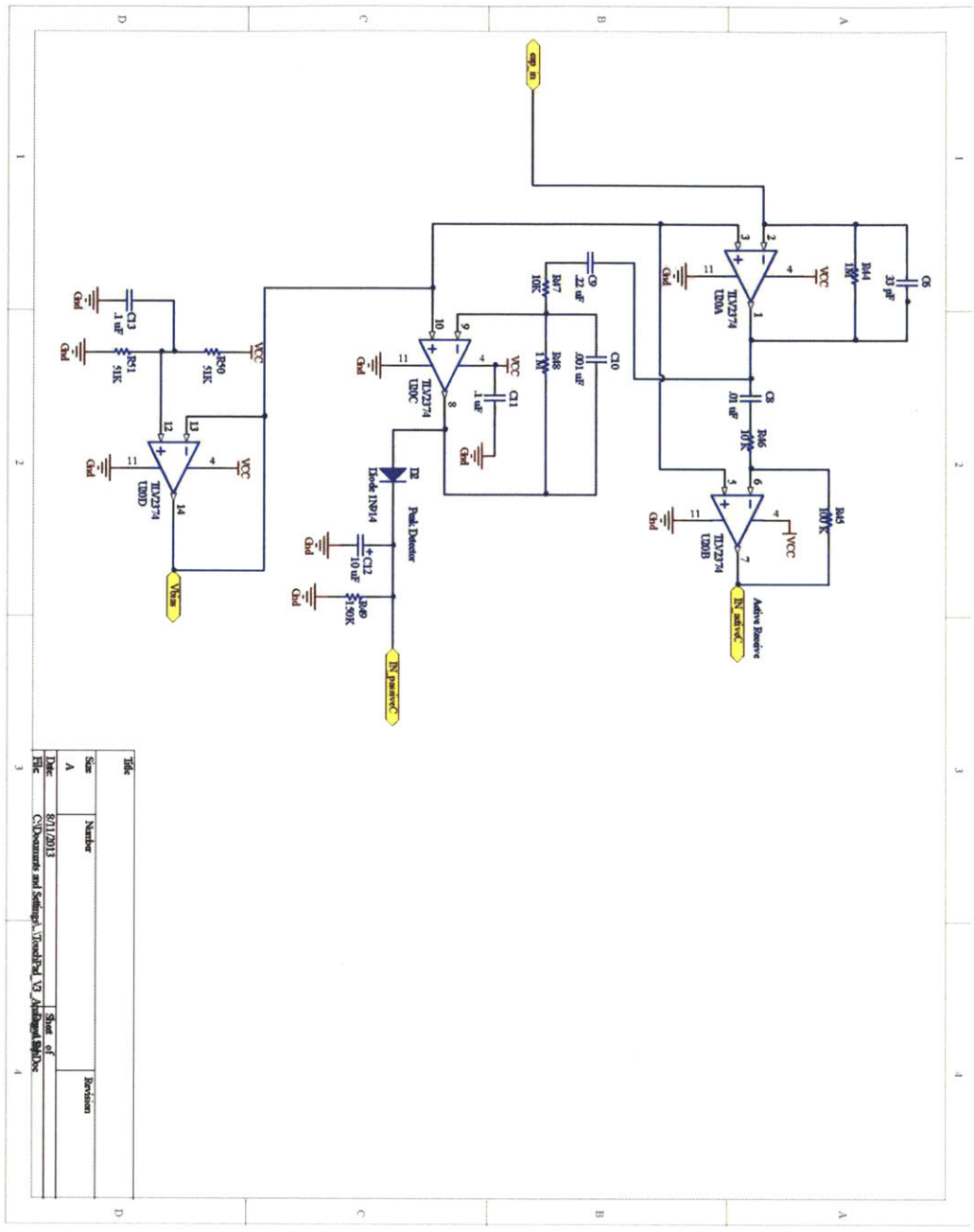

Title		
Size: A	Number	Revision
Date: 8/11/2013	Sheet of	
File: C:\Documents and Settings\...\TrondiPad_V3_AirBeam1.SchDoc		

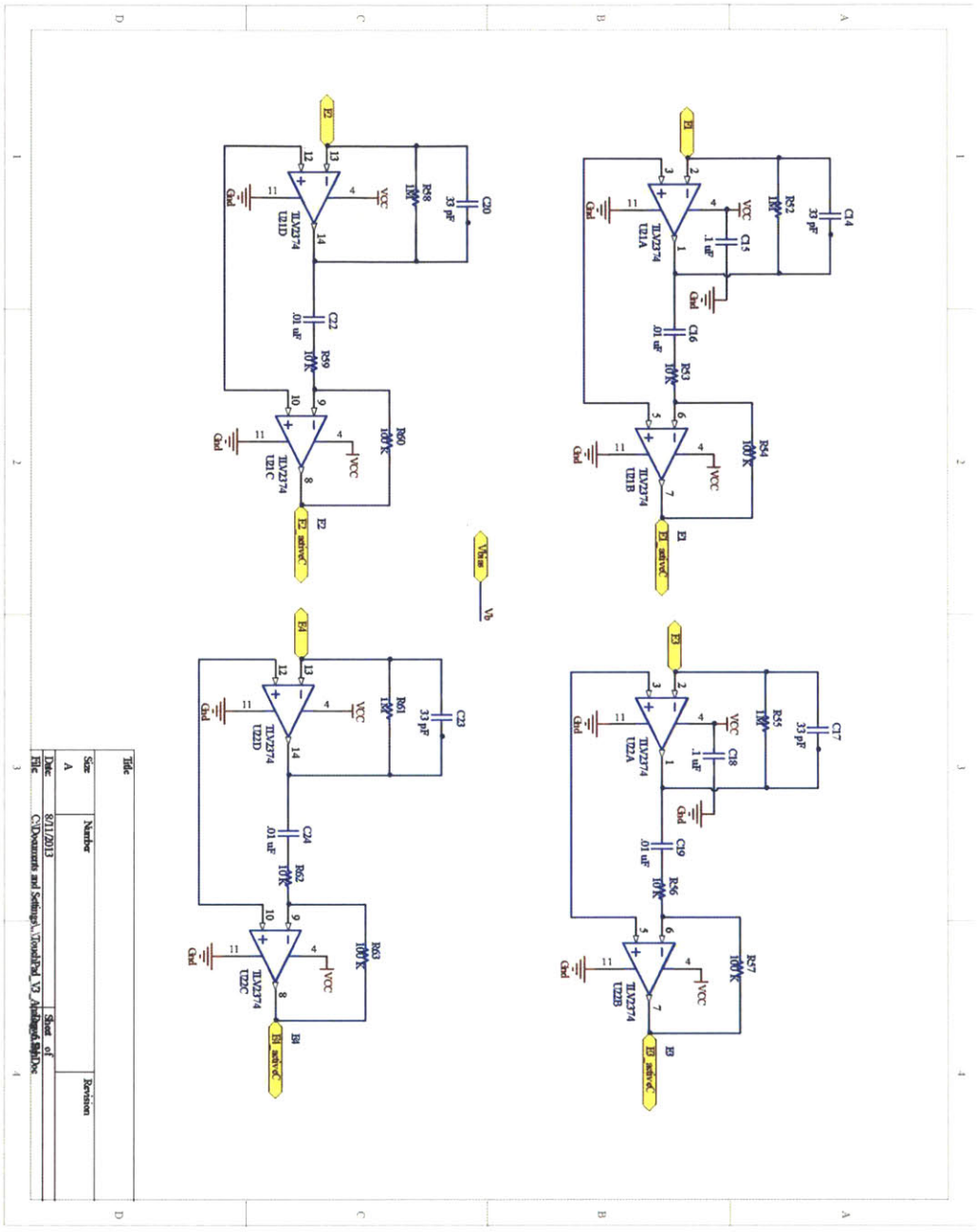
E1
E2
E3
E4
Vbias
Vb
TLV2374
U21A
U21B
U21C
U21D
U22A
U22B
U22C
U22D
R52
R53
R54
R55
R56
R57
R58
R59
R60
R61
R62
R63
C14
C15
C16
C17
C18
C19
C20
C22
C23
C24
VCC
Gnd
E1_activeC
E2_activeC
E3_activeC
E4_activeC
Title
Size
A
Number
Revision
Date:
8/11/2013
Sheet of
File:
C:\Documents and Settings\...\TouchPad_V3_...

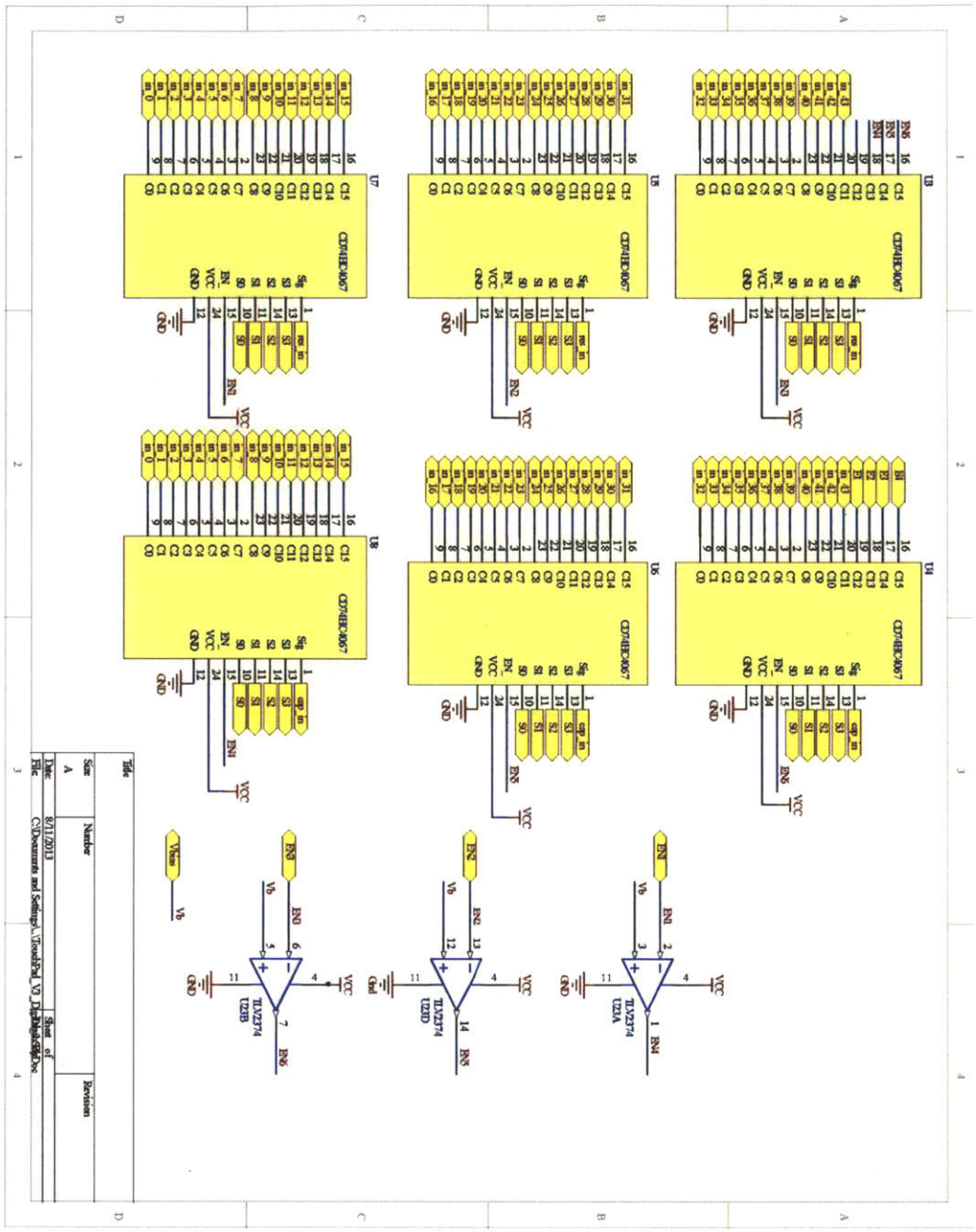

A.3 Design example of a sensate music controller surface

Bibliography

[1] M. Weiser, "The Computer for the 21st Century," *Scientific American* , vol. 265, pp. 94-104 , 1991.

[2] W. S. Wong. and A. Salleo, Flexible Electronics: Materials and Applications, Springer, 2010.

[3] V. J. Lumelsky, M. S. Shur and S. Wagner, "Sensitive Skin," *IEEE Sensor Journal,* pp. 41-51, 2001.

[4] D. Um and V. Lumelsky, "Fault tolerance via component redundancy for a modularizaed sensitive skin," *IEEE Internation Conference on Robotics and Automation,* 1999.

[5] M. Hakozaki, A. Hatori and H. Shinoda, "A sensitive skin using wireless stactile sensing elements," *Technocal Digest of the 19th Sensor Symposium,* 2001.

[6] J. Rekimoto, "Smartskin: an infrastrcture for freehand manipulation on interactive surfaces," *SIGCHI conference on Human Factors in Computing Systems: Changing Our World, Changing Ourselves,* 2002.

[7] I. Rosenberg and K. Perlin, "The UnMousePad: an interpolating multi-touch force-sensing input pad.," *ACM Trans. Graph,* vol. 3, no. 65, p. 28, 2009.

[8] C. Rendl, P. Greindl, M. Haller, M. Zirkl, B. Stadlober and P. Hartmann, "PyzoFlex: Printed Piezoelectric Pressure Sensing Foil," *UIST '12: Proceedings of the 25th Symposium on User Interface Software and Technology,* 2012.

[9] L. Buechley and M. Eisenberg, "Fabric PCBs, electronic sequins, and socket buttons: techniques for e-textile craft," *Personal and Ubiquitous Computing,* vol. 13, no. 2, pp. 133-150, 2009.

[10] Pacelli, M., "Sensing Fabrics for Monitoring Physiological and Biomechanical Variables: E-textile solutions," *Medical Devices and Biosensors,* pp. 1-4, 2006.

[11] Z. Ma, "An Electronic Second Skin," *Science,* vol. 333 , no. 6044 , pp. 830-831 , 12 August 2011.

[12] Dae-Hyeong Kim et al., "Epidermal Electronics," *Science,* vol. 333, no. 6044, pp. 838-843, 12 August 2011.

[13] "Roland," [Online]. Available: http://www.rolanddg.com/product/3d/3d/mdx-20_15/application.html. [Accessed July 2013].

[14] "Conductive Inkjet Technology," [Online]. Available: http://www.conductiveinkjet.com/. [Accessed July 2013].

[15] "Mitsubishi Paper Mills," [Online]. Available: http://www.mpm.co.jp/eng/cnews/pdf/20120426e.pdf. [Accessed July 2013].

[16] N.-W. Gong, S. Hodges and J. A. Paradiso, " Leveraging Conductive InkjetTechnology to Build a Scalable and Versatile Surface for Ubiquitous Sensing," in *Ubicomp 11*, Beijing, China, 2011.

[17] N.-W. Gong, C.-Y. Wang and J. A. Paradiso, "Low-cost Sensor Tape for Environmental Sensing Based on Roll-to-roll Manufacturing Process," in *IEEE SENSORS* , Taipei, 2012.

[18] K. A. Mirica, J. G. Weis, J. M. Schnorr, B. Esser and T. M. Swager, "Mechanical Drawing of Gas Sensors on Paper," *Angewandte Chemie International Edition,* vol. 51, no. 43, pp. 10740-10745, 2012.

[19] J. A. Paradiso, "Sensate Media," *Communications of the ACM,* vol. 48, no. 3, p. 70, 2005.

[20] J. Paradiso, J. Lifton and M. Broxton, "Sensate media: Multi-modal electronic skins as dense sensor networks," *BT Technology Journal,* vol. 22, no. 4, pp. 32-44, 2004.

[21] W.D.Stieh and C. Breaeal, "A Sensitive Skin for Robotic Companions Featuring Temperature, Force, and Electric Field Sensors," *IEEE/RSJ International Conference on Intelligent Robots and Systems,* pp. 1952-1959.

[22] B. Mistree and J. Paradiso, "ChainMail – A Configurable Multimodal Lining to Enable Sensate Surfaces and Interactive Objects," *Tangible, Embedded and Embodied Interaction,* pp. 65-72, 2010.

[23] J. Lifton, M. Broxton and J. A. Paradiso, "Distributed Sensor Networks as Sensate Skin," *IEEE Sensors,* 2003.

[24] G. B. Péerez, "S.N.A.K.E.: A Dynamically Reconfigurable Artificial Sensate Skin," MEng. Thesis, Massachusetts Institute of Technology, 2006.

[25] J. Lifton, M. Broxton and J. Paradiso, "Experiences and Directions in Pushpin Computing," *Proc. of IPSN,* vol. 05, pp. 416-421, 2004.

[26] K. Jain, M. Klosner, M. Zemel and S. Raghunandan, "Flexible Electronics and Displays: High--Resolution, Roll-to-Roll, Projection Lithography and Photoablation Processing Technologies for High Throughput Production," in *IEEE*, 2005.

[27] S. Liu and F. Guimbretière, "FlexAura: a flexible near-surface range sensor," in *UIST '12*, 2012.

[28] R. Balakrishnan, G. Fitzmaurice, G. Kurtenbach and K. Singh, "Exploring Interactive Curve and Surface Manipulation Using a Bend and Twist Sensitive Input Strip," in *Proceedings of 1999 ACM Symposium on Interactive 3D Graphics, pp 111-118.*

[29] d. Holman and R. Vertegaal, "TactileTape: Low-Cost Touch Sensing on Curved Surfaces," in *UIST '11*, 2011.

[30] R. Wimmer and P. Baudisch, "Modular and Deformable Touch-Sensitive Surfaces Based on Time Domain Reflectometry," in *UIST'11*, 2011.

[31] N. Villar et al., "Mouse 2.0: multi-touch meets the mouse," in *UIST 09'*, 2009.

[32] D. Wigdor, D. Leigh, C. Forlines, S. Shipman, J. Barnwell, R. Balakrishnan and C. Shen, "Under the table interaction.," in *in Proceedings of UIST '06.*

[33] B. T. Taylor and M. J. Bove, "Graspables: grasp-recognition as a user interface," in *CHI '09*, 2009.

[34] B. T. Taylor and V. M. Bove, "The bar of soap: a grasp recognition system implemented in a multi-functional handheld device," in *In CHI EA '08*, 2008.

[35] Sun, M. et al., "Enhancing naturalness of pen-and-tablet drawing through context sensing," in *Proceedings of ITS*, 2011.

[36] D. Pai et al., "The Tango: A Tangible Tango receptive Whole-Hand Human Interface. Proc. of World Haptics," in *IEEE Press*, 141-147, 2005.

[37] "http://www.phidgets.com/," 2013. [Online].

[38] B. Hartmann, S. R. Klemmer, M. Bernstein, L. Abdulla, B. Burr, A. Robinson-Mosher and J. Gee, "Reflective physical prototyping through integrated design, test, and analysis," *UIST,* pp. 299-308, 2006.

[39] D. Avrahami and S. E. Hudson, "Forming interactivity: a tool for rapid prototyping of physical interactive products," *Proceedings of the conference on Designing interactive systems: processes, practices, methods, and techniques,* 2002.

[40] R. Ballagas, M. Ringel, M. Stone and J. Borchers, "iStuff: a physical user interface toolkit for ubiquitous computing environments," *Proceedings of the SIGCHI conference on Human factors in computing systems,* 2003.

[41] "LEGO Mindstorms Robotic Invention System," [Online]. Available: http://www.mindstorms.lego.com/ .

[42] "http://research.microsoft.com/en-us/projects/gadgeteer/," Microsoft, 2013. [Online].

[43] "Cybelius," [Online]. Available: http://www.cybelius.com/products. [Accessed 2013].

[44] V. Savage, X. Zhang and B. Hartmann, "Midas: fabricating custom capacitive touch sensors to prototype interactive objects," *UIST ,* 2012.

[45] "Sketch-a-TUI: low cost prototyping of tangible interactions using cardboard and conductive ink," *TEI,* 2012.

[46] S. Jacoby and L. Buechley, "Drawing the Electric: Storytelling with Conductive Ink," *IDC,* 2013.

[47] "MaKey MaKey: An Invention Kit for Everyone," 2013. [Online]. Available: www.makeymakey.com/.

[48] J. Huang, H. Zhu, Y. Chen, C. Preston, K. Rohrbach, J. Cumings and L. Hu, "Highly Transparent and Flexible Nanopaper Transistors," *ACS NANO,* vol. 7, no. 3, pp. 2106-2113, 2013.

[49] "Blue Spark Technologies," [Online]. Available: http://www.bluesparktechnologies.com/.

[50] "eMbedded Organic Memory Arrays (MOMA project)," [Online]. Available: http://www.moma-project.eu/.

[51] T. Ng, A. C. Arias, J. H. Daniel, S. Garner, L. Lavery, S. Sambandan and G. L. Whiting, " Flexible printed sensor tape," *IDTechEx Printed Electronics Asia,* 2009.

[52] "FujiFilm Materials Printer," [Online]. Available: http://www.fujifilmusa.com/products/industrial_inkjet_printheads/deposition-products/dmp-2800/. [Accessed 2013].

[53] R. Vyas, V. Lakafosis, H. Lee, G. Shaker, L. Yang, G. Orecchini, A. Traille, M. M. Tentzeris and L. Roselli, "Inkjet Printed, Self Powered, Wireless Sensors for Environmental, Gas and Authentication-Based Sensing," *IEEE Sensors,* vol. 11, no.

12, pp. 3039-3052, 2011.

[54] Y. Kawahara, H. Lee and M. M. Tentzeris, "SenSprout: inkjet-printed soil moisture and leaf wetness sensor," *Ubicomp,* p. 545, 2012.

[55] [Online]. Available: http://www.nordson.com/en-us/divisions/efd/products/solder-paste/dispensing-paste/pages/default.aspx. [Accessed 2013].

[56] "3M Z-axis Conductive Adhesive Transfer Tape," [Online]. Available: http://www.3m.com/product/information/Electrically-Conductive-Adhesive-Transfer-Tape.html. [Accessed 2013].

[57] M. Wright, D. Wessel and A. Freed, "New Musical Control Structures from Standard Gestural Controllers," *In Proc. of the International Computer MusicConference,* pp. 387-390, 1997.

[58] P. Bruguière, D. Bethmann, D. E, F. Gaudin and P. Fonteneau, Musée de la Musique, Paris: Somogy Art Publishers, 2009.

[59] D. Kuronen, L. Kaye and C. Tremblay, Dangerous Curves: The Art of the Guitar, MFA Publications , 2000.

[60] O. Lähdeoja, M. M. Wanderley and J. Mallo, "Instrument Augmentation Using Ancillary Gestures for Subtle Sonic Eefects," *Proceedings of the SMC 2009 6th Sound and Music Computing Conference,* pp. 23-25, 2009.

[61] D. Thompson, The Stompbox: A History of Guitar Fuzzes, Flangers, Phasers, Echoes and Wahs, 1997.

[62] B. J. Rodriguez and H. Starr, "The Ztar MIDI Controller," *FORMAL,* 1998.

[63] D. Curves, The art of the guitar, I, SBN: 0878464786, MFA Publications, 2000.

[64] R. Koehly, D. Curtil and M. Wanderley., "Paper FSRs and latex/fabric traction sensors: Methods for the development of home-made touch sensors," *In Proc. of the 2006 Conf. on New Interfaces for Musical Expression (NIME-06,* p. 230–233, 2006.

[65] [Online]. Available: http://insidetv.ew.com/2008/10/27/nbc-chime-in-ca/.

[66] "Instructables," [Online]. Available: http://www.instructables.com/id/Make-a-Korg-Kaossilator-Guitar/.

[67] A. Zoran and J. Paradiso, "The chameleon guitar—guitar with a replaceable resonator.," *Journal of NewMusic Research,* vol. 40, p. 59–74, 2011.

[68] R. Jones et al., "A Force-Sensitive Surface for Intimate Control," *In Proceedings of the International Conference on New Interfaces for Musical Expression (NIME),* pp. 236-241.

[69] A. Freed and J. Rowland, "Collocated Surface Sound Interaction," *in CHI 2013, Interactivity Demo Session.*

[70] C. Roads and J. Strawn, "Foundations of Computer Music," Cambridge MA, MIT Press, 1985, pp. 257-260.

[71] H. Scharstein, "Input-output relationship of the Leaky-Integrator Neuron Model.," *Journal of Mathematical Biology. ,* vol. 8, no. 4, pp. 403-420, 1979.

[72] "Sensate Cooktops," [Online]. Available: http://resenv.media.mit.edu/Cooktops/index.html.

[73] "PSoC® 4 CapSense® Design Guide - Cypress Semiconductor," [Online]. Available: http://www.cypress.com/?docID=43145.

[74] S. Olberding, N.-W. Gong, J. Tiab, J. Paradiso and J. Steimle, "A Cuttable Multi-touch Sensor," *UIST,* 2013.

[75] M. K. Ghosh and K. L. Mittal, Polyimides: Fundamentals and Applications, CRC Press, 1996.

[76] H. Grange, C. Bieth, H. Boucher and G. Delapierre, "A capacitive humidity sensor with very fast response time and very low hysteresis," *Sens. & Actuators,* vol. 12, pp. 291-296, 1987.

[77] K. A. Mirica, J. G. Weis, J. M. Schnorr, B. Esser and T. M. Swager, "Mechanical Drawing of Gas Sensors on Paper," *Angewandte Chemie International Edition,* vol. 51, no. 43, pp. 10740-10745, 2012.

[78] R. J. Orr and G. D. Abowd, "The Smart Floor: A Mechanism for Natural User Identification and tracking," *CHI,* 2000.

[79] A. Schmidt.et al., "Context Acquisition Based on Load Sensing," *UbiComp 2002,* 2002.

[80] J. A. Paradiso et al., "The Magic Carpet: Physical Sensing for Immersive Environments.," *Ext. Abstracts CHI ,* no. ACM Press, pp. 277-278, 1997.

[81] N. Griffith and M. Fernström, ",LiteFoot: A floor space for recording dance and controlling media.," *In: Proceedings of ICMC,* p. 475–481, 1998.

[82] A. Kidané, A. Rodriguez, O. Cifdaloz and V. Harikrishnan, " ISA floor: A high resolution floor sensor with 3D visualization and multimedia interface capability.," *AME Program,AME-TR-2003-11p,* 2003.

[83] B. Richardson, K. Leydon, M. Fernström and J. Paradiso, "Z-Tiles: building blocks for modular, pressure-sensing floor spaces.,," *In: Extended Abstracts of the 2004 conference on Human factors and computing systems,* p. 1529–1532, 2004.

[84] T. Delbrück, A. M. Whatley, R. Douglas, K. Eng, K. Hepp and P. F. Verschure, "A tactile luminous floor for an interactive autonomous space," *Robotics and Autonomous Systems,* vol. 55, no. 6, pp. 433-443, 2007.

[85] Sankar Rangarajan et al., " The design of a pressure sensing floor for movement-based human computer interaction.," *In Proceedings of the 2nd European conference on Smart sensing and context (EuroSSC'07),* 2007.

[86] Sigurd Wagner et al., " Electronic skin: architecture and components," *Physica E: Low-dimensional Systems and Nano structures* , vol. 25, no. 2-3, pp. 326-334, 2004.

[87] J. A. Paradiso and N. Gershenfeld, "Musical Applications of Electric Field Sensing Sensing," *Computer Music Journal 21(2),* pp. 69-89, 1997.

[88] T. Chau, "A review of analytical techniques for gait data. Part 1: Fuzzy, statistical and fractal methods," *Gait Posture,* vol. 13, no. 1, pp. 49-66, 2001.

[89] S. e. a. Bamberg, "Gait Analysis Using a Shoe-Integrated Wireless Sensor System," *IEEE Transactions on Information Technology in Biomedicine,* vol. 12, no. 4, pp. 413-423, 2008.

[90] D. P and L. D, "DiamondTouch: a multi-user touch technology," *ACM UIST* , pp. 219-226, 2001.

[91] D. Cranor, Prototouch: A System for Prototyping Ubiquitous Computing Environments Mediated by Touch,, SM thesis, MIT Media Lab, 2011.

[92] R. Fletcher, M. Z. Poh and H. Eydgahi, "Wearable Sensors: Opportunities and Challenges for Low-Cost Health Care," *Conf Proc IEEE Eng Med Biol Soc,* pp. 1763-1766, , 2010.

[93] W. Boucsein, Electrodermal Activity, Springer, 2011.

[94] Lahey, B. et al., "PaperPhone: understanding the use of bend gestures in mobile devices with flexible electronic paper displays," *In Proceedings of CHI '11,* pp. 1303-1312 , 2011.

[95] T. V. Papakostas, J. Lima and M. Lowe, "5.3: A Large Area Force Sensor for Smart Skin Applications," *IEEE SENSORS,* pp. 0-7803-7454-1/02, 2002 .

[96] "Force Sensing Resistor Integration Guide and Evaluation Parts Catalog - 400 Series Evaluation Parts With Suggested Electrical Interfaces.," interlinkectronics.com.

[97] J. E. Dittes, "Galvanic skin response as a measure of patient's reaction to therapist's permissiveness.," *The Journal of Abnormal and Social Psychology,* vol. 55, no. 3, pp. 295-303, 1957.

[98] "http://www.t-ink.com," [Online]. [Accessed 2013].

[99] R. Koehly, D. Curtil and M. Wanderley, " Paper FSRs and latex/fabric traction sensors: Methods for the development of home-made touch sensors," *In Proc. of the 2006 Conf. on New Interfaces for Musical Expression (NIME-06),* p. 230–233, 2006.

[100] "Comductive Compounds," [Online]. Available: http://www.conductivecompounds.com.

[101] P. L. Davidson and J. Y. Han, "Extending 2D object arrangement with pressure-sensitive layering cues," *UIST '08,* pp. 87-90.